University of London

Imperial College of Science, Technology and Medicine
The Blackett Laboratory
Quantum Optics & Laser Science Group

Quantum Information Processing with Single Photons

Yuan Liang Lim

Thesis submitted in partial fulfilment of the
requirements for the degree of
Doctor of Philosophy
of the University of London
and the Diploma of Membership of Imperial College.

May 27, 2006

arXiv:quant-ph/0509168 v1 22 Sep 2005

Abstract

Photons are natural carriers of quantum information due to their ease of distribution and long lifetime. This thesis concerns various related aspects of quantum information processing with single photons. Firstly, we demonstrate N-photon entanglement generation through a generalised $N \times N$ symmetric beam splitter known as the Bell multiport. A wide variety of 4-photon entangled states as well as the N-photon W-state can be generated with an unexpected non-monotonic decreasing probability of success with N. We also show how the same setup can be used to generate multiatom entanglement. A further study of multiports also leads us to a multiparticle generalisation of the Hong-Ou-Mandel dip which holds for all Bell multiports of even number of input ports.

Next, we demonstrate a generalised linear optics based photon filter that has a constant success probability regardless of the number of photons involved. This filter has the highest reported success probability and is interferometrically robust. Finally, we demonstrate how repeat-until-success quantum computing can be performed with two distant nodes with unit success probability using only linear optics resource. We further show that using non-identical photon sources, robustness can still be achieved, an illustration of the nature and advantages of measurement-based quantum computation. A direct application to the same setup leads naturally to arbitrary multiphoton state generation on demand. Finally, we demonstrate how polarisation entanglement of photons can be detected from the emission of two atoms in a Young's double-slit type experiment without linear optics, resulting in both atoms being also maximally entangled.

Thesis Publications

---

1. Y. L. Lim and A. Beige, *Photon polarisation entanglement from distant dipole sources*, J. Phys. A **38**, L7 (2005), quant-ph/0308095
2. Y. L. Lim and A. Beige, *Push button generation of multiphoton entanglement*, Proc. SPIE **5436**, 118 (2004), quant-ph/0403125
3. Y. L. Lim and A. Beige, *An efficient quantum filter for multiphoton states*, J. Mod. Opt. **52**, 1073 (2005), quant-ph/0406008
4. Y. L. Lim and A. Beige, *Multiphoton entanglement through a Bell multiport beam splitter*, Phys. Rev. A **71**, 062311 (2005), quant-ph/0406047
5. Y. L. Lim and A. Beige and L. C. Kwek, *Repeat-Until-Success linear optics quantum computing*, Phys. Rev. Lett. **95**, 030505 (2005), quant-ph/0408043
6. Y. L. Lim and A. Beige, *Generalised Hong-Ou-Mandel Experiments with Bosons and Fermions*, New J. Phys **7**, 155 (2005), quant-ph/0505034
7. Y. L. Lim, S. Barrett, A. Beige, P. Kok and L. C. Kwek, *Repeat-until-success distributed quantum computing with stationary and flying qubits*,(submitted to Phys. Rev. A), quant-ph/0508218

Acknowledgements

I thank both Dr Almut Beige and Prof Sir Peter Knight for being my PhD supervisors. Almut has patiently guided me from being a novice to the stage where I can hopefully say interesting and new things about physics. A valuable lesson which I have learnt from her is the importance of being dogged and persevering in research. She has also taught me to believe in the impossible. Had it not been for her encouragement, I might have given up too easily on a difficult problem! Peter has been very encouraging and supportive to my education and have helped to ensure that I get the support and opportunities to attend summer schools and conferences, all of which have proven to be crucial to this PhD experience. I also thank both of them for guiding me in my thesis and giving me many valuable comments. Furthermore, many of the results in this thesis have been inspired from my interactions with them.

I thank Dan Browne for kindly ploughing through my thesis and offering many valuable scientific feedback, as well as suggesting improvements to the English. I also thank him for our many discussions that has greatly enriched me, and his patience in answering my many curious questions. In addition, I also thank Shash for reading my introductory chapter and also patiently explaining things like stabilizers and POVMs to me. I also thank Terry Rudolph for providing me with many inspiring and provocative thoughts that has helped to shape my research.

I thank Jim Franson for many stimulating discussions and encouragement on many of the work in this thesis, when he was visiting Imperial College. I also thank Geoff Pryde and Marek Żukowski for their encouragement and interest in my work. I also appreciate Martin Plenio for his encouragement.

I thank Jesus Roger-Salazar for kindly giving me the latex template for this thesis. I also thank Jens Eisert for his kind help with Appendix A.

I thank my collaborators Sean Barrett and Pieter Kok for their friendship and sharing their valuable experience and knowledge in research and physics. I also thank another collaborator Kwek Leong Chuan from Quantum LAH for funding a few of my visits to my homeland Singapore to facilitate research collaborations, and also helping me to open up opportunities for future research. My appreciation goes also to Christian Kurtsiefer for getting me fired up with excitement on things that can be done back in Singapore after my PhD.

Special thanks goes to Hugo Cable for being the best of buddies to me in QOLS. We have both "grown up" much together through this PhD experience and I wish him all the best after his PhD.

I also thank Jae, Rachele, Jeremy and Adele for their friendship.

I want to specially thank Huang Sen and Emily for such a special and dear friendship that cannot be expressed with words.

I thank a special brother, Bae Joon Woo. By divine circumstances, our paths had crossed twice - once in IQING 2002 and the other time in Cargese 2004, and we have since maintained close contact. He has been a special encouragement and inspiration to me and I thank him for his friendship.

I would like to thank David Oliver, Ros, Carmel, Ladi and Iyiola of Riverpark Church who had so warmly welcomed me when I first arrived in London and eased my settling in. Also many thanks to all members of the church for their love and prayer support during my three years in London.

I thank David Ong, Adrian Ying, Patrick Wong as well as Melvin Tan for their friendship and encouragement, and for always remembering me in their prayers even when I was away from Singapore.

I also thank Kin Seng and Kien Boon who have been responsible for encouraging me to apply for the DSO postgraduate scholarship program and facilitating the application process. I thank Kin Seng in particular for his encouragement and belief in me. I also thank Yuqing and Ernest for their prayers and support. I thank Poh Boon for helping me to get into the Applied Physics Lab in DSO, where my love for physics was rekindled. Of course, many thanks to DSO for granting me the funding to complete the PhD program in Imperial College!

I thank everyone in my family, especially Daddy, Mummy, Granny, Aunty Lucia, Aunty Letitia, my dear sister Yuan Ping, brother Yuan Sing, as well as my parents-in-law for all their love, support and encouragement. My love of physics was first ignited when my dad bought me the book, *At the opening of the atomic era*, when I was only a child. Ever since, I had always wanted to be a physicist!

I thank my wife Puay-Sze for her neverending patience, support and love which have been so crucial to me. I also want to make special mention of my soon-to-be-born son, Isaac, for the joy and additional motivation that he brings to me during the last lap of my thesis-writing!

I thank God who has loved me, always guided me and taken care of me.

Contents

Publications **3**

1 Introduction **9**

1.1 Brief Introduction to quantum information processing and single photons 10

1.2 Thesis Overview 19

2 Multiphoton Entanglement through a Bell Multiport Beam Splitter using Indepe

2.1 Introduction 21

2.1.1 Photon sources 22

2.1.2 Weak Coherent laser pulse 23

2.1.3 Parametric downconversion 24

2.1.4 Atom-like systems for the generation of single photons on demand 25

2.1.5 Single photons and multiport 27

2.2 Photon scattering through a linear optics setup 29

2.2.1 The Bell multiport beam splitter 32

2.3 The generation of 4-photon states 33

2.3.1 Impossible output states 33

2.3.2 The 4-photon *W*-state 34

2.3.3 The 4-photon GHZ-state 37

2.3.4 The 4-photon double singlet state 38

2.3.5 The general 4-photon case 39

2.4 The generation of N-photon *W*-states 39

2.4.1 Success probabilities 42

2.5 Conclusions 43

3 Generalised Hong-Ou-Mandel Effect forBosons and Fermions **45**

3.1 Introduction 45

3.2 Scattering through a Bell multiport beam splitter 47
3.3 HOM interference of two particles 48
3.4 Multiparticle HOM interference 49
3.4.1 Bosonic particles 50
3.4.2 Fermionic particles 52
3.5 Conclusions 53

4 An Efficient Quantum Filter for Multiphoton States 55
4.1 Introduction 55
4.2 A multipartite quantum filter 57
4.2.1 The 2-photon case 58
4.2.2 The N-photon case 60
4.3 Conclusions 63

5 Distributed Quantum Computing with Distant Single Photon Sources 65
5.1 Introduction 65
5.2 Basic Idea of a remote two-qubit phase gate 68
5.2.1 Encoding 68
5.2.2 Mutually Unbiased Basis 69
5.2.3 A deterministic entangling gate 70
5.2.4 Gate implementation with insurance 72
5.2.5 Teleportation with insurance 74
5.3 Entangled Atom-Photon generation from Atom-Cavity Systems . . . 76
5.3.1 Introduction 76
5.3.2 Photon gun encoder 76
5.4 Measurements on photon pairs 82
5.4.1 Canonical Bell-state measurement 83
5.4.2 Measurement for polarisation encoded photon pair 84
5.4.3 Measurement for dual-rail encoded photon pair 84
5.4.4 Time-resolved detection for non-identical photonsources 86
5.5 Conclusions and discussions 92

6 Distributed Photon Entanglement on Demand 94
6.1 Multiatom entanglement and multiphoton entanglement on demand . 94

7 Photon Polarisation Entanglement from Distant Sources in Free Space 98
7.1 Introduction 98
7.2 Theory 100

7.2.1 Entangled photon and entanged dipole generation 101
7.3 Experimental Implementation 108
7.4 Conclusion 109

8 Summary and Outlook **111**

A Inferring the singlet state from polarisation statistics **115**
References 117

1

Introduction

Photons are natural carriers of quantum information owing to their long lifetimes and ease of distribution and this constitutes the main motivation for this thesis. In quantum information processing, entanglement plays its role in diverse applications such as quantum cryptography, implementation of universal quantum gates, tests of non-locality, and is prevalent in all known quantum algorithms that provide an exponential speedup compared to classical algorithms. Entanglement, a still elusive concept, is strictly defined as the situation where a quantum state cannot be decomposed into a convex sum of tensor product density matrix states. The ability to generate or manipulate entanglement is thus a key ingredient to quantum information processing. In this thesis, we focus primarily on various aspects of entangled state generation, detection, manipulation and exploitation for quantum information processing using single photons. We consider novel means of how single photon sources can be manipulated through the photons they emit and vice-versa the way photons can be manipulated with the aid of single photon sources. Furthermore, as will be seen, these two apparently different tasks can often be exploited for each other. Therefore, an alternative title to this thesis could well be "Photon assisted quantum computation". We start here by giving a brief overview to quantum information processing bringing single photons into a general context. A more detailed survey of the research done in this thesis can be found in the relevant chapters.

1.1 Brief Introduction to quantum information processing and single photons

Quantum information processing is a remarkably diverse and interdisciplinary field. In the words of Knill and Nielsen [Knill02], it is "The science of the theoretical, experimental and technological areas covering the use of quantum mechanics for communication and computation." It includes quantum information theory, quantum communication, quantum computation, quantum algorithms and their complexity and quantum control. In general, these fields are not mutually exclusive and often have substantial overlaps. It is therefore somewhat artificial to attempt to classify them as separate subfields.

Early ideas of quantum information processing began with Feynman, who considered the question of efficient simulation of a quantum system [Feynman82]. He speculated that the only efficient simulation of a quantum system that could be achieved would come from another quantum system. Following that, Deutsch and Jozsa [Deutsch85, Deutsch92] demonstrated the existence of quantum algorithms that are more efficient than classical algorithms. Later, Shor [Shor], building on the work of Simon [Simon] as well as Deutsch and Jozsa, demonstrated a quantum algorithm for prime factorisation that is exponentially faster than any known classical algorithm. Both the Shor and Deutsch-Jozsa algorithm, as well as the Simon algorithm are actually special cases of the more general algorithm for the problem known as the Hidden Subgroup Problem(HSP). In fact, all known algorithms belonging to HSP class, at least for the case of finite Abelian groups, are exponentially more efficient than the best known corresponding classical algorithms. Finally, Grover [Grover96] demonstrated a fundamentally different algorithm that is $\sqrt{N}$ faster than the best known classical algorithm for an N element database search without any partial information. Entanglement appears to be necessary for quantum algorithms that yield exponential speedups compared to classical algorithms [Linden01, Harrow03].

The basic logical unit in each of these algorithms are so-called qubits, which hold the quantum information. Each of these qubits can be in any superposition between two orthogonal logical states, denoted $|0\rangle$ and $|1\rangle$, constituting the computation basis states, in analogy to classical bits '0' and '1' in classical computing. For example, a qubit $|\psi\rangle$ can be written as a state vector in a 2-dimensional Hilbert space given by $|\psi\rangle = a|0\rangle + b|1\rangle$ where a and b are arbitrary normalised complex coefficients. In contrast, a classical bit can only be in the state '0' or '1'. In ad-

dition, there are many possible physical realisations of a qubit. For example, the computational basis states can be the Zeeman ground states of atoms, the direction of the spin of electrons or polarisation states of photons. The coherent evolution of many qubits which can be in an arbitrary superposition[1] can be thought as a mechanism that enables massive parallelism in the computation, hence leading to a possible exponential speedup compared to classical computation. At the same time, any N-qubit unitary operation can be decomposed to two-qubit unitary operations [Barenco95]. It is important to note that there exist two-qubit gates, which together with arbitrary single qubit operations, can simulate any two-qubit unitary operation [DiVincenzo95]. Any two-qubit gate fufilling the above universality criterion is known as a universal two-qubit gate. Notable examples of such gates are CNOT and CZ gates, which perform a controlled non-trivial single qubit unitary operation on a target qubit dependent on the state of the control qubit. Specifically, given two input qubits, a control and target one, the CNOT operation flips the target qubit only if the control qubit is in the logical state $|1\rangle_{\rm c}$. Similarly, the CZ gate yields a negative sign to the target qubit $|1\rangle_{\rm t}$ only if the control qubit is also in the state $|1\rangle_{\rm c}$.

In addition, application of these two-qubit gates to a suitable product state can entangle the input state and we shall now make a short detour to illustrate some basic properties of an entangled state. For example, the state $\frac{1}{\sqrt{2}}(|10\rangle - |11\rangle)$ is not entangled because it can be written as a tensor product of two qubit states given by $\frac{1}{\sqrt{2}}(|0\rangle - |1\rangle) \otimes |1\rangle$. We now treat this as an input state where the left qubit is treated as the control and the right qubit is treated as the target. The application of a CNOT gate to this separable state yields a particularly interesting maximally entangled bipartite state, known as the singlet state $|\Phi^-\rangle$ given by $|\Phi^-\rangle = \frac{1}{\sqrt{2}}(|01\rangle - |10\rangle)$ where the control and target subscripts have been dropped for clarity. This state is invariant under any qubit rotation applied equally to the two qubits. This means that in the basis given by $|0'\rangle$ and $|1'\rangle$, the state $|\Phi^-\rangle$ is again given by $\frac{1}{\sqrt{2}}(|0'1'\rangle - |1'0'\rangle)$. The two parties each holding a qubit will always measure different basis states, no matter what common basis states they share. We now try to construct a two party non-entangled state that might yield a similar measurement syndrome. For example, the non-entangled mixed-state $\rho_{\rm noent} = \frac{1}{2}(|01\rangle\langle 01| + |10\rangle\langle 10|)$ will no doubt yield positive correlations of different states in the measurement basis $|0\rangle$ and $|1\rangle$. Unfortunately, this will no longer be true in another measurement basis, say $|\pm\rangle = \frac{1}{\sqrt{2}}(|0\rangle \pm |1\rangle)$. This shows that an entangled state can have stronger

[1]Note that with N qubits, the Hilbert space spans an exponentially large dimension given by 2^N.

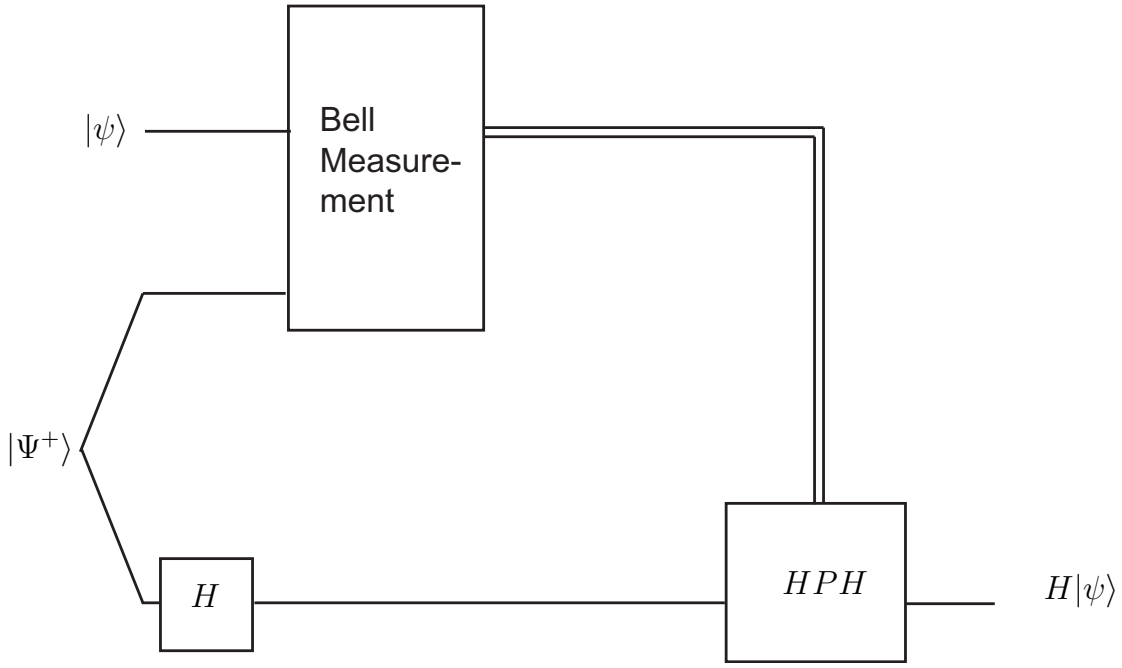

Figure 1.1: Teleportation of a unitary operation such as a Hadamard gate H over the input state $|\psi\rangle$. The action of a Hadamard gate is defined by $H|0\rangle = |+\rangle = \frac{1}{\sqrt{2}}(|0\rangle + |1\rangle)$ and $H|1\rangle = |-\rangle = \frac{1}{\sqrt{2}}(|0\rangle - |1\rangle)$. The entangled ancilla $\frac{1}{\sqrt{2}}(|0+\rangle + |1-\rangle)$ is given by acting H on $|\Psi^+\rangle = \frac{1}{\sqrt{2}}(|00\rangle + |11\rangle)$. A Bell measurement between one of the qubits of the entangled ancilla and the input state $|\psi\rangle$ is performed. P consists of a local unitary operation that depends on the measurement syndrome deriving from the Bell measurement. After measurement and the operation HPH, the teleported state becomes $H|\psi\rangle$. Note that ordinary teleportation is given by replacing the gate H with an identity operator.

correlations than is possible compared to a non-entangled state. Due to the existence of these special correlations, a bipartite entangled state for example, cannot be thought of as two separate parties. We give briefly an example of the exploitation of this correlation. Suppose we have an input state given by $|\psi\rangle = \alpha|0\rangle + \beta|1\rangle$ together with an ancilla $|\Phi^-\rangle$. We can then write the tripartite state $|\psi\rangle|\Phi^-\rangle$ as $\alpha|001\rangle - \alpha|010\rangle + \beta|101\rangle - \beta|110\rangle$ omitting the normalisation factor. If a projective measurement is performed on the first two parties such that a maximally entangled state say $|\Psi^+\rangle = \frac{1}{\sqrt{2}}(|00\rangle + |11\rangle)$ is detected (an example of a Bell measurement), this immediately projects the third qubit to the state $\alpha|1\rangle - \beta|0\rangle$, which is local unitary equivalent to the original input qubit $|\psi\rangle$. We have therefore transferred the input state by measurement to one of the qubits in the entangled ancilla using the correlation found in $|\Phi^-\rangle$ as well in $|\Psi^+\rangle$. This is also known as teleportation [Bennett93].

We have earlier defined what entanglement is by saying what it is not! Although we have already some limited success on entanglement measures (see Ref. [Plenio05] and references therein) and criteria [Horodecki96, Peres96] to help us establish whether a state is entangled or not, the full understanding of what entanglement really is remains elusive[2].

Returning to the discussion on universal gates, one might assume that such gate operations should be accomplished by coherent means, for example, with a controlled evolution of the Hamiltonian governing interactions between qubits possibly with an external control agent, such as a laser beam, with the Cirac-Zoller gate for trapped ions [Cirac95] as a famous example. This is however too restrictive and it is worth commenting briefly on approaches which use entangled resources to simulate universal gates with a measurement-based approach instead of using purely coherent evolutions. These approaches may be important for a future scalable quantum computing implementation. Notable examples are teleportation-based [Gottesman99], and cluster state [Briegel01, Raussendorf01, Raussendorf03] approaches. Both approaches require the preparation of a highly entangled ancilla which subsequently acts as a useful resource for quantum computation. The basic philosophy of the measurement-based approach is to bury all the "difficult" quantum operations in the offline preparation of the entangled ancilla. Quantum computation then proceeds by measurement, which is hopefully an easier operation. Generally, to simulate any N-qubit operation by these approaches, we require at least two-qubit interactions or gates for the preparation of the entangled ancilla. In particular, cluster state approaches allow for universal quantum computation without the need of coherent qubit to qubit interaction once the cluster state[3] has been prepared. Appropriate single qubit measurements in a cluster state allows for any quantum algorithm to be simulated. This was proven by Raussendorf *et al.* [Raussendorf03] by exploiting the correlations found in the cluster state, which is a highly entangled one. These measurements destroy the entanglement of the cluster state and hence, the cluster state is not reusable. Therefore, the term "one-way quantum computing" is used interchangeably with cluster state quantum computing. In the so-called teleportation based approach, the desired unitary operation is "teleported" onto an output state with the help of a suitably prepared entangled resource and Bell measurements (see (1.2)). Refer to Fig. 1.1 for an example of the teleportation of a single

[2]This is the author's personal perception.

[3]A cluster state is prepared for example by first initialising a lattice arrangement of qubits in the state $\frac{1}{\sqrt{2}}(|0\rangle + |1\rangle)$. A CZ gate is then performed between each nearest neighbour to form the cluster state.

qubit unitary operation. Note that this can be extended to any multiqubit unitary operation. For a general discussion of the measurement-based approach, see Ref. [Aliferis04, Childs05].

There is however another kind of approach that seems to share properties of both the coherent and measurement-based approaches. Examples are given in [Beige00, Franson04] where a Zeno-type measurement induces a coherent evolution. A Zeno effect can be understood as the process of halting an evolution based on continuous strong measurements. This is a very useful tool to freeze undesired evolution. Applied to cavity QED [Beige00], an environment induced Zeno-type effect suppresses the cavity decay, that would usually decohere the system. Applied to photons, [Franson04] the Zeno effect can prevent the undesired 2-photon occupation, associated with a failure event, in a doped fiber with a very large 2-photon absorption cross-section and with negligible 1-photon absorption cross-section. Therefore, it is a special kind of "deterministic" postselection.

In parallel to these developments, came the invention of quantum error correction codes by Calderbank, Shor and Steane (CSS) [Shor95, Calderbank96, Steane96]. It was initially thought that this was impossible due to the notion that quantum states are fragile, characterised with a continuous degree of freedom and generally subjected to noise of continuous nature which leads to decoherence. Furthermore, the quantum no-cloning theorem [Wootters82] ruled out the naive method of state copy to combat against noise, as often used in classical communication and computation. CSS however showed that quantum error correction was possible with the help of encoding operations and the measurement of error syndromes. This important result led to the concept of fault-tolerant quantum computation where one can asymptopically approach error-free computation with suitable encodings and error corrections provided that the error probability of gates do not exceed a certain threshold [Gottesman98].

Therefore, a lot of effort both experimentally and theoretically, has been focussed on the physical implementation of universal two-qubit gates. General criteria for a scalable quantum computing system were formulated by DiVincenzo [DiVincenzo00]. Note that this criteria, based on the conventional gate model for quantum computation, have been formulated before the recent development of new paradigms of quantum computation, such as measurement-based approaches to quantum computation or even hybrid models. A relook of this criteria may be timely. To date, gate implementation has been implemented using NMR techniques on a molecule (perfluorobutadienyl iron complex) [Vandersypen01] where a seven-qubit Shor's algorithm for the prime factorisation of the number 15 was demonstrated.

In trapped ions, the Cirac-Zoller gate [Schmidt-Kaler03], a geometric two-ion phase gate [Leibfried03] the Deutsch-Jozsa algorithm [Gulde03], determinstic teleportation of ions [Barrett04, Riebe04], quantum error correction [Chiaverini04] as well as a semi-classical quantum Fourier transform [Chiaverini05] has been demonstrated. These systems consist of qubits which are stationary with a possibly long decoherence time which makes them suitable as quantum memories. On the other hand, disadvantages of using stationary qubits alone include the requirement for precise coherent control. Furthermore, interaction with remote stationary qubits is difficult.

Alternatively, single photons, generally loosely thought of as a single excitation in the electromagnetic field, are natural flying qubits with long decoherence time (compared to gate operations) and are useful for the distribution of quantum information. At optical frequencies, the background photon count rate is virtually zero. Furthermore, photons are bosons and they obey the following commutation rules,

$$\left[a_i, a_j^\dagger\right] = \delta_{ij} \ , [a_i, a_j] = \left[a_i^\dagger, a_j^\dagger\right] = 0 \tag{1.1}$$

where a_i ($a_i^\dagger$) is the photon annihilation (creation) operator for a certain mode i, $\left[\hat{a}, \hat{b}\right] = \hat{a}\hat{b} - \hat{b}\hat{a}$ and $\delta_{ij} = 1$ for $i = j$ or 0 otherwise. Photons can in general be described in various encodings or degree of freedom, such as polarisation, spatial or frequency, or even angular momentum. For example, in polarisation encoding, one can assign the logical qubit $|0\rangle_L$ and $|1\rangle_L$ to any two orthogonal polarisations, such as the horizontal and vertical polarisations. Single qubit operations for photons are extremely easy [James01, Englert01] to implement with waveplates, polarisation rotators etc. However, there exists practically no coupling between photons in vacuum and hence a two-qubit gate implementation between photons is difficult, which is one of the reasons why photons are so stable. Indeed, an early proposal [Milburn89] of a photonic universal three-qubit conditional SWAP gate, known as the Fredkin gate, requires Kerr nonlinearity to produce intensity-dependent phase shifts. The Kerr nonlinearity required is extremely huge[4] if operation at the single photon level is required, which pose a severe experimental challenge. One of the early explorations of how quantum logic can be simulated (inefficiently and requiring exponential resources) with linear optical elements alone is found in the paper by Cerf *et al.* [Cerf98]. The word "linear optics"[5] is defined in the sense in which the Hamiltonian

[4] See Ref. [Turhette95] for a proof-of-principle demonstration with cavity QED.

[5] This definition would certainly include squeezing which is not part of the standard linear optical quantum information processing toolbox. We do not have to include squeezing in this thesis, although weak squeezing with photon detectors can result in a heralded single photon source. The linear optical quantum information processing toolbox we consider consist only of

that describe the photon transformation has only at most quadratic terms in photon creation or destruction operators. In this way, the resulting Heisenberg equations of motion are linear in terms of photon creation or destruction operators. Cerf *et al.*'s scheme is however not generally applicable to quantum computation with different photons as it operates on a Hilbert space of two degrees of freedom(polarisation and momentum) on the same photon instead of different photons. Following that, a very important no-go theorem by Lütkenhaus *et al.* [Lütkenhaus99] showed that complete Bell state measurement with unit efficiency is impossible with linear optics resource alone, despite having ancillas and conditional measurements as resources. Note that their work covers the case where the Bell state is defined with two photons regardless of the type of encoding, which applies generally to quantum computation with different photons. Further work [Calsamiglia01] (see also related work by Vaidman and Yoran [Vaidman99]) in this direction led to the result that given no ancillas as resources, linear optics-based Bell measurement yields a success probability of at most 50% (see Chapter 5 where such an example is given). We define, without loss of generality, the basis states of a complete Bell measurement as

$$
\begin{aligned}
|\Phi^{\pm}\rangle &= \frac{1}{\sqrt{2}}(a^{\dagger}_{1,h}a^{\dagger}_{2,v} \pm a^{\dagger}_{1,v}a^{\dagger}_{2,h})|0\rangle_{\text{vac}}\,, \\
|\Psi^{\pm}\rangle &= \frac{1}{\sqrt{2}}(a^{\dagger}_{1,h}a^{\dagger}_{2,h} \pm a^{\dagger}_{1,v}a^{\dagger}_{2,v})|0\rangle_{\text{vac}}\,.
\end{aligned} \tag{1.2}
$$

Here, $a^{\dagger}_{i,\lambda}$ refers to a photon creation operator for spatial mode i with polarisation mode λ. Bell states, which are maximally entangled two-qubit states, provide quantum correlations which feature as a crucial ingredient in many aspects of quantum information processing such as teleportation, entanglement swapping etc..

Later, the seminal paper by Knill *et al.* [Knill01b] demonstrated that quantum computing can be implemented efficiently (i.e. with polynomial resource) with photons and linear optics elements if one has deterministic single photon sources with perfect photon-resolving detectors. They proposed a photon nonlinear gate operation based on photon interference in a linear optics setup together with postselection. Their scheme also makes use of a teleportation based approach [Gottesman98] with the help of Bell state measurements. They managed to approach near 100% efficient Bell measurement with the aid of asymtopically large number of highly entangled photons without contradicting the no-go theorem of Lütkenhaus *et al.* Franson *et al.* [Franson02] have subsequently improved this scaling tremendously, with feed-forward corrections, from the failure rate of $1/n$ to $1/n^2$ where n is the number of

photon sources, detectors, beam splitters and phase plates.

ancilla photons. Probabilistic gate operations, based on Ref. [Knill01b] with some clever improvements, between photons have since been demonstrated experimentally [O'Brien03, Pittman03, Gasparoni04, Zhao05] and serve as a testbed for quantum computation.

Unfortunately, approaches using purely photon and linear optics alone seem to require huge practical resources for scaling even if they are polynomial [Scheel03, Scheel04b, Eisert05]. In principle, this can be alleviated through a photonic cluster state computation model in which the cluster state can be built in an efficient manner [Browne05, Nielsen04]. The cluster state than serves as a universal palette for any quantum computation that should proceed by measurement with unit efficiency in principle. A recent working demonstration of a postselected 4-photon cluster state quantum computation is found in Ref. [Walther05]. It is however still necessary to implement photon memory and this is currently still a great experimental challenge.

Going by a different thread from the usual linear optics quantum computation, it has been recently shown that relatively weak, but non-zero Kerr nonlinearity [Munro05, Nemoto04] is sufficient for implementing universal gates between photons with unit efficiency. The surprising thing is that one does not really need strong Kerr nonlinearity for this. The trick is to use a homodyne measurement with an intense coherent state source to compensate for the weak nonlinearity. This promising approach has many applications useful to photonic based quantum computation. Besides implementing photonic gates with unit efficiency, it can be used as a photon counting non-demolition measurement or to turn a weak coherent pulse into a heralded single photon source.

One might envision a hybrid approach using the best properties of both stationary and flying qubits (photons) which is a key feature in this thesis. Motivations of such hybrid approaches have been first considered by Van Enk *et al.* [Enk97, Enk98] in quantum networking, where information can be sent to distant nodes via flying qubits between stationary nodes consisting of stationary qubits. The stationary qubit (for example, atoms or ions) function as a qubit with long decoherence time as well as acting as a quantum memory. Such an approach opens the possibility of distributed quantum computing.

The basic component of such a network requires stationary qubit to flying qubit interfaces which is commonly found in cavity QED and atomic ensemble implementations.

Parallel developments in the field of quantum communication which essentially involves the exchange of classical or quantum information through classical and quantum channels includes quantum cryptography, teleportation, distributed quan-

tum computation etc. In the field of quantum cryptography, also widely known as quantum key distribution, protocols such as BB84, Ekert [Bennett84, Ekert91] show the possibility of two parties establishing a secret key with no possibility of an eavesdropper being able to share any part of the secret key. The main principles used are the quantum no-cloning theorem and the fact that a measurement of a state generally disturbs the original state. The eavesdropper attempting to learn anything of the secret key necessarily reduces the measured correlation observed between the two rightful parties, Alice and Bob. Such an observation signals the presence of a possible eavesdropper if the correlation is below a certain bound. Again, due to their nature of being flying qubits, all experiments to-date implementing quantum key distributions involve photons [Peng05, Kurtsiefer02, Gisin02]. Particularly, Ekert's protocol requires the preparation of an entangled pair of photons. Related to Ekert's protocol is the so-called Bell's inequality violation test [Bell65, Clauser69]. This is a deep test for ruling out a local hidden variable theory that can make predictions similar to quantum mechanics. Such a test involves the repeated preparation of an entangled pair of particles followed by independent measurements on each of the qubits to obtain a statistical correlation function. All local hidden-variable theories will yield a bound in the correlation function. According to quantum mechanics, this bound can be violated. The violation has been widely demonstrated[6] for the case where at least one of the particles is a photon. For that of two photons, the violation has been observed from atomic cascade emission [Aspect82] as well from spontaneous parametric downconversion [Ou88]. Particularly interesting, the experiment performed by Blinov *et al.* [Blinov04, Moehring04] demonstrated entanglement between an ion and a photon or in other words, a stationary and a flying qubit. They also demonstrated for the first time, a Bell inequality violation between particles of different species, namely an atom and a photon. This provides a building block to distributed quantum computation between distant ions assisted by photons. Teleportation also plays an especially important role in quantum communication. Augmented with quantum repeaters [Briegel98] based on entanglement purification [Bennett96], states can be transferred with high fidelity through teleportation with a robustly created perfect entangled ancilla. Experiments with photons over long distances have also been performed [Ursin04, Riedmatten04] further illustrating the use of photons as an information carrier.

[6]There exist two loopholes applying to experiments demonstrating the violation of the Bell's inequality. One is the lightcone loophole that would still allow a possible local realistic interpretation. The other is the detection loophole where the whole ensemble may not violate the Bell's inequality although the detected subensemble is perceived to violate it. To date, there has been no experiments that closes both loopholes.

As attractive as it is to use single photons in quantum information processing, five major sources of decoherence and errors are relevant. They are interferometric stability, mode matching (spatial and temporal), photon loss as well as detector accuracy and efficiency. Various aspects of these issues will be addressed in this thesis although we do not claim to fully resolve all these issues.

We have also seen in this section how important entanglement generation and manipulation of single photons is to the field of quantum information processing. This short introduction, in which we have not discussed those aspects of quantum information theory which are out of the scope of this thesis, obviously does not do justice to the wide field of quantum information processing. The interested reader is invited to refer to the book by Nielsen and Chuang [Nielsen00] for an excellent exposition.

1.2 Thesis Overview

The central theme of this thesis is the manipulation and preparation of qubits (be it stationary or flying qubits) with single photons. The bulk of the research work based on this theme is described from Chapters 2 to 7 and a brief overview is given as follows.

In Chapter 2, we show that a wide range of highly entangled multiphoton states, including *W*-states, can be prepared by interfering *single* photons inside a Bell multiport beam splitter and using postselection. Multiphoton entanglement being an important resource for linear optics quantum computing motivates the work in this chapter. The results that we obtain is photon encoding independent and thus have wide applicability. We perform further studies on the multiport in the next chapter for a different application.

In Chapter 3, we study an important aspect of multiphoton interference, namely, the generalised Hong-Ou-Mandel(HOM) effect that plays a crucial role to many aspects of linear optics based quantum computation with photons. The famous HOM dip for two photons, where two identical photons entering separate input arms of a 50:50 beamsplitter never exit in separate output arms, plays an important role in quantum information processing such as the characterisation of single photon sources, Bell measurements etc. Here, we present a new generalisation of the HOM dip for multiparticle scattering through a multiport.

In Chapter 4, we propose a scheme for implementing a multipartite quantum filter that uses entangled photons as a resource. Such filters have applications in the

building of cluster states and are shown to be universal. The scheme that we propose is highly efficient and uses the least resources of all comparable current schemes.

In Chapter 5, we describe an architecture of distributed quantum computing that can be realised with single photon sources without the need of highly entangled ancilla states. The ability to perform gate operations between arbitrary qubits, and not only between next neighbours, yields a significant improvement of the scalability of quantum computing architectures. This can be achieved with the help of distributed quantum computing, where the information of stationary qubits is encoded in the states of flying qubits (i.e. single photons), which then allow to establish a communication between distant sources. We describe the implementation of an eventually deterministic universal two-qubit gate operation between single photon sources, despite the restriction of the no-go theorem on deterministic Bell measurements with linear optics. This is a novel demonstration of an efficient repeat-until-success architecture to quantum computation.

In Chapters 2 and 7, the entangled photons are shown to be generated postselectively or at best preselectively. Ideally, one would like to generate these entangled photons on demand. Interestingly, by combining ideas of photon interaction with their sources together with measurements from Chapters 2 and 5, we show in Chapter 6 that distributed photon entanglement can be generated on demand. This can then serve as a useful tool for the diverse applications already mentioned.

So far, linear optics has played a crucial component in the preceding chapters. Penultimately, in Chapter 7, we do not consider any linear optics manipulation of light at all. Indeed, we recall the Young's double-slit experiment in the context of two distant dipole sources in free space without cavities. Experiments have shown that interference fringes can be observed by coherent light scattered by the dipole sources. Taking a step further, we show that polarisation entanglement can also be produced by initially unentangled *distant* single photon sources in free space which at the same time also results in entanglement between the sources. This adds new perspectives to common notions where it is widely thought that photon polarisation entanglement can only be obtained via pair creation within the *same* source or via postselective measurements on photons that overlapped within their coherence time inside a linear optics setup.

Finally, we close in Chapter 8 with a summary and give limitations and an outlook of the work of this thesis.

2

Multiphoton Entanglement through a Bell Multiport Beam Splitter using Independent Photons

2.1 Introduction

In this chapter, we are concerned with the practical generation of multiphoton entanglement. It is not possible to create a direct interaction between photons and hence they are difficult to entangle as already highlighted in Chapter 1. One way to overcome this problem is to create polarisation or time-bin entanglement via photon pair creation within the same source as in atomic cascade and parametric down-conversion experiments. This has already been demonstrated experimentally by many groups [Aspect82, Kwiat95, Brendel99, Thew02, Riedmatten04]. Other, still theoretical proposals employ certain features of the combined level structure of atom-cavity systems [Gheri98, Lange00, Schön05], photon emission from atoms in free space (described in Chapter 7) or suitably initialised distant single photon sources (to be demonstrated in Chapter 6).

Alternatively, highly entangled multiphoton states can be prepared using independently generated single photons with no entanglement in the initial state, linear optics and postselection. This method shall be the main focus of this chapter. In general, the photons should enter the linear optics network such that all information about the origin of each photon is erased. Afterwards postselective measurements are performed in the output ports of the network [Lapaire03]. Using this approach,

Shih and Alley verified the generation of maximally entangled photon pairs in 1988 by passing two photons simultaneously through a 50:50 beam splitter and detecting them in different output ports of the setup [Shih88]. For a recent experiment based on this idea using quantum dot technology, see Ref. [Fattal04].

Currently, many groups experimenting with single photons favour parametric down conversion because of the quality of the output states produced. However, these experiments cannot be scaled up easily, since they do not provide efficient control over the arrival times of the emitted photons. It is therefore experimentally challenging to interfere more than two photons successfully. Interesting experiments involving up to five photons have nevertheless been performed [Eibl03, Bourennane04a, Zhao03, Zhao04, Zhao05] but going to higher photon numbers might require different technologies. To find alternatives to parametric down conversion, a lot of effort has been made over the last years to propose experimentally realisable sources for the generation of single photons on demand [Law97, Kuhn99, Duan03, Jeffrey04]. Following these proposals, a variety of experiments has already been performed, demonstrating the feasibility and characterising the quality of sources based on atom-cavity systems [Hennrich00, Kuhn02, Keller04a, Mckeever04], quantum dots [Benson00, Pelton02] and NV color centres [Kurtsiefer00, Beveratos02]. Before we proceed further, it is appropriate to give a more detailed survey of the above mentioned single photon sources.

2.1.1 Photon sources

Photon sources can be generally subdivided into sources that give strictly antibunched photons, (i.e. the normalised intensity time correlation, also known as $g^{(2)}(\tau)$, is smaller than unity for zero time separation) or sources that yield otherwise. True single photon sources yield only antibunched photons with $g^{(2)}(0) = 0$. Furthermore, an ideal turnstile single photon source should consistently yield exactly one photon in the same pure quantum state whenever required. Particularly for applications [Knill01b] relying on Hong-Ou-Mandel two-photon type interference, it is important for photons to be indistinguishable and of high purity. An example of such a candidate source is an atom-like system which includes quantum dots, diamond NV-color centers and atom-cavity systems. These systems also afford push-button photon generation, which is an ideal requirement for experiments requiring single photons such as quantum cryptography or linear optics based quantum computing. When a photon is required, the source can be triggered to yield a photon. There also exist approximate single photon sources that cannot be directly triggered on

demand. In principle, even these sources can simulate an on-demand single photon source with the help of photon memory and non-demolition measurement, a currently challenging experimental requirement that has undergone much interest and development. Two prominent examples of pseudo single photon sources are a weak coherent laser pulse and the parametric downconversion source. We review below a selection of single photon sources that are currently in use.

2.1.2 Weak Coherent laser pulse

A laser pulse can be modelled to a good approximation as a equal weighted mixture of coherent states of the same amplitude α but different phase ϕ [Enk02, Mølmer97]. This is equivalent to a mixture[1] of photon Fock states weighted with a Poissonian distribution,

$$\rho_{\text{laser}} = \int d\phi |\alpha e^{i\phi}\rangle\langle\alpha e^{i\phi}| = \sum_n \frac{e^{-\alpha^2}\alpha^{2n}}{n!}|n\rangle\langle n|. \tag{2.1}$$

The probability weight of an n-photon Fock state is thus given by $P(n) = \frac{e^{-\alpha^2}\alpha^{2n}}{n!}$. When $\alpha \ll 1$, then $P(0) \gg P(1) \gg P(2)$. This implies that a weak laser pulse can indeed function as a pseudo single photon source. This necessarily implies low count rate for single photons which is due to the necessity to use a weak pulse to suppress any multiphoton component weighted by Poissonian statistics. Furthermore, any single photon pulse generated must be detected postselectively and cannot be heralded(except with the help of a photon non-demolition measurement) since $P(0) \gg P(1)$ therefore implying a necessarily large vacuum component. The weak coherent laser pulse finds its application in quantum key distribution (QKD) for example. It was once thought that photon-number splitting attack would be a strong impediment to achieve a high key rate in the presence of channel loss. However, in the light of some recent advancement of secure QKD protocols robust against photon-number splitting attack, such as the decoy-state [Hwang03] and strong phase-reference pulse [Koashi04] protocol, the weak coherent laser pulse is likely to remain an important tool for QKD.

[1] In fact, the relative and not the absolute phase in quantum optics experiments turns out to be the crucial parameter. So, it is equally valid and may be more useful to model the laser pulse as an effective pure coherent state instead of a mixture of coherent states as in (2.1). One should however be careful to ascribe realism to such an interpretation. This issue has been a source of hot debate. See Ref. [Bartlett05] and references therein for further discussion.

2.1.3 Parametric downconversion

A useful photon source arises from the process of spontaneous parametric downconversion(SPDC). Such a source is used widely in a large number of quantum optics experiments such as the famous Hong-Ou-Mandel effect [Hong87]. Similar to the coherent laser pulse source, it is also not a true single photon source. It is, however able to yield a wide variety of multiphoton states postselectively. If only a single photon is desired, it can act as a heralded source where a trigger allows one to infer the emission of a photon in a certain mode. On the other hand, it is widely used to generate entangled photon pairs [Kwiat95, Tittel98, Brendel99, Thew02, Riedmatten04] in various encodings such as polarisation,energy-time, time-bin etc. and a wide variety of experiments ranging from fundamental test of quantum mechanics to linear optics quantum computation have been performed with it. SPDC can generally yield quite a high count rate of entangled photon pairs, for example about $10^5 - 10^6 s^{-1}$ [Kurtsiefer01, Kumar04]. However, experiments for multiphoton interferometery typically yield, for example for $N = 4$ photons, a coincidence count rate of $10^{-2} s^{-1}$[Pan98a]. This low count rate is partially due to both the random nature of photon emission as well as the need for frequency filters to erase the time-stamp of the generated photons for experiments such as entanglement swapping with Bell measurements [Żukowski93]. The reason is due to the strong temporal correlation of the signal and idler photons emitted. Due to this, only quantum optics experiment in the few photons level utilising the above states ($N \leq 5$) are viable.

Although there exist quasi-deterministic schemes, for example in Ref. [Pittman02a, Jeffrey04] for photon generation, they require photon recycling circuits or photon memories, both still experimentally challenging. On the other hand, parametric downconversion is useful for generating squeezed states (see for example Ref. [Wu86]), which are useful for applications in continuous variable quantum information processing. The SPDC process can be roughly understood in terms of a higher energy photon being converted by an energy conserving process to two lower energy photons, traditionally known as the signal and idler photons. If the signal and idler photons are of the same polarisation, this is known as a Type-I process. If their polarisation are mutually orthogonal, this is known as a Type-II process. To generate a photon pair, a birefringent noncentrasymmetric nonlinear crystal is pumped by a laser, either in cw mode or pulsed mode. Phase matching conditions determine the direction and frequencies of the signal and idler photon pair generated.

We now denote the photon creation operator with frequency ω, polarisation λ and

direction $\hat{\mathbf{k}}$ as $a^{\dagger}_{\hat{\mathbf{k}},\lambda}(\omega)$. We denote the emitted directions(polarisation) of a signal and idler photon as $\hat{\mathbf{k}}_s(\lambda_s)$ and $\hat{\mathbf{k}}_i(\lambda_i)$ respectively and we assume a type-II process. As in Kwiat *et al.*[Kwiat95], we assume the presence of two photon collection directions, $\hat{\mathbf{k}}_A$ and $\hat{\mathbf{k}}_B$ such that when $\hat{\mathbf{k}}_A = \hat{\mathbf{k}}_i$ or $\hat{\mathbf{k}}_s$, $\hat{\mathbf{k}}_B = \hat{\mathbf{k}}_s$ or $\hat{\mathbf{k}}_i$ respectively. In these two directions, together with frequency filters, the postselected 2-photon state $|\psi\rangle$ generated by SPDC [Żukowski95] is then given by

$$\begin{aligned} |\psi\rangle \;=\; & \int d\omega_p \int d\omega_i \int d\omega_s F(\omega_p,\omega_i,\omega_s) \\ & [a^{\dagger}_{\hat{\mathbf{k}}_A,\lambda_i}(\omega_i) a^{\dagger}_{\hat{\mathbf{k}}_B,\lambda_s}(\omega_s) + a^{\dagger}_{\hat{\mathbf{k}}_A,\lambda_s}(\omega_s) a^{\dagger}_{\hat{\mathbf{k}}_B,\lambda_i}(\omega_i)]|\text{vac}\rangle \end{aligned} \tag{2.2}$$

where ω_p is the pump frequency and $F(\omega_p,\omega_i,\omega_s)$ is a function dependent on the phase matching condition as well as the frequency envelope of the pump and the frequency filters. Under suitable phase matching condition, spatial pin-hole filtering, and or frequency filtering, $F(\omega_p,\omega_i,\omega_s)$ can be highly peaked at $F(\omega_p,\omega_p/2,\omega_p/2)$ and $|\psi\rangle$ therefore reduces approximately to a polarisation Bell state [Kwiat95, Żukowski95] that is widely used in quantum optics experiments.

2.1.4 Atom-like systems for the generation of single photons on demand

Candidate systems that could yield single photons on demand include mainly atom-like systems such as atoms, quantum dots, NV (Nitrogen-Vacancy) color centers or even molecules. These proposals are mainly based on the ability to excite the photon source which then decays back to a ground state as a result yielding a photon. Due to the fact that every photon generated by this method requires an excitation time overhead, this results in naturally antibunched photon production. These systems are more recent developments, compared to SPDC sources and weak coherent laser pulses. They benefit from recent technological advancements such as semiconductor processing, laser cooling and trapping etc. and are still an exciting development avenue. Quantum information processing has further served as an important motivating factor, as is investigated in this thesis, for the continual development of these sources.

The quantum dot single photon source is operated by performing a sharp laser pulse excitation to an excited level representing the creation of a so-called excited exciton which rapidly decays non-radiatively to the lowest excited state of the exciton. A subsequent slower decay back to the ground state yields a photon. In practice, biexcitonic excitation is usually preferable, due to the ability to spectrally

isolate the last but one photon [Santori00]. With the quantum dot integrated in monolithic cavity structures, the spontaneous emission rate can be increased substantially with the emission mainly into the cavity mode which results in directed photon emission. Due to the non-radiative decay in the excitation process, there is a slight uncertainty in the photon emission time. Even with this and all other effects contributing to decoherence, photon pulses of sufficient purity and indistinguishability can be generated consistently to observe a Hong-Ou-Mandel 2-photon interference[Santori02] at low temperatures. If spectral purity is not needed, single photon generation can still be performed at room temperature [Michler00]. The quantum dot also allows for coherent Raman excitation schemes [Kiraz04] and may lead to an attractive solid-state alternative to photon guns based on atom-cavity systems. A good review on the physics of photon generation through quantum dots is found in Santori *et al.* [Santori04]. It is worth mentioning also the quantum dot can be excited electronically via a Coloumb blockade and Pauli effect [Kim99] leading to an electronic turnstile single photon device.

NV color center, an optically active defect inside a diamond nanocrystal, is an alternative atom-like system for photon generation. Unlike the quantum dot, for applications in quantum cryptography where the purity of photons generated is not too important, NV color centers can be maintained at room temperature during operation. Their key advantage lies in the fact that they boast of extremely stable operation even at room temperature. The excitation of an NV color center to generate a single photon is similar to that of the quantum dot. To date, photon antibunching has been observed with this method [Kurtsiefer00, Beveratos02]. The demonstration of Hong-Ou-Mandel 2-photon interference would probably require cyrogenic temperature operation. Before moving to atom-cavity systems, we mention that single molecules are yet another attractive atom-like system capable of yielding single photons. In fact, the most recent experiment with a TDI (Terrylenediimide) molecule at cryogenic temperature have yielded photons demonstrating the Hong-Ou-Mandel 2-photon interference [Kiraz05].

The atom-cavity system consists of an atom ideally trapped in a high-finesse cavity. A laser and cavity-driven Raman process which is described in more detail in Chapter 5 transfers a photon in the cavity which subsequently leaks out. This has been experimentally demonstrated [Kuhn02, Mckeever04, Keller04a] and photons generated from such systems have a sufficient purity and consistency to observe the Hong-Ou-Mandel 2-photon interference [Legero04]. In principle, barring imperfections such as photon absorption, weak cavity coupling, the photon generation probability approaches unity. The atom-cavity system allows also for generation of

entangled photons on demand [Schön05, Gheri98]. More generally, it also allows for the state of an atom to be redundantly encoded to the photon it generates which is described in Chapter 5.

Current experimental achievements of all these sources have admittedly not yet achieved photon production on demand. The best reported photon production efficiency [Mckeever04] is still less than 70% although there is no limit in principle to achieving near unit efficiency. Compared to SPDC, these sources generally demand greater experimental complexity at the present. Moreover, these sources are generally not as wavelength tunable as SPDC sources, although this need not be a real disadvantage. However, with strong motivations for scalability in linear optics quantum computation and distributed quantum computing as well as quantum cryptography, much effort to the development of a robust true photon on demand source is ongoing.

2.1.5 Single photons and multiport

Motivated by the above recent developments, several authors studied the creation of multiphoton entanglement by passing photons generated by a single photon source through a linear optics network [Żukowski97, Lee02, Fiurasek02, Zou02a, Wang03, Sagi03, Pryde03, Mikami04, Shi05]. A variety of setups has been considered. Zukowski *et al.* showed that the $N \times N$ Bell multiport beam splitter (see below) can be used to produce higher dimensional EPR (Einstein-Podolsky-Rosen) correlations [Żukowski97]. Shi and Tomita [Shi05] for example studied 3 and 4-photon W-state preparation with multiports which led to high generation efficency. They also conjectured but did not prove that a symmetric $N \times N$ multiport may be used to generate an N-photon W-state. Mikami *et al.* studied the generation of N-photon states through parametric downconversion, coherent laser states and multiports with photon number-resolving detectors. Such multiports have an important application in boosting the success probability of linear optics teleportation to near unity [Knill01b] using a special highly entangled multiphoton ancilla.

Special attention has been paid to the optimisation of schemes for the generation of the so-called NOON state with special applications in lithography [Lee02, Fiurasek02, Zou02a, Pryde03]. Wang studied the event-ready generation of maximally entangled photon pairs without photon number-resolving detectors [Wang03] and Sagi proposed a scheme for the generation of N-photon polarisation entangled GHZ states [Sagi03]. It is also possible to prepare arbitrary multiphoton states [Fiurasek03] using for example probabilistic but universal linear optics quantum

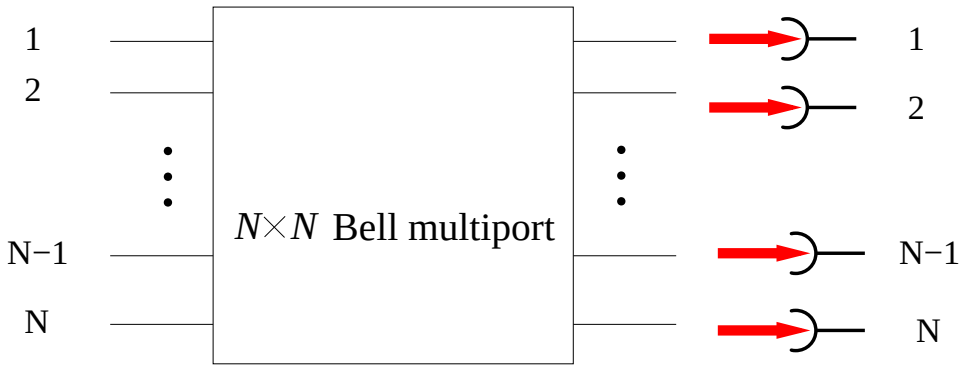

Figure 2.1: Experimental setup for the generation of multiphoton entanglement by passing N single photons through an $N \times N$ Bell multiport beam splitter. The state preparation is considered successful under the condition of the collection of one photon per output.

gates, like the one described in Refs. [Pittman02b, Knill01b] or using a large enough optical cluster state [Yoran03, Nielsen04, Browne05] which still remains an experimental challenge. However, these approaches are not always the most favourable and often require a large number of entangled photon ancillas.

Here we are interested in the generation of highly entangled qubit states of N photons using only a single photon source and a symmetric $N \times N$ Bell multiport beam splitter, which can be realised by combining single beam splitters into a symmetric linear optics network with N input and N output ports [Żukowski97, Törmä95]. In the two-photon case, the described scheme simplifies to the experiment by Shih and Alley [Shih98]. To entangle N photons, every input port i of the Bell multiport should be entered by a single photon prepared in a state $|\lambda_i\rangle$. The photons then interfere with each other before leaving the setup (see Fig. 2.1). We consider the state preparation as successful under the condition of the collection of one photon per output port, which can be relatively easily distinguished from cases with at least one empty output port. In general, this can be done with photon number-resolving non-demolition detectors [Munro05, Nemoto04] and we obtain preselected multiphoton entanglement. Otherwise, the entangled state is postselected without the need of photon number-resolving detectors. Postselected photon state preparation is nevertheless useful if one can accomplish a non-trivial task. Examples are teleportation [Joo03], quantum secret sharing, secure quantum key distribution [Chen05], testing entanglement with witnesses and observing a violation of Bell's inequality [Bourennane04b, Toth05] .

One advantage of using a Bell multiport beam splitter for the generation of multiphoton entanglement is that it redirects the photons without changing their inner

degrees of freedom, like polarisation, arrival time and frequency. The described setup can therefore be used to generate polarisation, time-bin and frequency entanglement. Especially, time-bin entanglement can be very robust against decoherence and has, for example, applications in long-distance fibre communication [Gisin02]. Moreover, the preparation of the input product state does not require control over the relative phases of the incoming photons, since the phase factor of each photon contributes at most to a global phase of the combined state with no physical consequences.

It is the purpose of this chapter to explore some novel properties of a Bell multiport beam splitter. This chapter is organised as follows. In Section 2.2 we introduce the notation for the description of photon scattering through a linear optics setup. Section 2.3 shows that a wide range of highly entangled photon states can be obtained for $N = 4$, including the W-state, the GHZ-state and a double singlet state. Afterwards we discuss the generation of W-states for arbitrary photon numbers N and calculate the corresponding probabilities for a successful state preparation. We observe an interesting non-monotonic decreasing trend in the success probability as N increases owing to quantum interference. Finally we conclude our results in Section 2.5.

2.2 Photon scattering through a linear optics setup

Let us first introduce the notation for the description of the transition of the photons through the $N \times N$ multiport beam splitter. In the following, $|+\rangle$ and $|-\rangle$ denote the state of a photon with polarisation "+" and "−" respectively. Alternatively, $|+\rangle$ could describe a single photon with an earlier arrival time or a higher frequency than a photon prepared in $|-\rangle$. As long as the states $|\pm\rangle$ are orthogonal and the incoming photons are in the same state with respect to all other degrees of freedom, except of course their input spatial positions, the calculations presented in this paper apply throughout. Moreover, we assume that each input port i is entered by one independently generated photon prepared in $|\lambda_i\rangle = \alpha_{i+}|+\rangle_i + \alpha_{i-}|-\rangle_i$, where $\alpha_{i\pm}$ are complex coefficients with $|\alpha_{i+}|^2 + |\alpha_{i-}|^2 = 1$. If $a^\dagger_{i\mu}$ denotes the creation operator for one photon with mode μ in input port i, the N-photon input state can be written as

$$|\phi_{\text{in}}\rangle \;=\; \prod_{i=1}^{N} \Big(\sum_{\mu=+,-} \alpha_{i\mu}\, a^\dagger_{i\mu} \Big)\, |0\rangle \tag{2.3}$$

with $|0\rangle$ being the vacuum state with no photons in the setup.

Let us now introduce the unitary $N \times N$-multiport transformation operator, namely the scattering matrix S, that relates the input state of the system to the corresponding output state

$$|\phi_{\rm out}\rangle \;=\; S\,|\phi_{\rm in}\rangle\,. \tag{2.4}$$

Using Eq. (2.3) and the relation $S^\dagger S = \mathit{I\!I}$ therefore yields

$$\begin{aligned} |\phi_{\rm out}\rangle &= S\Big(\sum_{\mu=+,-}\alpha_{1\mu}\,a^\dagger_{1\mu}\Big)\,S^\dagger S\Big(\sum_{\mu=+,-}\alpha_{2\mu}\,a^\dagger_{2\mu}\Big)\cdot\,\ldots\,\cdot S^\dagger S\Big(\sum_{\mu=+,-}\alpha_{N\mu}\,a^\dagger_{N\mu}\Big)\,S^\dagger S\,|0\rangle \\ &= \prod_{i=1}^{N}\Big(\sum_{\mu=+,-}\alpha_{i\mu}\,S\,a^\dagger_{i\mu}\,S^\dagger\Big)\,|0\rangle\,. \end{aligned} \tag{2.5}$$

In the following, the matrix elements U_{ji} of the unitary transformation matrix U denote the amplitudes for the redirection of a photon in input i to output j. Generally speaking, an $N \times N$ multiport described by any arbitrary transfer matrix U may be constructed by a pyramidal arrangement of beamsplitters and phase plates as shown in Fig. 2.2.

The most familiar example of a multiport is the 2×2 beamsplitter that has 2 input and 2 output ports. It can be described by a unitary 2×2 matrix $B(R,\phi)$ given by

$$B(R,\phi) = \begin{pmatrix} \sqrt{T} & {\rm e}^{{\rm i}\phi}\sqrt{R} \\ \sqrt{R} & -{\rm e}^{{\rm i}\phi}\sqrt{T} \end{pmatrix}, \tag{2.6}$$

where the R denotes the reflectivity and $T = 1 - R$ denotes the transmittivity of the beamsplitter. The phase ϕ is obtained by placing a phase shifter at one of the input ports.

Reck [Reck94, Reck96] (see also [Sun01]) has shown this using similar methods as used in Gaussian elimination. The key to his proof is to factorize the matrix U into a product of block matrices describing only 2×2 beam splitter matrices together with phase shifts. We begin by defining the $N \times N$ matrix $T_{pq}(R_{pq},\phi_{pq})$ which is essentially an identity matrix except for possibly four elements indexed by pp, pq, qp and qq which denote effectively a 2×2 unitary matrix. Note that $T_{pq}(R_{pq},\phi_{pq})$ represents a 2×2 beamsplitter with matrix $B(R_{pq},\phi_{pq})$ where the two input ports are p and q input ports of the $N \times N$ multiport.

For the inverse matrix of U denoted as U^{-1}, it is possible to find appropriate $T_{pq}(R_{pq},\phi_{pq})$ such that $U^{-1}\prod_{i=N-1}^{1} T_{Ni}(\omega_{Ni},\phi_{Ni})$ is another unitary matrix where the last row and column contains only zeros except on the diagonal element which

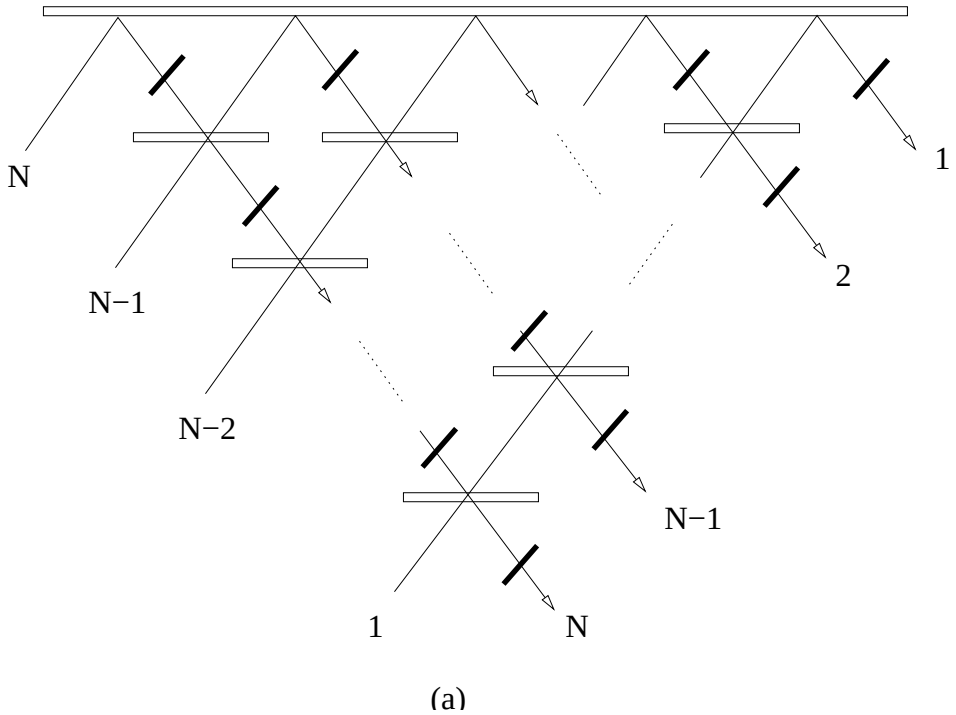

Figure 2.2: Pyramidal construction of a $N \times N$ multiport consisting of beamsplitters and phase plates

contains only a phase factor. Defining $\prod_{i=N-1}^{1} T_{Ni}(\omega_{Ni}, \phi_{Ni}) = L(N)$, we can systematically reduce U^{-1} to a diagonal matrix D^{-1} that contains only phase factors in the diagonal elements by the following operation,

$$U^{-1}L(N)L(N-1)...L(2) = D^{-1}. \tag{2.7}$$

It is clear that $U = L(N)L(N-1)...L(2)D$ can be built by a series of 2×2 beamplitters with phase shifters in each of the N output ports corresponding to the diagonal elements of D^{-1}. Indeed, the pyramidal construction shown in Fig. 2.2 corresponds precisely to such a decomposition operated in reverse. From this construction, the maximum number of 2×2 beamsplitters needed for the construction for a $N \times N$ multiport is given by $N(N-1)/2$.

Since the multiport beam splitter does not contain any elements that change the inner degrees of freedom of the incoming photons, the transition matrix U does not depend on μ. Denoting the creation operator for a single photon with parameter μ

in output port j by $b^\dagger_{j\mu}$ therefore yields

$$S\, a^\dagger_{i\mu}\, S^\dagger = \sum_j U_{ji}\, b^\dagger_{j\mu}\,. \tag{2.8}$$

Inserting this into Eq. (2.4) we can now calculate the output state of the $N \times N$ multiport given the initial state (2.3) and obtain

$$|\phi_{\rm out}\rangle \;=\; \prod_{i=1}^{N} \Big[\sum_{j=1}^{N} U_{ji} \Big(\sum_{\mu=+,-} \alpha_{i\mu}\, b^\dagger_{j\mu} \Big) \Big] |0\rangle\,. \tag{2.9}$$

This equation describes the independent redirection of all photons to their potential output ports. Conservation of the norm of the state vector is guaranteed by the unitarity of the transition matrix U. It is also important to note that any multiplication of phase factors in any of the input or output ports as well as any relabelling of the input or output ports constitutes a multiport which is essentially equivalent to the original multiport. In this sense, the original multiport is defined up to an equivalence class.

The state preparation is considered successful under the condition of the collection of one photon per output port. To calculate the final state, we apply the corresponding projector to the output state (2.9) and find that the thereby postselected N-photon state equals, up to normalisation,

$$|\phi_{\rm pro}\rangle = \sum_\sigma \Big[\prod_{i=1}^{N} U_{\sigma(i)i} \Big(\sum_{\mu=+,-} \alpha_{i\mu} b^\dagger_{\sigma(i)\mu} \Big) \Big] |0\rangle\,. \tag{2.10}$$

Here σ are the $N!$ possible permutations of the N items $\{1, 2, ..., N\}$. Note that the bosonic statistics of photons has been taken into account inherently in the formulation. A further elaboration on this is due in Chapter 3. Moreover, the norm of the state (2.10) squared, namely

$$P_{\rm suc} = \| \, |\phi_{\rm pro}\rangle \, \|^2\,, \tag{2.11}$$

is the success rate of the scheme and probability for the collection of one photon in each output j.

2.2.1 The Bell multiport beam splitter

Motivated by a great variety of applications, we are particularly interested in the generation of highly entangled photon states of a high symmetry, an example being

W-states. This suggests to consider symmetric multiports as described in 2.1.5, which redirect each incoming photon with equal probability to all potential output ports. A special example for such an $N \times N$ multiport is the Bell multiport beam splitter. Its transformation matrix

$$U_{ji} \;=\; \tfrac{1}{\sqrt{N}}\,\omega_N^{(j-1)(i-1)} \tag{2.12}$$

is also known as a discrete Fourier transform matrix and has been widely considered in the literature [Żukowski97, Törmä95, Törmä98]. Indeed, the Bell multiport is a linear optical realisation of a quantum Fourier transform. Here ω_N denotes the N-th root of unity,

$$\omega_N \equiv \exp\left(2\mathrm{i}\pi/N\right) . \tag{2.13}$$

Proceeding as in Section II.D of Ref. [Żukowski97], it can easily be verified that U is unitary as well as symmetric. Especially for $N = 2$, the transition matrix (2.12) describes a single 50:50 beam splitter.

2.3 The generation of 4-photon states

Before we discuss the N-photon case, we investigate the possibility of preparing highly entangled 4-photon states using specially prepared photons and a 4×4 Bell multiport beam splitter. For $N = 4$, the transition matrix (2.12) becomes

$$U \;=\; \tfrac{1}{2}\begin{pmatrix} 1 & 1 & 1 & 1 \\ 1 & \omega_4 & \omega_4^2 & \omega_4^3 \\ 1 & \omega_4^2 & \omega_4^4 & \omega_4^6 \\ 1 & \omega_4^3 & \omega_4^6 & \omega_4^9 \end{pmatrix} = \tfrac{1}{2}\begin{pmatrix} 1 & 1 & 1 & 1 \\ 1 & \mathrm{i} & -1 & -\mathrm{i} \\ 1 & -1 & 1 & -1 \\ 1 & -\mathrm{i} & -1 & \mathrm{i} \end{pmatrix} . \tag{2.14}$$

The following analysis illustrates the richness of the problem as well as motivating possible generalisations for the case of arbitrary photon numbers.

2.3.1 Impossible output states

Let us first look at the seemingly trivial situation, where every input port of the multiport beamspliter is entered by one photon in the same state, let us say in $|+\rangle$, so that

$$|\phi_{\mathrm{in}}\rangle = a_{1+}^\dagger a_{2+}^\dagger a_{3+}^\dagger a_{4+}^\dagger \,|0\rangle . \tag{2.15}$$

Using Eqs. (2.10) and (2.14), we then find that the collection of one photon per output port prepares the system in the postselected state

$$|\phi_{\rm pro}\rangle = \sum_{\sigma} \left[\prod_{i=1}^{4} U_{\sigma(i)i}\, b_{i+}^{\dagger} \right] |0\rangle = 0\,. \tag{2.16}$$

This means, that it is impossible to pass four photons in the same state through the considered setup with each of them leaving the multiport in a different output port. More generally speaking, the state with four photons in the same state does not contribute to the event of collecting one photon per output port. It is therefore impossible to prepare any superposition containing the states $b_{1+}^{\dagger} b_{2+}^{\dagger} b_{3+}^{\dagger} b_{4+}^{\dagger} |0\rangle$ or $b_{1-}^{\dagger} b_{2-}^{\dagger} b_{3-}^{\dagger} b_{4-}^{\dagger} |0\rangle$, respectively. The reason is destructive interference of certain photon states within the linear optics setup, which plays a crucial role for the generation of multiphoton entanglement via postselection. This effect is further studied and generalised in Chapter 3.

2.3.2 The 4-photon *W*-state

We now focus our attention on the case, where input port 1 is entered by a photon prepared in $|+\rangle$ while all other input ports are entered by a photon in $|-\rangle$, i.e.

$$|\phi_{\rm in}^{W}\rangle = a_{1+}^{\dagger} a_{2-}^{\dagger} a_{3-}^{\dagger} a_{4-}^{\dagger} |0\rangle\,. \tag{2.17}$$

Using again Eqs. (2.10) and (2.14), we find that the collection of one photon per output port corresponds to the postselected 4-photon state

$$|\phi_{\rm pro}^{W}\rangle \;=\; \sum_{j=1}^{4} U_{j1}\, b_{j+}^{\dagger} \sum_{\sigma_j} \left[\prod_{i=2}^{4} U_{\sigma_j(i)i}\, b_{\sigma_j(i)-}^{\dagger} \right] |0\rangle\,, \tag{2.18}$$

where the σ_j are the 3! permutations that map the list $\{2, 3, 4\}$ onto the list $\{1, ..., (j-1), (j+1), ..., 4\}$. If $|j_{\rm out}\rangle$ denotes the state with one photon in $|+\rangle$ in output port j and one photon in $|-\rangle$ everywhere else,

$$|j_{\rm out}\rangle \equiv b_{N-}^{\dagger} \ldots b_{(j+1)-}^{\dagger} b_{j+}^{\dagger} b_{(j-1)-}^{\dagger} \ldots b_{1-}^{\dagger} |0\rangle\,, \tag{2.19}$$

and β_j is a complex probability amplitude, then the output state (2.18) can be written as

$$|\phi^W_{\rm pro}\rangle \;=\; \sum_{j=1}^{4} \beta_j \, |j_{\rm out}\rangle \, . \tag{2.20}$$

Furthermore, we introduce the reduced transition matrices $U^{(j)}_{\rm red}$, which are obtained by deleting the first column and the j-th row of the transition matrix U. Then one can express each β_j as the permanent[2] [Horn85, Scheel04a, Minc78] of a matrix,

$$\beta_j = U_{j1} \sum_{\sigma_j} \prod_{i=2}^{4} U_{\sigma_j(i)i} = U_{j1} \, {\rm perm} \left(U^{(j){\rm T}}_{\rm red} \right) . \tag{2.21}$$

The output state (2.20) equals a W-state, if the coefficients β_j are all of the same size and differ from each other at most by a phase factor.

To show that this is indeed the case, we calculate the reduced matrices $U^{(j)}_{\rm red}$ explicitly[3] and obtain

$$\begin{aligned} U^{(1)}_{\rm red} &= \tfrac{1}{2} \begin{pmatrix} \omega_4 & \omega_4^2 & \omega_4^3 \\ \omega_4^2 & \omega_4^4 & \omega_4^6 \\ \omega_4^3 & \omega_4^6 & \omega_4^9 \end{pmatrix} , \; U^{(2)}_{\rm red} = \tfrac{1}{2} \begin{pmatrix} 1 & 1 & 1 \\ \omega_4^2 & \omega_4^4 & \omega_4^6 \\ \omega_4^3 & \omega_4^6 & \omega_4^9 \end{pmatrix} , \\ U^{(3)}_{\rm red} &= \tfrac{1}{2} \begin{pmatrix} 1 & 1 & 1 \\ \omega_4 & \omega_4^2 & \omega_4^3 \\ \omega_4^3 & \omega_4^6 & \omega_4^9 \end{pmatrix} , \; U^{(4)}_{\rm red} = \tfrac{1}{2} \begin{pmatrix} 1 & 1 & 1 \\ \omega_4 & \omega_4^2 & \omega_4^3 \\ \omega_4^2 & \omega_4^4 & \omega_4^6 \end{pmatrix} . \end{aligned} \tag{2.22}$$

The coefficients β_j differ at most by a phase factor, if the norm of the permanents of the transpose of these reduced matrices is for all j the same. To show that this is the case, we now define the vector

$$\mathbf{v} = (\omega_4, \omega_4^2, \omega_4^3) \, , \tag{2.23}$$

multiply each row of the matrix $U^{(1)}_{\rm red}$ exactly $(j-1)$ times with $\mathbf{v}$ and obtain the

[2]Note that the permanent of matrix U is ${\rm perm}(U) = \sum_\sigma \prod_{i=1}^{N} U_{i\sigma(i)}$.

[3]The reason for not simplifying these matrices is that the following equations provide the motivation for the proof of the general case in Section 2.4.

new matrices

$$\tilde{U}^{(1)}_{\rm red} = U^{(1)}_{\rm red}\,,\ \tilde{U}^{(2)}_{\rm red} = \tfrac{1}{2}\begin{pmatrix} \omega_4^2 & \omega_4^4 & \omega_4^6 \\ \omega_4^3 & \omega_4^6 & \omega_4^9 \\ 1 & 1 & 1 \end{pmatrix}\,,$$
$$\tilde{U}^{(3)}_{\rm red} = \tfrac{1}{2}\begin{pmatrix} \omega_4^3 & \omega_4^6 & \omega_4^9 \\ 1 & 1 & 1 \\ \omega_4 & \omega_4^2 & \omega_4^3 \end{pmatrix}\,,\ \tilde{U}^{(4)}_{\rm red} = U^{(4)}_{\rm red}\,. \tag{2.24}$$

The above described multiplication amounts physically to the multiplication of the photon input state with an overall phase factor and

$$\left|\,\mathrm{perm}\left(U^{(1)\mathrm{T}}_{\rm red}\right)\right| = \left|\,\mathrm{perm}\left(\tilde{U}^{(j)\mathrm{T}}_{\rm red}\right)\right|\,. \tag{2.25}$$

Moreover, using the cyclic symmetry of permanents [Horn85], we see that

$$\mathrm{perm}\left(U^{(j)\mathrm{T}}_{\rm red}\right) = \mathrm{perm}\left(\tilde{U}^{(j)\mathrm{T}}_{\rm red}\right)\,. \tag{2.26}$$

This implies together with Eq. (2.21) that the norm of the coefficients β_j is indeed the same for all j. Furthermore, using the above argument based on the multiplication of phase factors to the photon input state, one can show that

$$\beta_j = \beta_1 \left(\prod_{k=0}^{3} \omega_4^k\right)^{j-1}\,. \tag{2.27}$$

Inserting this into Eq. (2.18), we find that the postselected state with one photon per output port equals, after normalisation[4], the W-state

$$|\hat{\phi}^{W}_{\rm pro}\rangle = \tfrac{1}{2}\,[\,b^\dagger_{1+}b^\dagger_{2-}b^\dagger_{3-}b^\dagger_{4-} - b^\dagger_{1-}b^\dagger_{2+}b^\dagger_{3-}b^\dagger_{4-} + b^\dagger_{1-}b^\dagger_{2-}b^\dagger_{3+}b^\dagger_{4-} - b^\dagger_{1-}b^\dagger_{2-}b^\dagger_{3-}b^\dagger_{4+}\,]\,|0\rangle\,. \tag{2.28}$$

In analogy, we conclude that an input state with one photon in $|-\rangle$ in input port 1 and a photon in $|+\rangle$ in each of the other input ports, results in the preparation of the W-state

$$|\hat{\phi}^{W'}_{\rm pro}\rangle = \tfrac{1}{2}\,[\,b^\dagger_{1-}b^\dagger_{2+}b^\dagger_{3+}b^\dagger_{4+} - b^\dagger_{1+}b^\dagger_{2-}b^\dagger_{3+}b^\dagger_{4+} + b^\dagger_{1+}b^\dagger_{2+}b^\dagger_{3-}b^\dagger_{4+} - b^\dagger_{1+}b^\dagger_{2+}b^\dagger_{3+}b^\dagger_{4-}\,]\,|0\rangle \tag{2.29}$$

under the condition of the collection of one photon per output port. Both states,

[4] In the following we denote normalised states by marking them with the ˆ symbol.

(2.28) and (2.29), can be generated with probability

$$P_{\text{suc}} = \tfrac{1}{16}\,. \tag{2.30}$$

Transforming them into the usual form of a W-state with equal coefficients of all amplitudes [Dür00] only requires further implementation of a Pauli σ_z operation (i.e. a state dependent sign flip) on either the first and the third or the second and the fourth output photon, respectively.

Although symmetry considerations may suggest that one can obtain a W-state given the described input, it is not obvious from a rigorous point of view that this is the case. We have therefore performed explicit calculations to obtain the output state. In fact, naive application of a symmetry argument may lead to an incorrect predicted state which we will show in the next 2 subsections.

2.3.3 The 4-photon GHZ-state

Besides generating W-states, the proposed setup can also be used to prepare 4-photon GHZ-states. This requires, feeding each of the input ports 1 and 3 with one photon in $|+\rangle$ while the input ports 2 and 4 should each be entered by a photon in $|-\rangle$ such that

$$|\phi_{\text{in}}^{\text{GHZ}}\rangle = a_{1+}^{\dagger} a_{2-}^{\dagger} a_{3+}^{\dagger} a_{4-}^{\dagger}\,|0\rangle\,. \tag{2.31}$$

Calculating again the output state under the condition of collecting one photon per output port, we obtain

$$|\phi_{\text{pro}}^{\text{GHZ}}\rangle = \sum_{\sigma} U_{\sigma(1)1} U_{\sigma(2)2} U_{\sigma(3)3} U_{\sigma(4)4} b_{\sigma(1)+}^{\dagger} b_{\sigma(2)-}^{\dagger} b_{\sigma(3)+}^{\dagger} b_{\sigma(4)-}^{\dagger}\,|0\rangle\ , \tag{2.32}$$

where the σ are the 4! permutations that map the list $\{1, 2, 3, 4\}$ onto itself. On simplification, one finds that there are only two constituent states with non-zero coefficients and $|\phi_{\text{pro}}^{\text{GHZ}}\rangle$ becomes after normalisation

$$|\hat{\phi}_{\text{pro}}^{\text{GHZ}}\rangle = \tfrac{1}{\sqrt{2}}\,[\, b_{1+}^{\dagger} b_{2-}^{\dagger} b_{3+}^{\dagger} b_{4-}^{\dagger} - b_{1-}^{\dagger} b_{2+}^{\dagger} b_{3-}^{\dagger} b_{4+}^{\dagger}\,]\,|0\rangle \tag{2.33}$$

which equals the GHZ-state up to local operations. Transforming (2.33) into the usual form of the GHZ-state requires changing the state of two of the photons, for example, from $|+\rangle$ into $|-\rangle$. This can be realised by applying a Pauli σ_x operation to the first output port as well as a σ_y operation to the third output.

Finally, we remark that the probability for the creation of the GHZ-state (2.34)

is twice as high as the probability for the generation of a W-state (2.30),

$$P_{\rm suc} = \tfrac{1}{8}\,. \tag{2.34}$$

Unfortunately, the experimental setup shown in Fig. 2.1 does not allow for the preparation of GHZ-states for arbitrary photon numbers N. For a detailed description of polarisation entangled GHZ states using a different network of 50 : 50 and polarising beam splitters, see Ref. [Sagi03].

2.3.4 The 4-photon double singlet state

For completeness, we now ask for the output of the proposed state preparation scheme, given that the input state equals

$$|\phi_{\rm in}\rangle = a^\dagger_{1+}a^\dagger_{2+}a^\dagger_{3-}a^\dagger_{4-}|0\rangle\,. \tag{2.35}$$

Proceeding as above, we find that this results in the preparation of the state

$$|\phi^{\rm DS}_{\rm pro}\rangle = \sum_\sigma U_{\sigma(1)1}U_{\sigma(2)2}U_{\sigma(3)3}U_{\sigma(4)4}b^\dagger_{\sigma(1)+}b^\dagger_{\sigma(2)+}b^\dagger_{\sigma(3)-}b^\dagger_{\sigma(4)-}\,|0\rangle \tag{2.36}$$

under the condition of the collection of one photon per output port. Here the permutation operators σ are defined as in Section 2.3.3, which yields

$$\begin{aligned} |\hat{\phi}^{\rm DS}_{\rm pro}\rangle &= \tfrac{1}{2}\,[\,b^\dagger_{1+}b^\dagger_{2+}b^\dagger_{3-}b^\dagger_{4-} + b^\dagger_{1-}b^\dagger_{2-}b^\dagger_{3+}b^\dagger_{4+} - b^\dagger_{1+}b^\dagger_{2-}b^\dagger_{3-}b^\dagger_{4+} - b^\dagger_{1-}b^\dagger_{2+}b^\dagger_{3+}b^\dagger_{4-}\,]\,|0\rangle \\ &= \frac{1}{\sqrt{2}}[b^\dagger_{1+}b^\dagger_{3-} - b^\dagger_{3+}b^\dagger_{1-}] \otimes \frac{1}{\sqrt{2}}[b^\dagger_{2+}b^\dagger_{4-} - b^\dagger_{2+}b^\dagger_{4-}]|0\rangle\,. \end{aligned} \tag{2.37}$$

This state can be prepared with probability

$$P_{\rm suc} = \tfrac{1}{16}\,. \tag{2.38}$$

The state (2.37) is a double singlet state, i.e. a tensor product of two 2-photon singlet states, with a high robustness against decoherence [Eibl03, Bourennane04a]. In this 2 subsections, naive symmetry considerations may suggest a state with equal superpositions of all permutations of the given input state as the output. We have seen here clearly that this is not the case.

2.3.5 The general 4-photon case

Finally, we consider the situation where the input state is of the general form (2.3). Calculating Eq. (2.10), we find that the unnormalised output state under the condition of one photon per output port equals in this case

$$\begin{aligned} |\phi_{\rm pro}\rangle \;=\; & \tfrac{\rm i}{4}(\,\gamma_1+\gamma_2-\gamma_3-\gamma_4\,)\,|\hat{\phi}^{\rm DS}_{\rm pro}\rangle+\tfrac{1}{2\sqrt{2}}(\,\gamma_6-\gamma_5\,)\,|\hat{\phi}^{\rm GHZ}_{\rm pro}\rangle \\ & +\tfrac{1}{4}(\,\gamma_8+\gamma_{10}-\gamma_7-\gamma_9\,)\,|\hat{\phi}^{W}_{\rm pro}\rangle+\tfrac{1}{4}(\,\gamma_{12}+\gamma_{14}-\gamma_{11}-\gamma_{13}\,)\,|\hat{\phi}^{W'}_{\rm pro}\rangle \end{aligned} \tag{2.39}$$

with the coefficients

$$\begin{aligned} \gamma_1 &= \alpha_{1+}\alpha_{2+}\alpha_{3-}\alpha_{4-}\,, & \gamma_2 &= \alpha_{1-}\alpha_{2-}\alpha_{3+}\alpha_{4+}\,, \\ \gamma_3 &= \alpha_{1-}\alpha_{2+}\alpha_{3+}\alpha_{4-}\,, & \gamma_4 &= \alpha_{1+}\alpha_{2-}\alpha_{3-}\alpha_{4+}\,, \\ \gamma_5 &= \alpha_{1+}\alpha_{2-}\alpha_{3+}\alpha_{4-}\,, & \gamma_6 &= \alpha_{1-}\alpha_{2+}\alpha_{3-}\alpha_{4+}\,, \\ \gamma_7 &= \alpha_{1+}\alpha_{2-}\alpha_{3-}\alpha_{4-}\,, & \gamma_8 &= \alpha_{1-}\alpha_{2+}\alpha_{3-}\alpha_{4-}\,, \\ \gamma_9 &= \alpha_{1-}\alpha_{2-}\alpha_{3+}\alpha_{4-}\,, & \gamma_{10} &= \alpha_{1-}\alpha_{2-}\alpha_{3-}\alpha_{4+}\,, \\ \gamma_{11} &= \alpha_{1-}\alpha_{2+}\alpha_{3+}\alpha_{4+}\,, & \gamma_{12} &= \alpha_{1+}\alpha_{2-}\alpha_{3+}\alpha_{4+}\,, \\ \gamma_{13} &= \alpha_{1+}\alpha_{2+}\alpha_{3-}\alpha_{4+}\,, & \gamma_{14} &= \alpha_{1+}\alpha_{2+}\alpha_{3+}\alpha_{4-}\,. \end{aligned} \tag{2.40}$$

The form of the coefficients (2.40) reflects the full symmetry of the transformation of the input state. Each of the entangled states $|\hat{\phi}^{\rm DS}_{\rm pro}\rangle$, $|\hat{\phi}^{\rm GHZ}_{\rm pro}\rangle$, $|\hat{\phi}^{W}_{\rm pro}\rangle$ and $|\hat{\phi}^{W'}_{\rm pro}\rangle$ are generated independently from the different constituent parts of the input (2.3). Besides, Eq. (2.39) shows that the output state is constrained to be of a certain symmetry, namely the symmetry introduced by the $N\times N$ Bell multiport and the postselection criteria of finding one photon per output port.

2.4 The generation of N-photon *W*-states

Using the same arguments as in Section 2.3.2, we now show that the $N\times N$ Bell multiport beam splitter can be used for the generation of *W*-states for arbitrary photon numbers N. Like Bell states, *W*-states are highly entangled but their entanglement is more robust [Dür00]. Moreover, as N increases, *W*-states perform better than the corresponding GHZ states against noise admixture in experiments to violate local realism [Sen(De)03] and are important for optimal cloning protocols [Bužek96].

In analogy to Eq. (2.17), we assume that the initial state contains one photon in $|+\rangle$ in the first input port, while every other input port is entered by a photon

prepared in $|-\rangle$ so that

$$|\phi_{\rm in}\rangle \;=\; a_{1+}^{\dagger}\prod_{i=2}^{N} a_{i-}^{\dagger}\,|0\rangle\,. \tag{2.41}$$

Using Eq. (2.10), we find that the state of the system under the condition of the collection of one photon per output port equals

$$|\phi_{\rm pro}\rangle \;=\; \sum_{j=1}^{N} U_{j1}\,b_{j+}^{\dagger}\sum_{\sigma_j}\left[\prod_{i=2}^{N} U_{\sigma_j(i)i}\,b_{\sigma_j(i)-}^{\dagger}\right]|0\rangle\,, \tag{2.42}$$

where the σ_j are the $(N-1)!$ permutations that map the list $\{2,\,3,\,...,\,N\}$ onto the list $\{1,\,2,\,...,\,(j-1),\,(j+1),\,...,\,N\}$. As expected, the output is a superposition of all states with one photon in $|+\rangle$ and all other photons prepared in $|-\rangle$.

To prove that Eq. (2.42) describes indeed a W-state, we use again the notation introduced in Eqs. (2.19) and (2.20) and write

$$|\phi_{\rm pro}\rangle \;\equiv\; \sum_{j}\beta_j\,|j_{\rm out}\rangle\,. \tag{2.43}$$

To show that the coefficients β_j differ from β_1 at most by a phase factor, we express the amplitudes β_j as in Eq. (2.21) using the permanents of the reduced transition matrices and find

$$\beta_j = U_{j1}\sum_{\sigma_j}\prod_{i=2}^{N} U_{\sigma_j(i)i} = U_{j1}\,{\rm perm}\,\left(U_{\rm red}^{\rm T}(j)\right)\,. \tag{2.44}$$

Inserting the concrete form of the transition matrix U, this yields

$$\beta_j = \frac{1}{\sqrt{N^N}}\sum_{\sigma_j}\prod_{i=2}^{N}\omega_N^{(\sigma_j(i)-1)(i-1)}\,. \tag{2.45}$$

Proceeding as in Section 2.3.2, we now multiply β_j with the phase factor

$$v_j \equiv \left(\prod_{k=0}^{N-1}\omega_N^{k}\right)^{-(j-1)} \tag{2.46}$$

and obtain

$$\begin{aligned} v_j\,\beta_j &= \tfrac{1}{\sqrt{N^N}} \sum_{\sigma_j} \prod_{i=2}^{N} \omega_N^{(\sigma_j(i)-j)(i-1)} \\ &= \tfrac{1}{\sqrt{N^N}} \sum_{\sigma_j} \prod_{i=2}^{N} \omega_N^{\left(\mathrm{mod}_N(\sigma_j(i)-j)\right)(i-1)} \,. \end{aligned} \tag{2.47}$$

The expression $\mathrm{mod}_N(\sigma_j(i)-j)+1$ represents a set of $(N-1)!$ permutations that map $\{2,\,3,\,...,\,N\}$ onto the list $\{2,\,3,\,...,\,N\}$. It is therefore equivalent to the permutations $\sigma_1(i)$, which allows us to simplify Eq. (2.47) even further and to show that

$$v_j\,\beta_j = \tfrac{1}{\sqrt{N^N}} \sum_{\sigma_1} \prod_{i=2}^{N} \omega_N^{(\sigma_1(i)-1)(i-1)} = \beta_1\,. \tag{2.48}$$

From this and the fact that $1+2+...+(N-1) = \frac{1}{2}N(N-1)$ we finally arrive at the relation

$$\begin{aligned} \beta_j &= \left(\prod_{k=0}^{N-1} \omega_N^k\right)^{j-1} \beta_1 \\ &= \begin{cases} \beta_1\,, & \text{if } N \text{ is odd}\,, \\ (-1)^{j-1}\,\beta_1\,, & \text{if } N \text{ is even}\,. \end{cases} \end{aligned} \tag{2.49}$$

This shows that the amplitudes β_j are all of the same size and the Bell multiport can indeed generate N-photon W-states. If one wants the coefficients β_j to be exactly the same, one can remove unwanted minus signs in case of even photon numbers by applying a σ_z operation in each output port with an even number j.

The logic of the described proof exploits the symmetry of a Bell multiport and avoids calculating the coefficients of the constituent states of the output photon. Indeed, there exist no known efficient method [Scheel04a, Minc78] to calculate these coefficients in general.

In the case $N=2$, the above described state preparation scheme reduces to the familiar example, where two photons prepared in the two orthogonal states $|+\rangle$ and $|-\rangle$ pass through a 50:50 beam splitter. The collection of one photon in the each output port prepares the system in this case in the state $\frac{1}{\sqrt{2}}\,[\,b_{1+}^\dagger b_{2-}^\dagger - b_{1-}^\dagger b_{2+}^\dagger\,]\,|0\rangle$, which can be transformed into $\frac{1}{\sqrt{2}}\,[\,b_{1+}^\dagger b_{2-}^\dagger + b_{1-}^\dagger b_{2+}^\dagger\,]\,|0\rangle$ by flipping the sign of the state, i.e. depending on whether the photon is in $|+\rangle$ or $|-\rangle$, in one of the output ports.

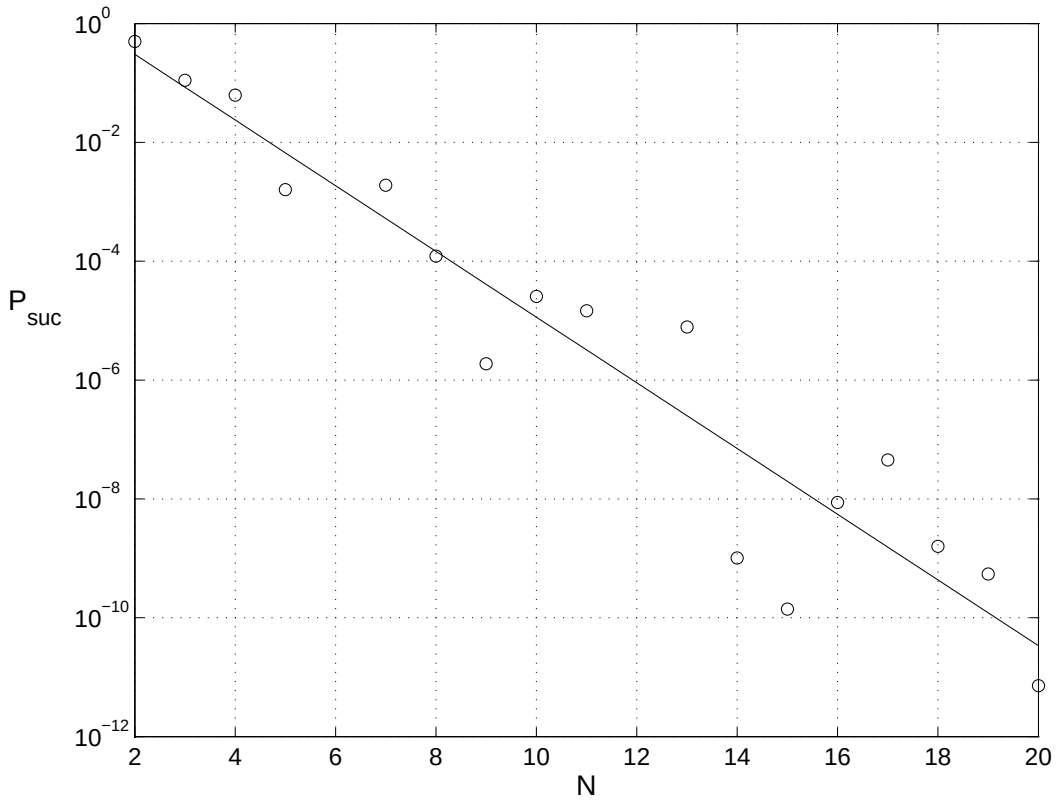

Figure 2.3: The success rate for the generation of N-photon W-states P_{suc} as a function of N. The solid line approximates the exact results via the equation $P_{\text{suc}} = \mathrm{e}^{a-bN}$ with $a = 1.35 \pm 1.32$ and $b = 1.27 \pm 0.10$

2.4.1 Success probabilities

Let us finally comment on the success rate of the proposed W-state preparation scheme. Computing the probability (2.11) can be done by finding the amplitude β_1 with the help of Eq. (2.44). Although the definition of the permanent of a matrix resembles the definition of the determinant, there exist only few theorems that can be used to simplify their calculation [Horn85, Scheel04a, Minc78]. In fact, the computation of the permanent is an NP-complete problem compared to that of a determinant which is only of complexity P. We therefore calculated P_{suc} numerically (see Fig. 2.3).

As it applies to linear optics schemes in general, the success probability decreases unfavourably as the number of qubits involved increases. Here the probability of success drops on average exponentially with N. We observe the interesting effect of a non-monotonic decreasing success probability as N increases. For example, the

probabilty of success for $N = 13$ is higher than for $N = 9$. Moreover, for $N = 6$ and $N = 12$, W-state generation is not permitted due to destructive interference. This may lead one to speculate that this is the case for all multiples of $N = 6$. Unfortunately, this does not apply to $N = 18$ and precludes an easy explanation of this effect.

2.5 Conclusions

We analysed the generation of multiphoton entanglement with the help of interference and postselection in a linear optics network consisting of an $N \times N$ Bell multiport beam splitter. Each input port should be entered by a single photon prepared in a certain state $|\lambda_i\rangle$. As long as the photons are the same with respect to all other degrees of freedom and it can be guaranteed that photons prepared in the same state overlap within their coherence time inside the linear optics network, the described scheme can be implemented using only a single photon source [Kuhn02, Mckeever04, Keller04a, Benson00, Pelton02, Kurtsiefer00, Beveratos02]. We believe that the described approach allows one to entangle much higher photon numbers than what can be achieved in parametric down conversion experiments.

In general, a highly entangled output state is obtained under the condition of the collection of one photon per output port. The motivation for this postselection criteria is that distinguishing this state from other output states does not require photon number resolving detectors, and can also accommodate lossy photon production. Ideally, the detectors should have negligible dark counts which is possible with current technology [Rosenberg05]. For simplicity of discussion, we would take this to be the assumption in the rest of the thesis. Moreover, the photons can easily be processed further and provide a resource for linear optics quantum computing and quantum cryptographic protocols.

Firstly, we analysed the case $N = 4$ and showed that the 4×4 Bell multiport allows for the creation of a variety of highly-symmetric entangled states including the W-state, the GHZ-state and double singlet states. It was found that some states are easier to prepare than others. A straightforward generalisation of the 4-photon case yields a scheme for the creation of N-photon W-states. We calculated the rates for successful state preparations and showed that they decrease in a non-monotonic fashion and on average exponentially with N.

The motivation for considering a Bell multiport beam splitter was that it only redirects the photons without affecting their inner degrees of freedom. The proposed

setup can therefore be used to produce polarisation, time-bin and frequency entanglement, respectively. To generate, for example, polarisation entangled photons, the initial photon states may differ in polarisation but should otherwise be exactly the same. The high symmetry of the Bell multiport beam splitter allows for the generation of a variety of highly entangled symmetric states. Furthermore, except for interferometric stability being required for the multiport, the scheme is highly robust to slow external and unknown phase fluctutation as this contributes to only a trivial global phase in the scheme.

The results in this chapter need not be limited only to postselected photon entanglement generation. As a foretaste, we will highlight an even more important application based on this chapter in Chapter 6. We continue our study on multiports in the next chapter with the aim of studying multiparticle interference, which is the crucial underlying mechanism in much of this thesis.

3

Generalised Hong-Ou-Mandel Effect for Bosons and Fermions

3.1 Introduction

The 2-photon Hong-Ou-Mandel (HOM) dip has been demonstrated first in 1987 [Hong87]. In their experiment, Hong, Ou and Mandel sent two identical photons through the separate input ports of a $50:50$ beam splitter. Each output port contained a photon detector. No coincidence detections within the temporal coherence length of the photons, i.e. no simultaneous clicks in both detectors, were recorded when there is no relative delay of the input photons[1]. Crucial for the observation of this effect was the indistinguishability of the pure quantum states of the input photons, which differed only in the directions of their wave vectors. This allowed the photons to interfere within the setup. The detectors could not resolve the origin of each observed photon.

Due to the nature of this experiment, the HOM dip was soon employed for quantum mechanical tests of local realism and for the generation of postselected entanglement between two photons [Shih88]. Linear optics Bell measurements on photon pairs rely intrinsically on the HOM dip [Braunstein95, Mattle96], which has also been a building block for the implementation of linear optics gates for quantum information processing with photonic qubits [Knill01b]. Shor's factorisation algorithm [Shor], for example, relies on multiple path interference to achieve massive

[1]The term "HOM dip" refers to the "dip" of the coincidence counts in both detectors under zero relative time delay of the input photons or photon detection.

parallelism [Ou99a] and multiphoton interference has to play a crucial role in any implementation of this algorithm using linear optics.

Since it requires temporal and spatial mode-matched photons, observing the HOM dip for two photons is also a good test of their indistinguishability. HOM interference has been applied to characterise recently introduced sources for the generation of single photons on demand by testing the identicalness of successively generated photons [Fattal04, Legero04, Kiraz05]. Another interesting test based on the HOM dip has been studied by Bose and Home, who showed that it can reveal whether the statistics of two identical particles passing through a 50 : 50 beam splitter is fermionic or bosonic [Bose02].

Motivated by the variety of possible applications of the 2-photon HOM dip, this chapter investigates generalised HOM experiments. We consider a straightforward generalisation of the scattering of two particles through a 50 : 50 beam splitter, namely the scattering of N particles through a symmetric $N \times N$ Bell multiport beam splitter. While numerous studies on N photon interference in the *constructive* sense, i.e. resulting in the enhancement of a certain photon detection syndrome, have been made (see e.g. Refs. [Ou99a]), not much attention has been paid to multiple path interference in the *destructive* sense. Mattle *et al.* [Mattle95] has studied both constructive and destructive detection syndromes for two photons scattering through an $N \times N$ Bell multiport. Recently, Walborn *et al.* studied so-called multimode HOM effects for photon pairs with several inner degrees of freedom, including the spatial and the polarisation degrees of freedom [Walborn03]. A notable example for destructive HOM interference has been given by Campos [Campos00], who studied certain triple coincidences in the output ports of an asymmetric 3×3 multiport beam splitter, which is also known as a tritter.

We consider *bosons* as well as the simultaneous scattering of *fermions*. The difference between both classes of particles is most elegantly summarised in the following commutation rules. While the annihilation and creation operators a_i and $a_i^\dagger$ for a boson in mode i obey the relation

$$[a_i, a_j^\dagger] \equiv a_i a_j^\dagger - a_j^\dagger a_i = \delta_{ij} \quad \text{and} \quad [a_i^\dagger, a_j^\dagger] = [a_i, a_j] = 0 \;\; \forall\, i,\, j \tag{3.1}$$

with $\delta_{ij} = 0$ for $i \neq j$ and $\delta_{ii} = 1$, the annihilation and creation operators a_i and $a_i^\dagger$ of fermionic particles obey the anticommutation relation

$$\{a_i, a_j^\dagger\} \equiv a_i a_j^\dagger + a_j^\dagger a_i = \delta_{ij} \quad \text{and} \quad \{a_i^\dagger, a_j^\dagger\} = \{a_i, a_j\} = 0 \;\; \forall\, i,\, j\,. \tag{3.2}$$

Here i and j refer to the inner degrees of freedom of the particles, like their respective path, polarisation, spin, frequency or energy.

Multiport beam splitters exist in general for a wide variety of fermionic and bosonic particles. Possible realisations of a photonic multiport have been discussed in Chapter 2. For example, multiports for bosonic or fermionic atoms can consist of a network of electrode wave guide beam splitters on an atom chip [Cassettari00]. Multiports for electrons, which behave like fermions, can be realised by fabricating a network of quantum point contacts acting as 2-electron beam splitters [Samuelsson04]. Specially doped optical fibres have recently been introduced in the literature and are expected to constitute beam splitters for "fermion-like" photons [Franson04].

As in the original HOM experiment [Hong87], we assume in the following that a particle detector is placed in each output port of the scattering beam splitter array. The incoming particles should enter the different input ports more or less simultaneously and in such a way that there is one particle per input port. Moreover, we assume that the particles are identical. We will show that it is impossible to observe a particle in each output port for even numbers N of bosons. We denote this effect of zero coincidence detection as the *generalised HOM dip*. We will also show that fermions always leave the setup separately exhibiting perfect coincidence detection. Since the interference behaviour of both types of particles is very different, the Bell multiport can be used to reveal their quantum statistics.

This chapter is organised as follows. In Section 3.2, we introduce the theoretical description of particle scattering through a symmetric Bell multiport. Section 3.3 describes the scattering of two particles through a $50:50$ beam splitter as an example. In Section 3.4, we derive the condition for the generalised HOM dip for bosons and analyse the scattering of fermions through the same setup for comparison. Finally we conclude our results in Section 3.5.

3.2 Scattering through a Bell multiport beam splitter

The description of particle scattering through a multiport is essentially the same as the previous Chapter 2. Suppose each input port i is entered by a particle with creation operator $a_i^\dagger$. Then the input state of the system equals

$$|\phi_{\text{in}}\rangle \;=\; \prod_{i=1}^{N} a_i^\dagger \,|0\rangle\,, \tag{3.3}$$

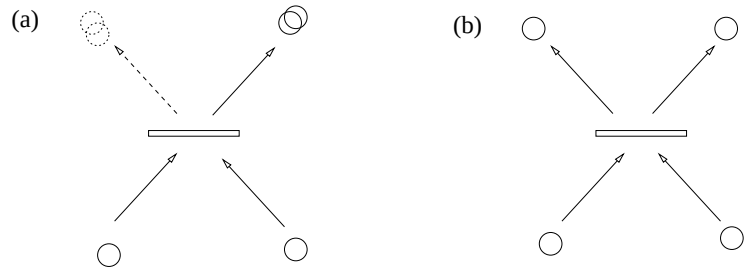

Figure 3.1: (a) HOM dip for two bosons scattering through a 50 : 50 beam splitter. (b) Perfect coincidence in the output ports for fermion scattering.

where $|0\rangle$ is the vacuum state with no particles in the setup.

If $b_j^\dagger$ denotes the creation operator for a single particle in output port j, similar to Chapter 2, we obtain for the output state of the photons given the input state (3.3),

$$|\phi_{\text{out}}\rangle \;=\; \prod_{i=1}^{N} \left(\sum_{j=1}^{N} U_{ji}\, b_j^\dagger \right) |0\rangle \,. \tag{3.4}$$

Again, U_{ji} denotes the matrix element representing the transition amplitude of the ith input port to the jth output port of the matrix U defining the multiport. Specially for a Bell multiport, U is a discrete fourier transform matrix defined in Chapter 2. Note that up to now, we have not invoked any assumptions about the nature of the particles. The formalism in this section applies to bosons and fermions equally.

3.3 HOM interference of two particles

Before analysing the general case, we motivate our discussion by considering two identical particles entering the different input ports of a 50 : 50 beam splitter. For $N = 2$, the transition matrix (2.12) becomes the Hadamard matrix[2]

$$U \;=\; \tfrac{1}{\sqrt{2}} \begin{pmatrix} 1 & 1 \\ 1 & -1 \end{pmatrix} \tag{3.5}$$

and the input state (4.6) becomes $|\phi_{\text{in}}\rangle = a_1^\dagger a_2^\dagger |0\rangle$. Note that local measurements on this input state cannot reveal any information about the bosonic or fermionic

[2]We remind the reader that the transition matrix chosen here is not unique. It represents rather an equivalence class of 50 : 50 beam splitters with can be transformed to each other via phase shifts. Our discussion on the bunching or antibunching of particles apply to this equivalence class.

nature of the two particles. However, using Eq. (3.4), we find that the beam splitter prepares the system in the state

$$|\phi_{\text{out}}\rangle = \tfrac{1}{2}\,(b_1^\dagger + b_2^\dagger)(b_1^\dagger - b_2^\dagger)\,|0\rangle = \tfrac{1}{2}\left[(b_1^\dagger)^2 - b_1^\dagger b_2^\dagger + b_2^\dagger b_1^\dagger - (b_2^\dagger)^2\right]|0\rangle\,. \tag{3.6}$$

This state no longer contains any information about the origin of the particles, since each incoming one is equally likely transferred to any of the two output ports. Passing through the setup, the input particles become indistinguishable by detection (see Fig. 3.1). Their quantum statistics can now be revealed using local measurements.

Bosons obey the commutation law (3.1). Using this, the output state (3.6) becomes

$$|\phi_{\text{out}}\rangle = \tfrac{1}{2}\left[(b_1^\dagger)^2 - (b_2^\dagger)^2\right]|0\rangle\,, \tag{3.7}$$

which implies a zero-coincidence count rate at the output ports. The particles bunch together in the same output port and exhibit the famous HOM dip (see Fig. 3.1(a)). In contrast, fermions obey the anticommutation relation (3.2) and their output state

$$|\phi_{\text{out}}\rangle = b_1^\dagger b_2^\dagger\,|0\rangle \tag{3.8}$$

implies perfect particle coincidence. This means that the fermions always arrive in separate output ports and never bunch together (see Fig. 3.1(b)). A $50:50$ beam splitter can therefore be used to distinguish bosons and fermions indeed [Bose02].

3.4 Multiparticle HOM interference

We now consider the general case of N particles passing through an $N \times N$ Bell multiport beam splitter. As in the $N = 2$ case, the setup redirects each incoming particle with equal probability to any of the possible output ports, thereby erasing the information about the origin of each particle and making them indistinguishable by detection. For even numbers of bosons, this results in the generalised HOM dip and zero coincidence detection. In contrast, fermions leave the setup always separately, thus demonstrating maximum coincidence detection. Observing this extreme behaviour can be used, for example, to verify the quantum statistics of *many* particles experimentally.

3.4.1 Bosonic particles

In order to derive the necessary condition for the appearance of the generalised HOM dip for even numbers of bosons, we calculate the output state (3.4) of the system under the condition of the collection of one particle per output port. Each term contributing to the projected conditional output state $|\phi_{\mathrm{pro}}\rangle$ can be characterised by a certain permutation, which maps the particles in the input ports 1, 2, ..., N to the output ports 1, 2, ..., N. In the following, we denote any of the $N!$ permutations by σ with $\sigma(i)$ being the i-th element of the list obtained when applying the permutation σ onto the list $\{1, 2, ..., N\}$. Using this notation, $|\phi_{\mathrm{pro}}\rangle$ equals up to normalisation

$$|\phi_{\mathrm{pro}}\rangle = \sum_{\sigma} \left[\prod_{i=1}^{N} U_{\sigma(i)i}\, b^{\dagger}_{\sigma(i)} \right] |0\rangle \,. \tag{3.9}$$

The norm of this state has been chosen such that

$$P_{\mathrm{coinc}} = \| \, |\phi_{\mathrm{pro}}\rangle \, \|^2 \tag{3.10}$$

is the probability to detect one particle per output port. It is therefore also the probability for observing coincidence counts in all N detectors as in Chapter 2.

Up to now, the nature of the particles has not yet been taken into account. Using the commutation relation (3.1) for bosons, the conditional output state (3.9) becomes

$$|\phi_{\mathrm{pro}}\rangle = \mathrm{perm}\, U \cdot \prod_{i=1}^{N} b^{\dagger}_{i} \, |0\rangle \tag{3.11}$$

with the permanent of the square matrix U defined as [Scheel04a, Horn85, Minc78]

$$\mathrm{perm}\, U \equiv \mathrm{perm}\, U^{T} \equiv \sum_{\sigma} \prod_{i=1}^{N} U_{\sigma(i)\, i} \,. \tag{3.12}$$

The permanent of a matrix is superficially similar to the determinant. However, there exist hardly any mathematical theorems that can simplify the calculation of the permanent of an arbitrary matrix.

To derive a condition for the impossibility of coincidence detections, we have to see when the probability (3.10) equals zero. Using Eq. (3.11), we find

$$P_{\mathrm{coinc}} = |\, \mathrm{perm}\, U \,|^2 \,. \tag{3.13}$$

The key to the following proof is to show that the transition matrix U of the Bell

multiport possesses a certain symmetry such that its permanent vanishes in certain cases. Suppose the matrix U is multiplied by a diagonal matrix Λ with matrix elements

$$\Lambda_{jk} \equiv \omega_N^{j-1}\,\delta_{jk}\,. \tag{3.14}$$

This generates a matrix ΛU with

$$(\Lambda U)_{ji} = \sum_{k=1}^{N} \Lambda_{jk} U_{ki} = \Lambda_{jj} U_{ji} = \tfrac{1}{\sqrt{N}}\,\omega_N^{(j-1)i}\,. \tag{3.15}$$

We now introduce the modulus function defined as $\mathrm{mod}_N(x) = j$, if $x - j$ is dividable by N and $0 \leq j < N$. Since $\omega_N^N = \omega_N^0 = 1$, the matrix elements (3.15) can be expressed as

$$(\Lambda U)_{ji} = \tfrac{1}{\sqrt{N}}\,\omega_N^{(j-1)(\mathrm{mod}_N(i)+1-1)}\,. \tag{3.16}$$

Note that the function $\tilde{\sigma}(i) = \mathrm{mod}_N(i)+1$ maps each element of the list $\{1, 2, ...N-1, N\}$ respectively to the list $\{2, 3, ...N, 1\}$. A comparison with Eq. (2.12) therefore shows that

$$(\Lambda U)_{ji} = U_{j\,\tilde{\sigma}(i)}\,. \tag{3.17}$$

In other words, the multiplication with Λ amounts to nothing more than a cyclic permutation of the columns of the matrix U. Taking the cyclic permutation symmetry of the permanent of a matrix (see definition (3.12)) into account, we obtain

$$\mathrm{perm}\,U = \mathrm{perm}\,(\Lambda U)\,. \tag{3.18}$$

However, we also have the relation

$$\mathrm{perm}\,(\Lambda U) = \mathrm{perm}\,\Lambda \cdot \mathrm{perm}\,U \tag{3.19}$$

with the permanent of the diagonal matrix Λ given by

$$\mathrm{perm}\,\Lambda = \prod_{k=1}^{N} \omega_N^{k-1} = \omega_N^{\sum_{k=1}^{N} k} = \omega_N^{N(N+1)/2} = \mathrm{e}^{\mathrm{i}\pi(N+1)} = \begin{cases} 1\,, & \text{if } N \text{ is odd}\,, \\ -1\,, & \text{if } N \text{ is even}\,. \end{cases} \tag{3.20}$$

For N being even, a comparison of Eqs. (3.18) - (3.20) reveals that

$$\mathrm{perm}\,U = -\mathrm{perm}\,U = 0\,. \tag{3.21}$$

As a consequence, Eq. (3.13) implies that $P_{\text{coinc}} = 0$. Coincidence detection in all output ports of the setup is impossible for even numbers of bosons. This is not necessarily so, if the number of particles is odd. For example, for $N = 3$ one can check that there is no HOM dip by calculating $\operatorname{perm} U$ explicitly. Campos showed that observing a HOM dip for $N = 3$ is nevertheless possible with the help of a specially designed asymmetric multiport beam splitter [Campos00].

Furthermore, even if the number of particles is even, the HOM dip does not appear to hold for all symmetric multiports. For example, it is known that all symmetric 4×4 multiport can be represented generally by the transition matrix U given in the form as [Żukowski97]

$$U = \frac{1}{2}\begin{pmatrix} 1 & 1 & 1 & 1 \\ 1 & \mathrm{e}^{\mathrm{i}\phi} & -1 & -\mathrm{e}^{\mathrm{i}\phi} \\ 1 & -1 & 1 & -1 \\ 1 & -\mathrm{e}^{\mathrm{i}\phi} & -1 & \mathrm{e}^{\mathrm{i}\phi} \end{pmatrix}, \tag{3.22}$$

where each choice of ϕ in the range between 0 and π parameterize an equivalence class. Note that the Bell multiport coincides with the choice of $\phi = \frac{\pi}{2}$. As before, one can compute the probability of coincidence detection and it is given by

$$P_{\text{coinc}} = \frac{1}{8}(1 + \cos(2\phi)) \,. \tag{3.23}$$

This suggest that by performing a HOM experiment on coincidence detection, one can characterise an unknown symmetric 4×4 multiport. This may find new application in symmetric multiports made by fiber splicing [Pryde03][3]. In the case of a Bell multiport, one recovers the HOM dip.

3.4.2 Fermionic particles

Fermions scattering through a Bell multiport show another extreme behaviour. Independent of the number N of particles involved, they always leave the setup via different output ports, thereby guaranteeing perfect coincidence detection. As expected, particles obeying the quantum statistics of fermions cannot populate the same mode.

Again, we assume that each input port is simultaneously entered by one particle and denote the creation operator of a fermion in output port i by $b_i^\dagger$. Proceeding

[3]For example, it was communicated to me by Geoff Pryde that the phase factor ϕ in Eq. (3.22) is not a parameter easily controllable in fiber splicing.

as in Section 3.4.1, one finds again that the output state of the system under the condition of the collection of one particle per output port is given by Eq. (3.9). To simplify this equation, we now introduce the sign function of a permutation with $\mathrm{sgn}(\sigma) = \pm 1$, depending on whether the permutation σ is even or odd. An even (odd) permutation is one, that can be decomposed into an even (odd) number of interchanges. Using this notation and taking the anticommutation relation for fermions (3.2) into account, we find

$$|\phi_{\mathrm{pro}}\rangle = \sum_{\sigma} \mathrm{sgn}(\sigma) \left(\prod_{i=1}^{N} U_{\sigma(i)\,i}\, b_i^{\dagger} \right) |0\rangle \,. \tag{3.24}$$

A closer look at this equation shows that the amplitude of this state relates to the determinant of the transformation matrix given by

$$\det U = \sum_{\sigma} \mathrm{sgn}(\sigma) \prod_{i=1}^{N} U_{\sigma(i)\,i} \,. \tag{3.25}$$

Since U is unitary, one has $|\det U| = 1$ and therefore also, as Eq. (3.10) shows,

$$P_{\mathrm{coinc}} = |\det U|^2 = 1 \,. \tag{3.26}$$

This means that fermions leave the system separately indeed, i.e. with one particle per output port. In the above, we only used the unitarity of the transition matrix U but not its concrete form. Perfect coincidence detection therefore applies to any situation where fermions pass through an $N \times N$ multiport, i.e. independent of its realisation.

3.5 Conclusions

We analysed a situation, where N particles enter the N different input ports of a symmetric Bell multiport beam splitter simultaneously. If these particles obey fermionic quantum statistics, they always leave the setup independently with one particle per output port. This results in perfect coincidence detection, if detectors are placed in the output ports of the setup. In contrast to this, even numbers N of bosons have been shown to never leave the setup with one particle per output port. This constitutes a generalisation of the 2-photon HOM dip to the case of arbitrary even numbers N of bosons. The generalised HOM dip is in general not observable when N is odd.

The proof exploits the cyclic symmetry of the setup. We related the coincidence detection in the output ports to the permanent or the determinant of the transition matrix U describing the multiport, depending on the bosonic or fermionic nature of the scattered particles. The NP complexity of computing the permanent compared to the determinant has been discussed in Chapter 2. Experimental setups involving the scattering of bosons through a multiport therefore have important applications in quantum information processing.

For example, part of the linear optics quantum computing scheme by Knill, Laflamme and Milburn [Knill01b] is based on photon scattering through a Bell multiport beam splitter. In contrast to this, the scattering of non-interacting fermions through the same corresponding circuit, can be efficiently simulated on a classical computer [Terhal02, Knill01a]. Moreover, the quantum statistics of particles has been used for a variety of quantum information processing tasks such as entanglement concentration [Paunkóvic02] and entanglement transfer [Omar02]. Completely new perspectives might open when using setups that can change the quantum behaviour of particles and convert, for example, photons into fermions [Franson04].

Finally, we remark that observing HOM interference of many particles is experimentally very robust. Our results can therefore also be used to verify the quantum statistics of particles experimentally as well as to characterise or align an experimental setup. Testing the predicted results does not require phase stability in the input or output ports nor detectors with maximum efficiency. The reason is that any phase factor that a particle accumulates in any of the input or output ports contributes at most to an overall phase factor of the output state $|\phi_{\text{out}}\rangle$. However, the coincidence statistics are sensitive to the phase factors accumulated inside the multiport beam splitter as they affect the form of the transition matrix U.

In the next chapter, we propose a scheme for an entanglement assisted photon manipulation. The required entangled photon ancillas can be either generated on demand (see Chapter 6) or postselectively (see Chapter 2).

4

An Efficient Quantum Filter for Multiphoton States

4.1 Introduction

Much effort has been made to find efficient schemes for the realisation of useful operations between photons contributing to quantum information processing. For example, we have discussed the process of entangling photons in Chapter 2. In this chapter, we discuss a very useful operation, namely the *parity* or *quantum filter* [Pan98b, Franson01, Hofmann02, Grudka02, Zou02b]. The application of parity filters is diverse, ranging from quantum non demolition measurements of entanglement to the generation of multiphoton quantum codes [Hofmann02] and the generation of multipartite entanglement [Zou02b]. Moreover, it has been shown that the parity filter can constitute a crucial component for the generation of cluster states for one-way quantum computing [Verstraete04, Browne05]. Furthermore, Nemoto and Munro[Nemoto04] applied the parity filter based on weak nonlinearity to achieve nearly deterministic linear optics quantum computing. Together with single qubit rotations and measurements, the parity filter constitutes a universal set of gate operations [Browne05].

Applied to two photons, the parity filter projects their state onto the 2-dimensional subspace of states where the photons have identical polarisation in the $|H\rangle$ and $|V\rangle$

basis[1]. We denote the corresponding operator as P_2 and define

$$P_2 = \sqrt{p_2}\Big(|HH\rangle\langle HH| + |VV\rangle\langle VV| \Big) , \tag{4.1}$$

where H and V describe a horizontally and a vertically polarised photon, respectively. Besides, p_2 is the success probability for the performance of the parity projection on an arbitrary input state. This means, even when applied to a parity eigenstate, the photons only pass through the filter with probability p_2. Here, the term *success probability* denotes the projection efficiency of a given setup.

In the original proposal of a linear optics implementation of the 2-photon parity filter [Hofmann02], Hofmann and Takeuchi obtained a success probability of $p_2 = \frac{1}{16}$ after passing the photons through several beam splitters and performing postselective measurements. Two other proposals yield a higher success probability of $p_2 = \frac{1}{4}$ [Grudka02, Zou02b]. Grudka and Wojcik achieve this by using the idea of teleportation [Knill01b] and by employing ancilla states containing six photons. Zou and Pahlke use a single mode quantum filter that separates the 1-photon state from the vacuum and the 2-photon state. By combining two such single mode filters, a parity filter can be realised that requires a 4-photon ancilla state as a resource [Zou02b].

In direct analogy to the 2-photon parity filter (4.1), a quantum filter for N photons can be defined by the operator

$$P_N = \sqrt{p_N}\Big(|HH\ldots H\rangle\langle HH\ldots H| + |VV\ldots V\rangle\langle VV\ldots V| \Big) . \tag{4.2}$$

Applied to an arbitrary input state with N photons, this filter projects the system with probability p_N onto the 2-dimensional subspace where all photons have the same polarisation in the $|H\rangle$ and $|V\rangle$ basis. One way to implement this gate is to pass the input state through $(N-1)$ 2-photon parity filters, which succeeds with overall probability $p_N = p_2^{N-1}$. This approach presents a steep challenge for large photon number N, given the above mentioned success probabilities of a single 2-photon parity check.

In this chapter, we describe a potential implementation of the N-photon quantum filter (4.2) with a success rate as high as $p_N = \frac{1}{2}$, which is much more effective than performing operation (4.2) with the previously proposed 2-photon parity filters. As a resource we require the presence of the N-photon GHZ-state

$$|A^{(N)}\rangle = \tfrac{1}{\sqrt{2}}\Big(|HH\ldots H\rangle + |VV\ldots V\rangle \Big) . \tag{4.3}$$

[1]This is also known as the states of even parity

In principle, this photon state can be prepared on demand [Gheri98, Lange00, Lim04]. Furthermore, we require a photon-number resolving detector that can distinguish between 0, 1 and 2 photons. To implement the quantum filter (4.2), we use ideas that have been inspired by a recently performed entanglement purification protocol [Pan03]. Indeed, the same setup can be reconfigured and interpreted as a 2-photon parity filter. It should also be emphasised, with some changes in the definition of the photon basis in our setup, our quantum filter also maps to the CNOT gate proposed by Pittman *et al.* [Pittman01] with a $\frac{1}{4}$ probability of success.

4.2 A multipartite quantum filter

The most important component of our scheme is the polarising beam splitter, which redirects a photon depending on its polarisation to one of the output modes. In the following, $|\lambda_i\rangle$ describes a photon with polarisation λ travelling in mode i. Besides, we denote the input modes $i = 1$ and 2 and the output modes $i = 1'$ and $2'$ such that a V polarised photon entering input mode 1 and an H polarised photon entering input mode 2 leave the setup through output $1'$. Suppose two photons enter the setup in different modes. Then the effect of the beam splitter can be summarised in the transformation

$$|\lambda_1\mu_2\rangle \otimes |0_{1'}0_{2'}\rangle \longrightarrow \begin{cases} |0_1 0_2\rangle \otimes |H_{1'}H_{2'}\rangle \ , & \text{if } \ \lambda = \mu = H \ , \\ |0_1 0_2\rangle \otimes |V_{1'}V_{2'}\rangle \ , & \text{if } \ \lambda = \mu = V \ , \\ |0_1 0_2\rangle \otimes |(HV)_{1'}0_{2'}\rangle \ , & \text{if } \ \lambda = V \ \text{ and } \ \mu = H \ , \\ |0_1 0_2\rangle \otimes |0_{1'}(HV)_{2'}\rangle \ , & \text{if } \ \lambda = H \ \text{ and } \ \mu = V \ . \end{cases} \tag{4.4}$$

We show now that this operation can be used to realise a filter which compares the polarisation λ of a target photon with the polarisation of an ancilla photon prepared in $|\mu_2\rangle$. With μ being either V or H, the filter operation corresponds to the projector $|\mu\rangle\langle\mu|$ and can be implemented with *unit* efficiency.

Suppose a photon number resolving detector is placed in one of the output modes, say output $2'$, and the target photon enters the system prepared in $|\lambda_1\rangle = \alpha\,|H_1\rangle + \beta\,|V_1\rangle$. Using Eq. (4.4), one can calculate the unnormalised output state after a click in the detector corresponding to polarisation μ. It is either $\alpha\,|H_{1'}\rangle$ or $\beta\,|V_{1'}\rangle$, depending on whether μ equals H or V. Note that the probability for a 1-photon detection ($|\alpha|^2$ or $|\beta|^2$, respectively) is exactly what one would expect after applying the filter operation $|\mu\rangle\langle\mu|$ with efficiency 1 to the incoming photon. Remarkably, the target photon is effectively not destroyed in the process. The reason is that it does

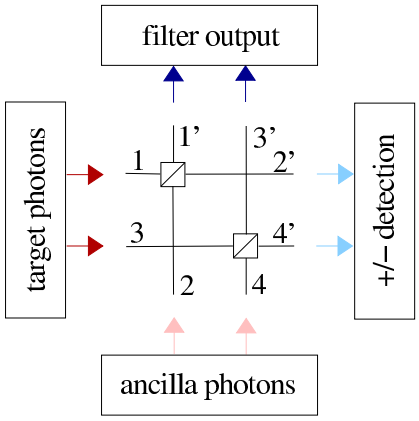

Figure 4.1: Experimental setup for the realisation of a 2-photon parity filter. The target photons enter the setup via the input modes 1 and 3, while the ancilla photons enter the setup via inputs 2 and 4. Within the setup, each photon has to pass one polarising beam splitter. Under the condition of the detection of one photon in each of the outputs $2'$ and $4'$, the filter succeeded and the projected output state leaves the system via the modes $1'$ and $3'$.

not matter whether the detector absorbs the target photon or the ancilla photon, if both have the same polarisation and are anyway indistinguishable.

4.2.1 The 2-photon case

Let us now describe how the polarising beam splitter (4.4) can be used for the implementation of a 2-photon parity filter. The setup we consider here contains two polarising beam splitters and two polarisation sensitive detectors (see Fig. 4.1). The target state enters the setup via the input modes 1 and 3. We further require the presence of the 2-photon ancilla state $|A^{(2)}\rangle$, which is a 2-photon Bell state. The ancilla photons should enter the setup via the input modes 2 and 4. The two detectors are placed in the output modes $2'$ and $4'$. If they both receive a photon each, the filter operation is deemed a success. Output modes $1'$ and $3'$ are designated the filter output.

In the following, we consider the general input pure state

$$|\psi_{\text{in}}^{(2)}\rangle = \alpha\,|H_1H_3\rangle + \beta\,|V_1V_3\rangle + \gamma\,|H_1V_3\rangle + \delta\,|V_1H_3\rangle\ . \tag{4.5}$$

Our aim is to eliminate the components, where the photons are of different polarisation. Together with the ancilla state $|A^{(2)}\rangle$, the setup in Fig. 4.1 is entered by the

4-photon state

$$\begin{aligned}|\tilde{\psi}^{(2)}_{\text{in}}\rangle &= |\psi^{(2)}_{\text{in}}\rangle \otimes |A^{(2)}\rangle \\ &= \tfrac{1}{\sqrt{2}}\Big(\alpha\,|H_1H_2H_3H_4\rangle + \alpha\,|H_1V_2H_3V_4\rangle + \beta\,|V_1V_2V_3V_4\rangle + \beta\,|V_1H_2V_3H_4\rangle \\ &\quad +\gamma\,|H_1H_2V_3H_4\rangle + \gamma\,|H_1V_2V_3V_4\rangle + \delta\,|V_1V_2H_3V_4\rangle + \delta\,|V_1H_2H_3H_4\rangle\Big)\,.\end{aligned} \tag{4.6}$$

We now show that the system can act like a parity filter, if one photon is collected in output mode $2'$ and another one is collected in output mode $4'$. Using Eq. (4.4), one can show that the 4-photon states (4.6) becomes in this case, the unnormalised state

$$|\tilde{\psi}^{(2)}_{\text{out}}\rangle = \tfrac{1}{\sqrt{2}}\Big(\alpha\,|H_{1'}H_{2'}H_{3'}H_{4'}\rangle + \beta\,|V_{1'}V_{2'}V_{3'}V_{4'}\rangle\Big)\,. \tag{4.7}$$

We further assume that the detectors measure the polarisation of the incoming photons in the rotated basis defined by the 1-photon states

$$|\pm\rangle \equiv \tfrac{1}{\sqrt{2}}\Big(|H\rangle \pm |V\rangle\Big)\,. \tag{4.8}$$

It is important that the detectors distinguish the polarisation of each incoming photon in this basis (opposed to just absorbing the photon), since this approach guarantees that the output becomes the expected pure state. Using the definition (4.8), we can rewrite the state (4.7) as

$$\begin{aligned}|\tilde{\psi}^{(2)}_{\text{out}}\rangle &= \tfrac{1}{2}\Big(\alpha\,|H_{1'}H_{3'}\rangle + \beta\,|V_{1'}V_{3'}\rangle\Big)\otimes\tfrac{1}{\sqrt{2}}\Big(|+_{2'}+_{4'}\rangle + |-_{2'}-_{4'}\rangle\Big) \\ &\quad +\tfrac{1}{2}\Big(\alpha\,|H_{1'}H_{3'}\rangle - \beta\,|V_{1'}V_{3'}\rangle\Big)\otimes\tfrac{1}{\sqrt{2}}\Big(|+_{2'}-_{4'}\rangle + |-_{2'}+_{4'}\rangle\Big)\,.\end{aligned} \tag{4.9}$$

Suppose the photons in output ports $2'$ and $4'$ are absorbed in the measurement process. Then the output state of the system equals in case of a single click in each of the detectors

$$|\psi^{(2)}_{\text{out}}\rangle = \tfrac{1}{2}\Big(\alpha\,|H_{1'}H_{3'}\rangle \pm \beta\,|V_{1'}V_{3'}\rangle\Big)\,. \tag{4.10}$$

The "+" sign applies when both detectors measure the same polarisation (which happens with probability $\frac{1}{2}$); the "−" sign applies when both detectors measure different polarisations (which also happens with probability $\frac{1}{2}$). More generally, every measurement of the state $|-\rangle$ yields a phase flip error on the output state. Therefore, measuring even numbers of $|-\rangle$(or in this case, the same polarisations) yield no phase flip error or identity operation on the output state. The implementation of the parity filter only needs a correction of this phase flip error in the event of

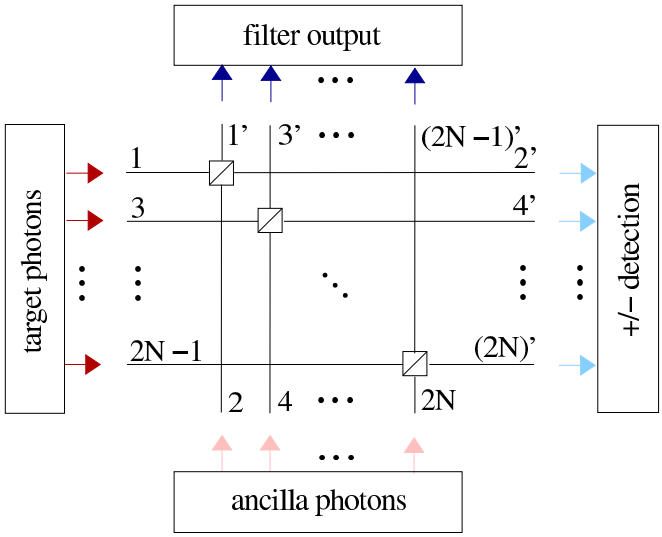

Figure 4.2: Experimental setup for the realisation of the N-photon quantum filter (4.2). The N polarising beam splitters each compare the state of one of the target photons with the state of one of the ancilla photons, which are initially prepared in the GHZ state $|A^{(N)}\rangle$. Besides, N detectors perform photon measurements in the polarisation basis (4.8). The output photons leave the system via the odd numbered output ports.

measuring odd numbers of $|-\rangle$ (in this case, different polarisations) which can be implemented with the help of a Pauli σ_z operation on any of the output photons. In any case, the 4-photon state (4.6) can be reduced by measurement in the $|\pm\rangle$ with appropriate σ_z correction to the following 2-photon state,

$$|\psi^{(2)}_{\text{out}}\rangle = \tfrac{1}{\sqrt{2}}\Big(\,\alpha\,|H_{1'}H_{3'}\rangle + \beta\,|V_{1'}V_{3'}\rangle\,\Big)\;, \tag{4.11}$$

with unit efficiency. We have taken into account all appropriate measurement syndromes which explains the normalisation. A closer look at the normalisation of this state tells us that the parity filter shown in Fig. 4.1 works with efficiency $p_2 = \frac{1}{2}$. If the success probability of the scheme would be 1, the output state (4.11) would be $\alpha\,|H_{1'}H_{3'}\rangle + \beta\,|V_{1'}V_{3'}\rangle$. It can be shown that the filter can also be operated with mixed states as inputs.

4.2.2 The N-photon case

The generalisation of the above described 2-photon parity filter to the N-photon quantum filter (4.2) is straightforward and requires N polarising beam splitters and N polarisation sensitive detectors (see Fig. 4.2). One side of the setup is entered

by the N-photon input state $|\psi_{\text{in}}^{(N)}\rangle$ with one photon in each odd-numbered input mode, while the other side is entered by an N-photon ancilla state $|A^{(N)}\rangle$ with one photon in each even numbered input mode. In the following we denote the modes containing the detectors by $2'$, $4'$, ..., $(2N)'$, while the modes $1'$, $3'$, ..., $(2N-1)'$ contain the output state.

Again, the successful operation of the quantum filter is indicated by a single click in each of the detectors. Suppose α denotes the amplitude of the state $|H_1 H_3 \dots H_{2N-1}\rangle$ while β is the amplitude of the state $|V_1 V_3 \dots V_{2N-1}\rangle$ with respect to the target state $|\psi_{\text{in}}^{(N)}\rangle$. Then we find, using Eq. (4.4) and in analogy to Eq. (4.7), that the collection of one photon in each of the detector output ports transforms the total input state $|\tilde{\psi}_{\text{in}}^{(N)}\rangle = |\psi_{\text{in}}^{(N)}\rangle \otimes |A^{(N)}\rangle$ into

$$|\tilde{\psi}_{\text{out}}^{(N)}\rangle = \tfrac{1}{\sqrt{2}} \left(\alpha \, |H_{1'} H_{2'} \dots H_{(2N)'}\rangle + \beta \, |V_{1'} V_{2'} \dots V_{(2N)'}\rangle \right) . \tag{4.12}$$

For the same reason as in the 2-photon case, we assume that the detectors measure the polarisation of the incoming photons in the polarisation basis (4.8) by absorption. Suppose J is the number of photons found in the $|-\rangle$ state, then one can show using Eq. (4.12) and proceeding as in Section 4.2.1 that the output state of the remaining N photons equals

$$|\psi_{\text{out}}^{(N)}\rangle = \tfrac{1}{2} \left(\alpha \, |H_{1'} H_{3'} \dots H_{(2N-1)'}\rangle + (-1)^J \beta \, |V_{1'} V_{3'} \dots V_{(2N-1)'}\rangle \right) . \tag{4.13}$$

Note that the probability of J being an odd number, which incurs a phase flip error on the output state in analogy to the 2-photon filter, is $\frac{1}{2}$. As before, we can transform with unit efficiency the state (4.12) with the help of a phase flip correction to the final state given by

$$|\psi_{\text{out}}^{(N)}\rangle = \tfrac{1}{\sqrt{2}} \left(\alpha \, |H_{1'} H_{3'} \dots H_{(2N-1)'}\rangle + \beta \, |V_{1'} V_{3'} \dots V_{(2N-1)'}\rangle \right) . \tag{4.14}$$

This is exactly the output state that one expects after the application of the quantum filter (4.2) to the input state $|\psi_{\text{in}}^{(N)}\rangle$ with success probability $p_N = \frac{1}{2}$, which is the highest that has been predicted so far without the use of universal two-qubit quantum gate operation such as the CNOT or CZ gates[2]. Naively, one might expect

[2] Alternatively, a straightforward way of implementing the quantum filter (4.2) is to replace each polarising beam splitter in the setup (see Fig. 4.2) by a CNOT gate(which is difficult to realise with linear optics alone). Furthermore, the detectors in all even numbered output modes should perform a polarisation sensitive measurement in the H/V basis. The projection efficiency of such a scheme would only be limited by the success probability p of a single controlled-NOT operation and would scale like p^N. For sufficiently large photon numbers N, this might decrease below $\frac{1}{2}$.

that the efficiency of the filter decreases with the number of photons in the setup. However, this is not the case here. Furthermore, we remark that the described quantum filter also works for mixed N-photon input states.

Taking into account real detector efficiencies and dark count rates will diminish both the success probability and fidelity of the above described filter. In general, the success probability and fidelity depend on the nature of the input state as well as the ancilla. Here, we focus on a simple example of analysing the error probability of a 2-photon parity filter by assuming imperfect photon detectors but perfect ancilla state. It is shown in [Saavedra00] that the ancilla states considered here can be prepared with high fidelity and success probability. As in [Hofmann02], we assume that the dark count rate can be reduced by time gating and consider the effect of detector inefficiencies causing an error due to a mistake of registering a 2-photon detection event as a single photon event. This is known as preselective error. If we also postselect the output state, then such an error can in principle be eliminated. Without loss of generality, we analyse the case where the detectors each register a click for an alleged photon in the state $|+\rangle$. This can be represented by a POVM(Positive operator valued measure) element $E_{i'}$ given by [Lee04]

$$E_{i'} = p_d|+_{i'}\rangle\langle+_{i'}| + 2p_d(1-p_d)|(++)_{i'}\rangle\langle(++)_{i'}|\,, \tag{4.15}$$

where p_d is the single photon detection efficiency. From Kok and Braunstein [Kok01, Barnett98], we know that the reduced projected state is $\rho_{1'3'} = \frac{\mathrm{Tr}_{2'4'}(E_{2'}E_{4'}\rho_{1'2'3'4'})}{\mathrm{Tr}_{1'3'}(\cdot)}$ where $\rho_{1'2'3'4'}$ is the state after passing $|\tilde{\psi}^{(2)}_{\mathrm{in}}\rangle$ through the 2 polarising beam splitters. We also fix $|\alpha|^2 = |\beta|^2 = |\gamma|^2 = |\delta|^2 = \frac{1}{4}$ to compute for the most typical input state to obtain the average fidelity. One can show that the fidelity[3] of the quantum filter is given by $F = \langle\psi^{(2)}_{\mathrm{out}}|\rho_{1'3'}|\psi^{(2)}_{\mathrm{out}}\rangle / \langle\psi^{(2)}_{\mathrm{out}}|\psi^{(2)}_{\mathrm{out}}\rangle = (5 - 6p_d + 2p_d^2)^{-1}$. For example, given a p_d of 0.88 ([Takeuchi99, Rosenberg05]), the maximum error rate $1 - F$ would be 0.19 in the light of current technology. Especially for the recent work by Rosenberg *et al.* [Rosenberg05], superconducting transition-edge sensors are expected to have photon-number resolution with negligible dark counts at arbitrary high efficiency in the future.

Therefore the use of polarising beam splitters, which can operate with a very high fidelity, should be favoured [Pan03].

[3]This is analogous to the true QND or preselective fidelity discussed in Ref [Kok05b]. Clearly, if we define our fidelity based on coincidence counting, where a photon is detected in all outputs 1', 2' 3' 4', the postselective fidelity can be much higher.

4.3 Conclusions

We described the realisation of a 2-photon parity filter that requires only two polarising beam splitters, two photons prepared in a maximally entangled Bell state and two polarisation sensitive detectors. The success rate of the scheme $p_2 = \frac{1}{2}$ is the highest that has been predicted so far without the help of universal two-qubit quantum gate operations and is reached here due to employing an entangled ancilla state as a resource. A generalisation of the proposed scheme to the N-photon case is straightforward. We showed that the quantum filter (4.2) can be implemented with the help of N polarising beam splitters and an N-photon GHZ state as a resource. Remarkably, the success rate of the filter remains $\frac{1}{2}$, irregardless of the size of the input state.

To implement the quantum filter (4.2), the N polarising beam splitters compare the state of the incoming photons pairwise with the state of the ancilla photons. In Section 4.2, we showed that a single polarising beam splitter can be used to realise a filter, which measures polarisation H or V, respectively, with unit efficiency. Preparing the ancilla photons, for example, in the state $|HH\ldots H\rangle$, would result in a filter that measures whether all target photons are prepared in $|H\rangle$. However, since we compare the input state with a GHZ state, which contains two terms, namely $|HH\ldots H\rangle$ and $|VV\ldots V\rangle$, the probability of the described filter is only as high as $\frac{1}{2}$. Indeed, the highly entangled N-photon GHZ state acts as a "mask" for the filter.

A straightforward extension of the ideas of this chapter is to consider a different form of the "mask" or ancilla state $|A^{CZ}\rangle$ given by $\frac{1}{2}(|H_2H_4\rangle + |H_2V_4\rangle + |V_2H_4\rangle - |V_2V_4\rangle)$. Under the condition that the photons pass the filter, heralded by single photon detection in both output detectors in $|\pm\rangle$, the output state, with correction of sign errors, would instead be given by

$$|\psi_{\text{out}}^{(CZ)}\rangle = \frac{1}{2}(\alpha|H_{1'}H_{3'}\rangle + \beta|V_{1'}V_{3'}\rangle + \gamma|H_{1'}V_{3'}\rangle - \delta|V_{1'}H_{3'}\rangle)\,. \tag{4.16}$$

This is the same as the application of a CZ filter or gate P_{CZ}

$$P_{CZ} = \frac{1}{2}(|H_{1'}H_{3'}\rangle\langle H_1H_3| - |V_{1'}V_{3'}\rangle\langle V_1V_3| + |H_{1'}V_{3'}\rangle\langle H_1V_3| + |V_{1'}H_{3'}\rangle\langle V_1H_3|) \tag{4.17}$$

with efficiency $\frac{1}{4}$ to the input state (4.5). This is analogous to the CNOT gate proposed by Pittman *et al.* [Pittman01] with success probability $\frac{1}{4}$.

We have seen an example of how quantum computing with photons assisted with entangled ancillas can result in a more efficient implementation. However, the

scheme is still necessarily probabilistic as are all known linear optics based schemes where the input state is not already necessarily encoded offline. We move to the next chapter where we add just one more ingredient, a special single photon source with encoding ability, and show how quantum computing with linear optics can become effectively deterministic.

5

Distributed Quantum Computing with Distant Single Photon Sources

5.1 Introduction

Practical implementations of quantum computing to solve non-trivial problems require a scalable architecture, i.e. the ability to process, address and store many qubits. This is particularly challenging if all the interactions between qubits are controlled locally and coherently. Particular advances in this aspect have been made in ion traps [Kielpinsksi02] and atoms trapped in optical lattices [Jaksch99]. Even with optical lattices, with the inherent capability to store many qubits, controlled addressibility and manipulation of individual qubits still remains an experimental challenge despite advances to alleviate these requirements [You00, Kay04, Calarco04] through the help of marker atoms. In ion traps, while addressibility is not an issue, interaction between distant qubits still requires some form of ion transport to the range where coherent interaction is possible between two ions [Duan04a, Kielpinsksi02].

An attractive alternative approach is the concept of distributed quantum computing [Eisert00, Grover96, Cirac99]. This consists of a network of nodes with each node processing and storing a small number of qubits, which is comparatively easy to realise. The qubits in each node are stationary qubits, i.e. qubits that are not transported, with long decoherence times and serve as a quantum memory. The stationary qubits in each node communicate with distant nodes through the means of flying qubits, i.e. qubits that are transported. Distributed quantum computing can lead to a more efficient implementation of the phase estimation problem com-

pared to a classical computer in the presence of decoherence [Grover96, Cirac99]. Furthermore, distributed quantum computing allows distant users to share quantum resources.

Traditionally, the stationary qubit of a certain node maps its state to a flying qubit which leaves the node. On the arrival at the target node, the flying qubit maps its state to a stationary qubit in the target node. It is thus assumed that interconvertability of stationary and flying qubits are required. Schemes related to this have been proposed based on atom-cavity as stationary qubits and photons as flying qubits [Enk97, Cirac97, Sørensen98, Xiao04, Cho04, Zhou05, Duan05]. All these schemes involve single photon sources with direct transmisions of photons through cavities. In all these cases, such transmissions occur one or several times to complete the gate operation protocol. Another scheme by Mancini *et al.* involves engineering a direct interaction between 2 distant coupled cavities via fibers [Mancini04]. All these schemes demand a high level of precision and might pose a great experimental challenge [Browne03] if one requires a high success probability.

In contrast to this, we avoid all these challenges by not requiring any form of photon transmission through cavities. Note that we do not really require the interconversion of stationary qubits and flying qubits for quantum computation in a network. The unidirectional encoding of stationary to flying qubits is already sufficient for distributed quantum computation. Schemes along these lines [Protsenko02, Schlosser03, Zou05, Barrett05] have already been proposed[1]. To implement a two-qubit universal gate between two distant stationary qubits, the basic idea is to redundantly encode the pair of stationary qubits to a pair of flying qubits. Following that, a maximally entangling or Bell measurement, which is normally accomplished with linear optics, is performed on the pair of flying qubits. A universal two-qubit gate is accomplished between the stationary qubits if the entangling measurement is successful. Another related scheme based on trapped ions has been proposed [Duan04b] which uses ancilla ions in which they have to be pre-entangled.

In this chapter, we will demonstrate that scalable quantum computing between distant stationary qubits, where the stationary qubits are single photon sources which generate the photons naturally as flying qubits, can be made deterministic even if the entangling measurement does not succeed.[2] We *do not* require any ancilla

[1] Very recently, after this work has been submitted for publication in August 2004, Benjamin *et al.* [Benjamin05] reported a scheme on creating graph states by optical excitation in stationary qubits. They also obtain the insurance scenario reported in this chapter with a 4×4 multiport at the cost of having two distant stationary qubits encoding a qubit. Furthermore, interferometric stability is not inherent in their scheme.

[2] We remind the reader here that a never-failing complete Bell measurement on two photons is

stationary qubits nor any photon transmission through cavities to achieve this. The ability to encode the state of the atom unto the photon is all that is required. We use linear optics to perform the Bell measurements on the photon. Generally, the measurement basis we choose does not yield any information about the stationary qubits and therefore cannot destroy the qubits in any case. As above, for a successful Bell measurement, a two-qubit gate is accomplished. If not, the state of the stationary qubit is not destroyed and this allows us to repeat the encoding and subsequent measurement until it succeeds. We have shown that this can be done by carefully choosing the measurement basis in the entangling measurement with linear optics. A related idea to protect a photon state against gate failure has been proposed in the past by Knill *et al.* [Knill01b] in the context of photon gate implementation by a two-qubit quantum code in their teleportation-based gate. Such ideas are closely related to quantum error correction [Shor95, Calderbank96, Steane96]. We however use a form of redundant encoding natural to diverse kinds of single photon sources and show that distributed quantum computation between stationary qubits can require similar experimental resources as linear optics computation, i.e. single photon sources, optical elements and photon detectors. At the same time, it can be performed much more efficiently[3] as compared to conventional linear optics computation [Knill01b].

The single photon sources that we use can take the form of atom-cavity systems [Law97, Kuhn99], quantum dots, diamond NV colour centers or even atomic ensembles [Matsukevich04]. In principle, any photon source that allows redundant encoding of the state of the source to the photon it generates is a viable candidate for our scheme.

Having generated the photons, the photons must subsequently travel to the linear optics apparatus that performs the entangling or partial Bell measurement. Finally, the partial Bell measurements on the encoded photons are performed and based on measurement results, we either halt the scheme upon a heralded success or repeat the scheme until success.

This chapter is organised as follows. The next section details the general principle of a remote two-qubit gate implementation with our scheme. We also show how teleportation with insurance can be accomplished with minimal change to the setup. Following that, in Section 5.3 and 5.4 we describe the two ingredients of the scheme, photon encoding and measurements. Finally, we conclude in the last section with a short discussion on possible applications to cluster state buildup for

not possible with linear optics [Lütkenhaus99].

[3]We require no prepared ancillas nor any photon storage and feedforward operations.

robust computing.

5.2 Basic Idea of a remote two-qubit phase gate

One of the requirements for universal quantum computing is the ability to perform a universal two-qubit gate operation, like a controlled phase gate. Here we describe the general concept for the implementation of such an entangling two-qubit phase gate between two distant single photon sources. Note that our method of distributed quantum computing only allows the realisation of non-local phase gates, since the measurement on a photon pair can imprint a phase on the state of the corresponding sources but cannot change the distribution of their populations. This is however sufficient for universal quantum computation. The first step for the implementation of a two-qubit gate is the generation of a photon within each respective source, which encodes the information of the stationary qubit.

5.2.1 Encoding

Let us denote the states of the photon sources, which encode the logical qubits $|0\rangle_{\mathrm{L}}$ and $|1\rangle_{\mathrm{L}}$ as $|0\rangle$ and $|1\rangle$, respectively. For example, for atom-like single photon sources, the stable ground states can be chosen as the logical qubits. An arbitrary pure state of two stationary qubits can be written as

$$|\psi_{\mathrm{in}}\rangle = \alpha\,|00\rangle + \beta\,|01\rangle + \gamma\,|10\rangle + \delta\,|11\rangle\,, \tag{5.1}$$

where α, β, γ and δ are the corresponding complex coefficients with $|\alpha|^2 + |\beta|^2 + |\gamma|^2 + |\delta|^2 = 1$. Suppose a photon is now generated in each of the two sources, whose state (i.e. polarisation, frequency or generation time) depends on the state of the source. As we see below, it is helpful to assume that the encoding is for both sources different. In the following, we assume that source 1 prepared in $|i\rangle$ leads to the creation of one photon in state $|\mathsf{x}_i\rangle$, while source 2 prepared in $|i\rangle$ leads to the creation of one photon in state $|\mathsf{y}_i\rangle$, such that

$$|i\rangle_1 \rightarrow |i;\mathsf{x}_i\rangle_1\,, \quad |i\rangle_2 \rightarrow |i;\mathsf{y}_i\rangle_2\,. \tag{5.2}$$

The simultaneous creation of a photon in both sources then transfers the initial state (5.1) into

$$|\psi_{\mathrm{enc}}\rangle = \alpha\,|00;\mathsf{x}_0\mathsf{y}_0\rangle + \beta\,|01;\mathsf{x}_0\mathsf{y}_1\rangle + \gamma\,|10;\mathsf{x}_1\mathsf{y}_0\rangle + \delta\,|11;\mathsf{x}_1\mathsf{y}_1\rangle\,. \tag{5.3}$$

The way this encoding step can be realised experimentally using either emission time or polarisation degrees of freedom to encode the stationary qubits is discussed in Section 5.3.

5.2.2 Mutually Unbiased Basis

Once the photons have been created, an entangling phase gate can be implemented by performing an absorbing measurement on the photon pair. Therefore, it is important to choose the photon measurement such that none of the possible outcomes reveals any information about the coefficients α, β, γ and δ. That such measurements exists is well known [Wootters89]. The corresponding measurement basis forms a so-called *mutually unbiased basis* (MUB) with respect to the computational basis. Here we are interested in photon pair measurements in a MUB[4] given the computational basis $\{|\mathsf{x}_0\mathsf{y}_0\rangle, |\mathsf{x}_0\mathsf{y}_1\rangle, |\mathsf{x}_1\mathsf{y}_0\rangle, |\mathsf{x}_1\mathsf{y}_1\rangle\}$.

More concretely, the potential outcomes of the photon measurement should all be of the form

$$|\Phi\rangle = \tfrac{1}{2}[|\mathsf{x}_0\mathsf{y}_0\rangle + \mathrm{e}^{\mathrm{i}\varphi_1}\,|\mathsf{x}_0\mathsf{y}_1\rangle + \mathrm{e}^{\mathrm{i}\varphi_2}\,|\mathsf{x}_1\mathsf{y}_0\rangle + \mathrm{e}^{\mathrm{i}\varphi_3}\,|\mathsf{x}_1\mathsf{y}_1\rangle]\,. \tag{5.4}$$

Indeed, this is possible with linear optics as we will show in this thesis. Detecting this state and absorbing the two photons in the process transfers the encoded state (5.3) into

$$|\psi_{\mathrm{out}}\rangle = \alpha\,|00\rangle + \mathrm{e}^{-\mathrm{i}\varphi_1}\,\beta\,|01\rangle + \mathrm{e}^{-\mathrm{i}\varphi_2}\,\gamma\,|10\rangle + \mathrm{e}^{-\mathrm{i}\varphi_3}\,\delta\,|11\rangle\,, \tag{5.5}$$

and therefore does not reveal any information about the input state (5.1) indeed. It is thus equivalent to a phase gate implementation on the stationary qubit.

Here we are especially interested in the implementation of an entangling phase gate with maximum entangling power. This requires detecting the photons in one of the four Bell states. If

$$\varphi_3 = \varphi_1 + \varphi_2\,, \tag{5.6}$$

the state $|\Phi\rangle$ is a product state and the output (5.5) differs from the initial state (5.1) only by local operations. However, the state (5.4) becomes a maximally entangled one if and only if

$$\varphi_3 = \varphi_1 + \varphi_2 \pm (2n-1)\pi\,. \tag{5.7}$$

.

[4]In this chapter, our MUB basis is always defined with respect to the computational basis.

5.2.3 A deterministic entangling gate

Let us denote the states of the measurement basis, i.e. the mutually unbiased basis, in the following by $\{|\Phi_i\rangle\}$. In order to find a complete Bell basis with all states of the form (5.4), we introduce the following notation,

$$\begin{aligned} |\Phi_1\rangle &\equiv \tfrac{1}{\sqrt{2}}[|\mathsf{a}_1\mathsf{b}_1\rangle + |\mathsf{a}_2\mathsf{b}_2\rangle] \;,\; |\Phi_2\rangle \equiv \tfrac{1}{\sqrt{2}}[|\mathsf{a}_1\mathsf{b}_1\rangle - |\mathsf{a}_2\mathsf{b}_2\rangle]\,, \\ |\Phi_3\rangle &\equiv \tfrac{1}{\sqrt{2}}[|\mathsf{a}_1\mathsf{b}_2\rangle + |\mathsf{a}_2\mathsf{b}_1\rangle] \;,\; |\Phi_4\rangle \equiv \tfrac{1}{\sqrt{2}}[|\mathsf{a}_1\mathsf{b}_2\rangle - |\mathsf{a}_2\mathsf{b}_1\rangle]\,, \end{aligned} \tag{5.8}$$

where the states $|\mathsf{a}_i\rangle$ describe photon 1 and the states $|\mathsf{b}_i\rangle$ describe photon 2 and $\langle\mathsf{a}_1|\mathsf{a}_2\rangle = 0$ and $\langle\mathsf{b}_1|\mathsf{b}_2\rangle = 0$. One can then write the photon states on the right hand side of Eq. (5.8) without loss of generality as

$$\begin{aligned} |\mathsf{a}_1\rangle &= \cos\theta_1\,|\mathsf{x}_0\rangle + \mathrm{e}^{\mathrm{i}\vartheta_1}\sin\theta_1\,|\mathsf{x}_1\rangle \;,\; |\mathsf{a}_2\rangle = \mathrm{e}^{-\mathrm{i}\xi_1}(\mathrm{e}^{-\mathrm{i}\vartheta_1}\sin\theta_1\,|\mathsf{x}_0\rangle - \cos\theta_1\,|\mathsf{x}_1\rangle) \\ |\mathsf{b}_1\rangle &= \cos\theta_2\,|\mathsf{y}_0\rangle + \mathrm{e}^{\mathrm{i}\vartheta_2}\sin\theta_2\,|\mathsf{y}_1\rangle \;,\; |\mathsf{b}_2\rangle = \mathrm{e}^{-\mathrm{i}\xi_2}(\mathrm{e}^{-\mathrm{i}\vartheta_2}\sin\theta_2\,|\mathsf{y}_0\rangle - \cos\theta_2\,|\mathsf{y}_1\rangle)\,. \end{aligned} \tag{5.9}$$

Inserting this into Eq. (5.8), we find

$$\begin{aligned} |\Phi_1\rangle &= \tfrac{1}{\sqrt{2}}[(\cos\theta_1\cos\theta_2 + \mathrm{e}^{-\mathrm{i}(\vartheta_1+\vartheta_2)}\mathrm{e}^{-\mathrm{i}(\xi_1+\xi_2)}\sin\theta_1\sin\theta_2)|\mathsf{x}_0\mathsf{y}_0\rangle \\ &\quad +(\mathrm{e}^{\mathrm{i}\vartheta_2}\cos\theta_1\sin\theta_2 - \mathrm{e}^{-\mathrm{i}\vartheta_1}\mathrm{e}^{-\mathrm{i}(\xi_1+\xi_2)}\sin\theta_1\cos\theta_2)|\mathsf{x}_0\mathsf{y}_1\rangle \\ &\quad +(\mathrm{e}^{\mathrm{i}\vartheta_1}\sin\theta_1\cos\theta_2 - \mathrm{e}^{-\mathrm{i}\vartheta_2}\mathrm{e}^{-\mathrm{i}(\xi_1+\xi_2)}\cos\theta_1\sin\theta_2)|\mathsf{x}_1\mathsf{y}_0\rangle \\ &\quad +(\mathrm{e}^{\mathrm{i}(\vartheta_1+\vartheta_2)}\sin\theta_1\sin\theta_2 + \mathrm{e}^{-\mathrm{i}(\xi_1+\xi_2)}\cos\theta_1\cos\theta_2)|\mathsf{x}_1\mathsf{y}_1\rangle], \\ |\Phi_2\rangle &= \tfrac{1}{\sqrt{2}}[(\cos\theta_1\cos\theta_2 - \mathrm{e}^{-\mathrm{i}(\vartheta_1+\vartheta_2)}\mathrm{e}^{-\mathrm{i}(\xi_1+\xi_2)}\sin\theta_1\sin\theta_2)|\mathsf{x}_0\mathsf{y}_0\rangle \\ &\quad +(\mathrm{e}^{\mathrm{i}\vartheta_2}\cos\theta_1\sin\theta_2 + \mathrm{e}^{-\mathrm{i}\vartheta_1}\mathrm{e}^{-\mathrm{i}(\xi_1+\xi_2)}\sin\theta_1\cos\theta_2)|\mathsf{x}_0\mathsf{y}_1\rangle \\ &\quad +(\mathrm{e}^{\mathrm{i}\vartheta_1}\sin\theta_1\cos\theta_2 + \mathrm{e}^{-\mathrm{i}\vartheta_2}\mathrm{e}^{-\mathrm{i}(\xi_1+\xi_2)}\cos\theta_1\sin\theta_2)|\mathsf{x}_1\mathsf{y}_0\rangle \\ &\quad +(\mathrm{e}^{\mathrm{i}(\vartheta_1+\vartheta_2)}\sin\theta_1\sin\theta_2 - \mathrm{e}^{-\mathrm{i}(\xi_1+\xi_2)}\cos\theta_1\cos\theta_2)|\mathsf{x}_1\mathsf{y}_1\rangle], \\ |\Phi_3\rangle &= \tfrac{1}{\sqrt{2}}[(\mathrm{e}^{-\mathrm{i}\vartheta_2}\mathrm{e}^{-\mathrm{i}\xi_2}\cos\theta_1\sin\theta_2 + \mathrm{e}^{-\mathrm{i}\vartheta_1}\mathrm{e}^{-\mathrm{i}\xi_1}\sin\theta_1\cos\theta_2)|\mathsf{x}_0\mathsf{y}_0\rangle \\ &\quad -(\mathrm{e}^{-\mathrm{i}\xi_2}\cos\theta_1\cos\theta_2 - \mathrm{e}^{-\mathrm{i}(\vartheta_1-\vartheta_2)}\mathrm{e}^{-\mathrm{i}\xi_1}\sin\theta_1\sin\theta_2)|\mathsf{x}_0\mathsf{y}_1\rangle \\ &\quad +(\mathrm{e}^{\mathrm{i}(\vartheta_1-\vartheta_2)}\mathrm{e}^{-\mathrm{i}\xi_2}\sin\theta_1\sin\theta_2 - \mathrm{e}^{-\mathrm{i}\xi_1}\cos\theta_1\cos\theta_2)|\mathsf{x}_1\mathsf{y}_0\rangle \\ &\quad -(\mathrm{e}^{\mathrm{i}\vartheta_1}\mathrm{e}^{-\mathrm{i}\xi_2}\sin\theta_1\cos\theta_2 + \mathrm{e}^{\mathrm{i}\vartheta_2}\mathrm{e}^{-\mathrm{i}\xi_1}\cos\theta_1\sin\theta_2)|\mathsf{x}_1\mathsf{y}_1\rangle], \\ |\Phi_4\rangle &= \tfrac{1}{\sqrt{2}}[(\mathrm{e}^{-\mathrm{i}\vartheta_2}\mathrm{e}^{-\mathrm{i}\xi_2}\cos\theta_1\sin\theta_2 - \mathrm{e}^{-\mathrm{i}\vartheta_1}\mathrm{e}^{-\mathrm{i}\xi_1}\sin\theta_1\cos\theta_2)|\mathsf{x}_0\mathsf{y}_0\rangle \\ &\quad -(\mathrm{e}^{-\mathrm{i}\xi_2}\cos\theta_1\cos\theta_2 + \mathrm{e}^{-\mathrm{i}(\vartheta_1-\vartheta_2)}\mathrm{e}^{-\mathrm{i}\xi_1}\sin\theta_1\sin\theta_2)|\mathsf{x}_0\mathsf{y}_1\rangle \\ &\quad +(\mathrm{e}^{\mathrm{i}(\vartheta_1-\vartheta_2)}\mathrm{e}^{-\mathrm{i}\xi_2}\sin\theta_1\sin\theta_2 + \mathrm{e}^{-\mathrm{i}\xi_1}\cos\theta_1\cos\theta_2)|\mathsf{x}_1\mathsf{y}_0\rangle \\ &\quad -(\mathrm{e}^{\mathrm{i}\vartheta_1}\mathrm{e}^{-\mathrm{i}\xi_2}\sin\theta_1\cos\theta_2 - \mathrm{e}^{\mathrm{i}\vartheta_2}\mathrm{e}^{-\mathrm{i}\xi_1}\cos\theta_1\sin\theta_2)|\mathsf{x}_1\mathsf{y}_1\rangle]. \end{aligned} \tag{5.10}$$

These states are of the form (5.4), if the amplitudes are all of the same size, which yields the conditions

$$\begin{aligned} &|\cos\theta_1\cos\theta_2 \pm \mathrm{e}^{-\mathrm{i}(\vartheta_1+\vartheta_2+\xi_1+\xi_2)}\sin\theta_1\sin\theta_2| \\ =\ &|\cos\theta_1\sin\theta_2 \pm \mathrm{e}^{-\mathrm{i}(\vartheta_1+\vartheta_2+\xi_1+\xi_2)}\sin\theta_1\cos\theta_2| = \tfrac{1}{\sqrt{2}}\,, \end{aligned} \tag{5.11}$$

and

$$\begin{aligned} &|\cos\theta_1\sin\theta_2 \pm \mathrm{e}^{-\mathrm{i}(\vartheta_1-\vartheta_2+\xi_1-\xi_2)}\sin\theta_1\cos\theta_2| \\ =\ &|\cos\theta_1\cos\theta_2 \pm \mathrm{e}^{-\mathrm{i}(\vartheta_1-\vartheta_2+\xi_1-\xi_2)}\sin\theta_1\sin\theta_2| = \tfrac{1}{\sqrt{2}}\,. \end{aligned} \tag{5.12}$$

The constraints (5.11) and (5.12) can be fulfilled by the condition,

$$\cos(2\theta_1)\cos(2\theta_2) = \cos(\vartheta_1 \pm \vartheta_2 + \xi_1 \pm \xi_2) = 0\,. \tag{5.13}$$

The $\pm$ sign in Eq. (5.13) apply to Eq. (5.11) and (5.12), respectively, provided that neither $\cos(2\theta_1)$ or $\cos(2\theta_2)$ equal 1. In the special case, where either $\cos(2\theta_1) = 1$ or $\cos(2\theta_2) = 1$, condition (5.13) simplifies to $\cos(2\theta_1)\cos(2\theta_2) = 0$ with no restrictions in the angles ϑ_1, ϑ_2, ξ_1 and ξ_2[5]. One particular way to fulfil these restrictions is to set

$$\xi_2 = -\tfrac{1}{2}\pi\,,\ \xi_1 = \vartheta_1 = \vartheta_2 = 0 \ \text{ and } \ \theta_1 = \theta_2 = \tfrac{1}{4}\pi\,, \tag{5.14}$$

which corresponds to the choice

$$\begin{aligned} |\mathsf{a}_1\rangle &= \tfrac{1}{\sqrt{2}}(|\mathsf{x}_0\rangle + |\mathsf{x}_1\rangle)\,, |\mathsf{a}_2\rangle = \tfrac{1}{\sqrt{2}}(|\mathsf{x}_0\rangle - |\mathsf{x}_1\rangle)\,, \\ |\mathsf{b}_1\rangle &= \tfrac{1}{\sqrt{2}}(|\mathsf{y}_0\rangle + |\mathsf{y}_1\rangle)\,, |\mathsf{b}_2\rangle = \tfrac{\mathrm{i}}{\sqrt{2}}(|\mathsf{y}_0\rangle - |\mathsf{y}_1\rangle)\,. \end{aligned} \tag{5.15}$$

Therefore, the Bell states (5.8) have the following form which satisfies the form of the mutually unbiased basis states (5.4),

$$\begin{aligned} |\Phi_1\rangle &= \tfrac{1}{2}\mathrm{e}^{\mathrm{i}\pi/4}[|\mathsf{x}_0\mathsf{y}_0\rangle - \mathrm{i}|\mathsf{x}_0\mathsf{y}_1\rangle - \mathrm{i}|\mathsf{x}_1\mathsf{y}_0\rangle + |\mathsf{x}_1\mathsf{y}_\mathsf{y}\rangle]\,, \\ |\Phi_2\rangle &= \tfrac{1}{2}\mathrm{e}^{-\mathrm{i}\pi/4}[|\mathsf{x}_0\mathsf{y}_0\rangle + \mathrm{i}|\mathsf{x}_0\mathsf{y}_1\rangle + \mathrm{i}|\mathsf{x}_1\mathsf{y}_0\rangle + |\mathsf{x}_1\mathsf{y}_\mathsf{y}\rangle]\,, \\ |\Phi_3\rangle &= \tfrac{1}{2}\mathrm{e}^{\mathrm{i}\pi/4}[|\mathsf{x}_0\mathsf{y}_0\rangle - \mathrm{i}|\mathsf{x}_0\mathsf{y}_1\rangle + \mathrm{i}|\mathsf{x}_1\mathsf{y}_0\rangle - |\mathsf{x}_1\mathsf{y}_\mathsf{y}\rangle]\,, \\ |\Phi_4\rangle &= -\tfrac{1}{2}\mathrm{e}^{-\mathrm{i}\pi/4}[|\mathsf{x}_0\mathsf{y}_0\rangle + \mathrm{i}|\mathsf{x}_0\mathsf{y}_1\rangle - \mathrm{i}|\mathsf{x}_1\mathsf{y}_0\rangle - |\mathsf{x}_1\mathsf{y}_\mathsf{y}\rangle]\,. \end{aligned} \tag{5.16}$$

[5] An example of this special case can be found in Ref. [Zou05]. However, this case does not yield a gate operation with insurance when a partial Bell measurement on the photons is performed.

To find out which gate operation the detection of the corresponding maximally entangled states (5.8) combined with a subsequent absorption of the photon pair results into, we decompose the encoded state (5.3) into a state of the form

$$|\psi_{\rm enc}\rangle = \tfrac{1}{2}\sum_{i}^{4} |\psi_i, \Phi_i\rangle \tag{5.17}$$

and determine the states $|\psi_i\rangle$ of the stationary qubits. Using the notation

$$U_{\rm CZ} \equiv |00\rangle\langle 00| + |01\rangle\langle 01| + |10\rangle\langle 10| - |11\rangle\langle 11| \tag{5.18}$$

for the controlled two-qubit phase gate and the notation

$$Z_i(\phi) \equiv |0\rangle_{\rm ii}\langle 0| + {\rm e}^{-{\rm i}\phi}|1\rangle_{\rm ii}\langle 1| \tag{5.19}$$

for the local controlled-Z gate on photon source i [6], we find

$$\begin{aligned}
|\psi_1\rangle &= \exp\left(-\tfrac{1}{4}{\rm i}\pi\right) Z_2(-\tfrac{1}{2}\pi)\, Z_1(-\tfrac{1}{2}\pi)\, U_{\rm CZ}\, |\psi_{\rm in}\rangle\,, \\
|\psi_2\rangle &= \exp\left(\tfrac{1}{4}{\rm i}\pi\right) Z_2(\tfrac{1}{2}\pi)\, Z_1(\tfrac{1}{2}\pi)\, U_{\rm CZ}\, |\psi_{\rm in}\rangle\,, \\
|\psi_3\rangle &= \exp\left(-\tfrac{1}{4}{\rm i}\pi\right) Z_2(-\tfrac{1}{2}\pi)\, Z_1(\tfrac{1}{2}\pi)\, U_{\rm CZ}\, |\psi_{\rm in}\rangle\,, \\
|\psi_4\rangle &= -\exp\left(\tfrac{1}{4}{\rm i}\pi\right) Z_2(\tfrac{1}{2}\pi)\, Z_1(-\tfrac{1}{2}\pi)\, U_{\rm CZ}\, |\psi_{\rm in}\rangle\,.
\end{aligned} \tag{5.20}$$

From this we see that one obtains the CZ gate operation (5.18) up to local unitary operations upon the detection of any of the four Bell states $|\Phi_i\rangle$.

5.2.4 Gate implementation with insurance

When implementing distributed quantum computing with photons as flying qubits and single photon sources as stationary qubits, the problem arises that it is impossible to perform a complete Bell measurement on the photons using only linear optics elements. As it has been shown in the past [Lütkenhaus99], in the best case, one can only distinguish two of the four Bell states on average. The construction of efficient non-linear optical elements remains a difficult problem experimentally. The above described phase gate could therefore be operated at most with success rate $\frac{1}{2}$.

Therefore, we choose the photon pair measurement basis $\{|\Phi_i\rangle\}$ such that two of the basis states are maximally entangled while the other two basis states are product states. This is also naturally motivated from the fact that such a measurement basis

[6] This gate can be accomplished by applying a strongly detuned laser field for a certain time t.

can be easily implemented using a linear optics setup [Braunstein95, Mattle96]. In the following, we choose $|\Phi_3\rangle$ and $|\Phi_4\rangle$ as in Eq. (5.8) and $|\Phi_1\rangle$ and $|\Phi_2\rangle$ as

$$|\Phi_1\rangle = |\mathsf{a_1 b_1}\rangle\,, \quad |\Phi_2\rangle = |\mathsf{a_2 b_2}\rangle\,. \tag{5.21}$$

As long as the states $\{|\Phi_i\rangle\}$ constitute a MUB, the implementation of an eventually deterministic entangling phase gate remains possible. In this way, we obtain quantum computing *with insurance*. In case of the failure of the gate implementation, a product state is detected and the system remains, up to a local phase gate, in the original qubit state. This means that the original qubit state (5.1) can be restored and the described protocol can be repeated, thereby eventually resulting in the performance of the universal controlled phase gate (5.18). The probability for the realisation of the gate operation within one step equals $\frac{1}{2}$ and the completion of the gate requires, on average, only two steps.

Let us now determine the conditions under which the states $\{|\Phi_i\rangle\}$ constitute a MUB. Proceeding as above, we find that $|\Phi_3\rangle$ and $|\Phi_4\rangle$ are of form (5.4) if the angles ϑ_i, ξ_i and θ_i in Eq. (5.9) fulfil, for example, Eq. (5.14). In analogy to Eqs. (5.11) and (5.12), we find that $|\Phi_1\rangle$ and $|\Phi_2\rangle$ belong to a MUB, if

$$|\cos\theta_1 \cos\theta_2| = |\cos\theta_1 \sin\theta_2| = |\sin\theta_1 \cos\theta_2| = |\sin\theta_1 \sin\theta_2| = \tfrac{1}{2}\,, \tag{5.22}$$

which also holds for the parameter choice in Eq. (5.14). Note that Eq. (5.22) is general and applies for any product state detection in a Partial Bell basis measurement. One can easily verify with the above choice that the product states $|\Phi_1\rangle$ and $|\Phi_2\rangle$ are given by

$$\begin{aligned} |\Phi_1\rangle &= \tfrac{1}{2}[|\mathsf{x_0 y_0}\rangle + |\mathsf{x_0 y_1}\rangle + |\mathsf{x_1 y_0}\rangle + |\mathsf{x_1 y_1}\rangle]\,, \\ |\Phi_2\rangle &= \tfrac{\mathrm{i}}{2}[|\mathsf{x_0 y_0}\rangle - |\mathsf{x_0 y_1}\rangle - |\mathsf{x_1 y_0}\rangle + |\mathsf{x_1 y_1}\rangle]\,, \end{aligned} \tag{5.23}$$

which fulfils (5.4). This means that choosing the states $|\mathsf{a}_i\rangle$ and $|\mathsf{b}_i\rangle$ as in Eq. (5.15) allows to implement the gate operation (5.18) with insurance[7].

Finally, we determine the gate operations corresponding to the detection of a certain measurement outcome $|\Phi_i\rangle$. To do this, we decompose the encoded state (5.3) again into a state of the form (5.17). Proceeding as in the previous subsection

[7]The term insurance was first coined by Bose *et al.* in the context of teleportation between atoms in different cavities with the aid of a backup atom in one of the cavities [Bose99].

we find

$$\begin{aligned}
|\psi_1\rangle &= |\psi_{\rm in}\rangle\,, \\
|\psi_2\rangle &= -{\rm i}\, Z_2(\pi)\, Z_2(\pi)\, |\psi_{\rm in}\rangle\,, \\
|\psi_3\rangle &= \exp\left(-\tfrac{1}{4}{\rm i}\pi\right) Z_2(-\tfrac{1}{2}\pi)\, Z_1(\tfrac{1}{2}\pi)\, U_{\rm CZ}\, |\psi_{\rm in}\rangle\,, \\
|\psi_4\rangle &= -\exp\left(\tfrac{1}{4}{\rm i}\pi\right) Z_2(\tfrac{1}{2}\pi)\, Z_1(-\tfrac{1}{2}\pi)\, U_{\rm CZ}\, |\psi_{\rm in}\rangle\,. \qquad (5.24)
\end{aligned}$$

From this, we see that one obtains indeed the CZ gate operation (5.18) up to local unitary operations upon the detection of either $|\Phi_3\rangle$ or $|\Phi_4\rangle$ as in (5.20). In case of the detection of the product states $|\Phi_1\rangle$ or $|\Phi_2\rangle$, the initial state can be restored with the help of one-qubit phase gates, which then allows to repeat the operation.

It should be emphasized that there are other possible photon pair measurement bases that yield a universal two-qubit phase gate upon the detection of a Bell-state but where the original state is destroyed upon the detection of a product state (see e.g. [Zou05]). The reason is that, while the detected Bell states might result in a universal gate operation, the corresponding product states are not mutually unbiased and their detection erases the qubit state in the photon sources. To achieve the effect of an *insurance*, the photon pair measurement basis should be chosen as described in this Section, as an example.

5.2.5 Teleportation with insurance

Here, we first show that the setup can be directly used to realise a quantum filter operation with insurance. This would lead us naturally to teleportation. Particularly, we describe a scheme for the implementation of the parity filter operation(see Chapter 4)

$$P^{1\pm}_{\rm filter} = |00\rangle\langle 00| \pm |11\rangle\langle 11|\,, \qquad (5.25)$$

which projects the initial qubit state $|\psi_{\rm in}\rangle$ with probability $|\alpha|^2 + |\delta|^2$ onto the even-parity state,

$$|\psi_{\rm fin}\rangle = (\alpha\,|00\rangle \pm \delta\,|11\rangle)/\sqrt{|\alpha|^2 + |\delta|^2}\,. \qquad (5.26)$$

or

$$P^{2\pm}_{\rm filter} = |01\rangle\langle 01| \pm |10\rangle\langle 10|\,, \qquad (5.27)$$

which projects $|\psi_{\rm in}\rangle$ with probability $|\beta|^2 + |\gamma|^2$ onto the odd-parity state,

$$|\psi_{\rm fin}\rangle = (\beta\,|01\rangle \pm \gamma\,|10\rangle)/\sqrt{|\beta|^2 + |\gamma|^2}\,. \qquad (5.28)$$

Again, this can be achieved if the photon states are detected in the desired form $\frac{1}{\sqrt{2}}(|\mathsf{x}_0\mathsf{y}_0\rangle \pm \mathrm{e}^{\mathrm{i}\delta_{1\pm}}|\mathsf{x}_1\mathsf{y}_1\rangle)$ or $\frac{1}{\sqrt{2}}(|\mathsf{x}_0\mathsf{y}_1\rangle \pm \mathrm{e}^{\mathrm{i}\delta_{2\pm}}|\mathsf{x}_1\mathsf{y}_0\rangle)$ where $\delta_{i\pm}$ is any arbitrary phase angle. Looking again at Eq. (5.10), all the basis states $|\Psi_i\rangle$ will be the desired form by setting

$$\sin(\theta_1 \mp \theta_2) = \cos(\theta_1 \pm \theta_2) = 0\,, \tag{5.29}$$

and

$$\sin(\vartheta_1 \pm \vartheta_2 + \xi_1 \pm \xi_2) = 0\,, \tag{5.30}$$

provided that $\sin(2\theta_1)\sin(2\theta_2) \neq 0$. In the special case where $\sin(2\theta_1)\sin(2\theta_2) = 0$, then the only constraint would be $\sin(2\theta_1) = \sin(2\theta_2) = 0$ with no restriction on the angles ϑ_1, ϑ_2, ξ_1 and ξ_2. However now, we redefine $|\Psi_1\rangle$ and $|\Psi_2\rangle$ as product states defined in Eq. (5.21), collectively forming a partial Bell-measurement basis. Combining with the condition of insurance in Eq. (5.22), we see that the choice

$$\theta_1 = \theta_2 = \frac{\pi}{4},\ \vartheta_1 = \vartheta_2 = \xi_1 = \xi_2 = 0, \tag{5.31}$$

allows us to implement a parity filter with insurance. This is the choice where

$$\begin{aligned} |\mathsf{a}_1\rangle &= \tfrac{1}{\sqrt{2}}(|\mathsf{x}_0\rangle + |\mathsf{x}_1\rangle)\,,\ |\mathsf{a}_2\rangle = \tfrac{1}{\sqrt{2}}(|\mathsf{x}_0\rangle - |\mathsf{x}_1\rangle)\,, \\ |\mathsf{b}_1\rangle &= \tfrac{1}{\sqrt{2}}(|\mathsf{y}_0\rangle + |\mathsf{y}_1\rangle)\,,\ |\mathsf{b}_2\rangle = \tfrac{1}{\sqrt{2}}(|\mathsf{y}_0\rangle - |\mathsf{y}_1\rangle)\,. \end{aligned} \tag{5.32}$$

which yields

$$\begin{aligned} |\Phi_1\rangle &= \tfrac{1}{2}(|\mathsf{x}_0\mathsf{y}_0\rangle + |\mathsf{x}_0\mathsf{y}_1\rangle + |\mathsf{x}_1\mathsf{y}_0\rangle + |\mathsf{x}_1\mathsf{y}_1\rangle)\,, \\ |\Phi_2\rangle &= \tfrac{1}{2}(|\mathsf{x}_0\mathsf{y}_0\rangle - |\mathsf{x}_0\mathsf{y}_1\rangle - |\mathsf{x}_1\mathsf{y}_0\rangle + |\mathsf{x}_1\mathsf{y}_1\rangle)\,, \\ |\Phi_3\rangle &= \tfrac{1}{\sqrt{2}}(|\mathsf{x}_0\mathsf{y}_0\rangle - |\mathsf{x}_1\mathsf{y}_1\rangle)\,, \\ |\Phi_4\rangle &= -\tfrac{1}{\sqrt{2}}(|\mathsf{x}_0\mathsf{y}_1\rangle - |\mathsf{x}_1\mathsf{y}_0\rangle)\,. \end{aligned} \tag{5.33}$$

To see this, we again decompose the input state (5.3) again into a state of the form (5.17). Proceedings as in the previous subsection, we find

$$\begin{aligned} |\psi_1\rangle &= |\psi_{\mathrm{in}}\rangle\,,\ |\psi_2\rangle = Z_2(\pi)\,Z_2(\pi)\,|\psi_{\mathrm{in}}\rangle\,, \\ |\psi_3\rangle &= P^{1-}_{\mathrm{filter}}|\psi_{\mathrm{in}}\rangle\,,\ |\psi_4\rangle = -P^{2-}_{\mathrm{filter}}|\psi_{\mathrm{in}}\rangle\,. \end{aligned} \tag{5.34}$$

One application of the quantum parity filter (5.25) is *teleportation with insurance*, which now requires less resources than previously proposed schemes [Bose99]. Suppose, a given state $\alpha\,|0\rangle + \beta\,|1\rangle$ of source A is to be teleported to another target

source B prepared in $\frac{1}{\sqrt{2}}(|0\rangle+|1\rangle)$. Application of the quantum filter to the combined state of the two sources, then ultimately transfers this state into $\alpha\,|00\rangle + \beta\,|11\rangle$ or $\alpha\,|01\rangle + \beta\,|10\rangle$. In order to complete the teleportation, the state of B should be disentangled from the state of source A without revealing the coefficients α and β. This can be achieved by measuring source A on the basis given by $|\pm\rangle \equiv \frac{1}{\sqrt{2}}(|0\rangle \pm |1\rangle)$. Depending on the outcome of this measurement, a further local operation on the state of B might be required.

We proceed next with the description of possible ways to realise the photon encoding.

5.3 Entangled Atom-Photon generation from Atom-Cavity Systems

5.3.1 Introduction

The purpose of this subsection is to show how a highly efficient encoder of a stationary qubit to the flying qubit can be performed in the context of an atom-cavity system. We use an atom-cavity photon gun [Law97, Kuhn99, Duan03, Saavedra00, Gheri98, Ciaramicoli01, Maurer04, Keller04b] in which either Raman transfer with detuning or the so-called stimulated Raman adabiatic passage (STIRAP) [Bergmann98, Oreg84] is employed. Gheri *et al.* [Gheri98] were the first to exploit a limited version of encoding with this technique. Here, we review by following closely the formalism of Duan *et al.* [Duan03], how a deterministic single photon encoder with a single or double Λ-type level configuration trapped in a cavity can be implemented in principle. We illustrate this using the STIRAP method as an example although the Raman transfer method using large detuning resulting in adiabatic elimination of the excited state will yield the same general conclusion. As in [Gheri98, Saavedra00], we make use of the superposition principle and the fact that no-cross couplings can occur between different subspaces as described by the system Hamiltonian to show how efficient encoding to the photon is possible.

5.3.2 Photon gun encoder

We consider the situation of a degenerate double Λ-type atom trapped in an optical cavity. Specifically, each Λ system i where $i = 0, 1$ consists of two ground states $|u_i\rangle$ and $|v_i\rangle$ as well as an excited state $|e_i\rangle$ as shown in Fig. 5.1. We assume that the

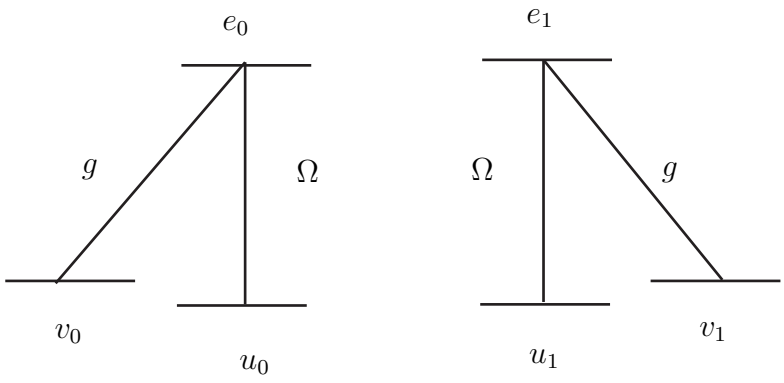

Figure 5.1: Schematic view of a single photon polarisation encoder and level configuration of the atomic structure containing the qubit.

atom is initially prepared in the state

$$|\psi(t=0)\rangle = (\alpha_0|u_0\rangle + \alpha_1|u_1\rangle)|0\rangle_{\text{cav}}|\text{vac}\rangle, \tag{5.35}$$

where $|0\rangle_{\text{cav}}$ and $|\text{vac}\rangle$ denotes the cavity vacuum field and the external photon vacuum field respectively.

Lasers with time-dependent Rabi frequency $\Omega_i(t)$ with frequency ω_L resonantly couple levels u_i to e_i. The cavity resonantly couples levels v_i to e_i with coupling strength g_i with the cavity resonant frequency ω_{cav}. In addition, the cavity field associated with creation(destruction) operator $a_i^\dagger(a_i)$ corresponding to both Λ systems i is required to be orthogonal (in this case, in polarisation) with respective decay rates κ_i. The external photon fields can be described by creation(destruction) operators $b_i(\omega)^\dagger(b_i(\omega))$ with mode i and frequency ω. They satisfy the commutation rules $[b_i(\omega_1), b_j^\dagger(\omega_2)] = \delta_{ij}\delta_{\omega_1\omega_2}$.

To solve the evolution of the system, it is convenient to borrow the concept of quantum jump formalism [Hegerfeldt93, Dalibard92, Carmichael93] with a non-event (i.e. no spontaneously emitted photon emitted outside the cavity mode) evolution described by a non-Hermitian Hamiltonian.

The conditional non-Hermitian Hamiltonian ($\hbar = 1$), in the case where no photon is spontaneously emitted outside the cavity mode, in the interaction picture with respect to the free evolution is given by [Tregenna02, Duan03]

$$H(t) = H_{\text{atom-cavity}}(t) + H_{\text{cavity-env}}(t) \tag{5.36}$$

where

$$H_{\text{atom-cavity}}(t) = \sum_i \Omega_i(t)|e_i\rangle\langle u_i| + g_i a_i|e_i\rangle\langle v_i| + \text{H.c.} - \text{i}\frac{\Gamma_i}{2}|e_i\rangle\langle e_i|\,, \tag{5.37}$$

$$H_{\text{cavity-env}}(t) = \sum_i \text{i}\sqrt{\frac{\kappa_i}{2\pi}}\int_{-\omega_b}^{\omega_b} d\omega a_i^\dagger b_i(\bar{\omega})\text{e}^{-\text{i}\omega t} + \text{H.c.}\,, \tag{5.38}$$

and $\bar{\omega} = \omega_{\text{cav}} + \omega$ and ω_b is the bandwidth. We assume ω_b to be relatively large but it has to be much smaller than ω_{cav}. Within this bandwidth, the coupling between the free field and the cavity mode is approximately constant and given by $\sqrt{\frac{\kappa_i}{2\pi}}$. The cavity coupling g_i, which derives from the quantisation of the vacuum field in the cavity, is a function of the cavity spatial mode function and the relevant dipole transition element [Chen04]. For the purpose of illustration, they can be set to be real and equal without loss of generality. We also see the effect of the damping factor Γ_i on the excited state $|e_i\rangle$ due to the possibility of spontaneous emission.

We now define the states $|D_i(t)\rangle$ and $|B_i(t)\rangle$ such that

$$\begin{aligned} |D_i(t)\rangle &= \cos\vartheta_i(t)|u_i\rangle|0\rangle_{\text{cav}} - \sin\vartheta_i(t)|v_i\rangle a_i^\dagger|0\rangle_{\text{cav}}\,, \\ |B_i(t)\rangle &= \sin\vartheta_i(t)|u_i\rangle|0\rangle_{\text{cav}} + \cos\vartheta_i(t)|v_i\rangle a_i^\dagger|0\rangle_{\text{cav}}\,, \end{aligned} \tag{5.39}$$

where

$$\cos\vartheta_i(t) = \frac{g_i}{\sqrt{g_i^2 + \Omega_i^2(t)}}. \tag{5.40}$$

One can easily see that $|D_i(t)\rangle$ and $|B_i(t)\rangle$ are orthogonal to each other. An important point, as pointed out by Duan *et. al.* is that the spatial dependence of $\cos\vartheta_i(t)$ can be made to vanish provided that $\Omega_i(t)$ and g_i share the same cavity spatial mode structure. This can be accomplished by collinear pumping where the external pumping laser couples to a similar spatial cavity mode of a different polarisation relative to the one used in generating the cavity photon that subsequently leaks out and is encoded to the atomic state. This suggests that the atom need not really be cooled to the Lamb-Dicke limit for operation which removes a huge experimental challenge. However, the same authors point out that cooling is still important to maintain a long trap lifetime of the atom in the cavity.

When Γ_i and κ_i vanish, $|D_i(t)\rangle$ is an exact eigenstate with zero eigenvalue of the Hamiltonian $H(t)$ and hence, known as a dark state. A system initially in the dark state always stays in the dark state provided that the adiabatic following condition is fulfilled. This is the essence of the STIRAP process, which allows for robust coherent state transfer by remaining always in a dark state. In the subspace

defined by the Hamiltonian $H(t)$ and making the assumption that only one photon excitation can be put to the external field, the general state after time t is given by

$$\begin{aligned} |\psi(t)\rangle &= \sum_i \alpha_i((c_{D_i}(t)|D_i(t)\rangle + c_{B_i}(t)|B_i(t)\rangle + \\ &\quad c_{e_i}(t)|e_i\rangle|0\rangle_{\rm cav})|{\rm vac}\rangle + |v_i\rangle|0\rangle_{\rm cav}\int_{-\omega_b}^{\omega_b} d\omega s(\omega,t)_i|\bar{\omega}\rangle_i)\,, \end{aligned} \tag{5.41}$$

where $|\bar{\omega}\rangle_i = b_i^\dagger(\bar{\omega})|{\rm vac}\rangle$. Note that the last term with the external photon excitation is associated with the state $|v_i\rangle|0\rangle_{\rm cav}$. This can be inferred by looking at the Hamiltonian given in Eq. (5.36). An external photon excitation of mode i comes only through the annihilation of a cavity photon $a_i^\dagger|0\rangle_{\rm cav}$ from $H_{\rm cavity-env}(t)$ which was created accompanying the projection of the atomic state to $|v_i\rangle$ from $H_{\rm atom-cavity}(t)$. Up to now, we have not made any adiabatic approximations. We can calculate the probability $P_{\rm cond}(t) = ||\,|\psi(t)\rangle||^2$ of the system evolving according to $H(t)$. It is this evolution that yields the photon in the cavity mode which leaks out subsequently. Otherwise, spontaneous emission occurs and this takes place with the probability $P_{\rm spon}(t) = 1 - P_{\rm cond}(t)$. Explictly, this is given by

$$P_{\rm spon}(t) = 1 - \sum_i |\alpha_i|^2(|c_{D_i}(t)|^2 + |c_{B_i}(t)|^2 + |c_{e_i}(t))|^2 + \int_{-\omega_b}^{\omega_b} d\omega|s(\omega,t)_i|^2) \tag{5.42}$$

When $P_{\rm spon}(t)$ is small or close to 0, the system can yield an effective photon source on demand. Now, the adiabatic condition, which we take as an ansatz (see further discussion by Duan *et al.* [Duan03]), results in a very slow change of $\cos\vartheta_i(t)$ which implies that the time derivatives of $|D_i(t)\rangle$ and $|B_i(t)\rangle$ vanish. This condition also implies that the population of $|B_i(t)\rangle$ and $|e_i\rangle$ is virtually zero and can be effectively neglected. This allows us to simplify the calculation of the evolution of $|\psi(t)\rangle$ with the Schrodinger's equation by calculating the two time-dependent coefficients given by

$$\begin{aligned} \dot{c}_{D_i}(t) &= -\sqrt{\frac{\kappa_i}{2\pi}}\sin\vartheta_i(t)\int_{-\omega_b}^{\omega_b} d\omega s(\omega,t)_i {\rm e}^{-{\rm i}\omega t}\,, \\ \dot{s}(\omega,t)_i &= \sqrt{\frac{\kappa_i}{2\pi}} c_{D_i}(t)\sin\vartheta_i(t){\rm e}^{{\rm i}\omega t}\,. \end{aligned} \tag{5.43}$$

The solutions of the two coefficients are given approximately by

$$\begin{aligned} c_{D_i}(t) &= \exp(-\frac{\kappa_i}{2}\int_0^t dt'\sin^2\vartheta_i(t'))\,, \\ s(\omega,t)_i &= \sqrt{\frac{\kappa_i}{2\pi}}\int_0^t dt'{\rm e}^{{\rm i}\omega t'} c_{D_i}(t')\sin\vartheta_i(t')\,. \end{aligned} \tag{5.44}$$

We have used the Markovian approximation in the process where the limits of integration of ω is artificially extended to $-\infty$ and ∞ due to the large bandwidth ω_b to yield a delta function. To have generated an external photon with unit probability by time $t = \tau$, we should start with $c_{D_i}(0) = 1$ at time $t = 0$ and end up with $c_{D_i}(\tau) = 0$ by looking at Eq. (5.41) where τ is chosen to be a characteristic time in the tail end of the pumping laser pulse when the amplitude is near zero. This is fulfilled by choosing a large τ and(or) increasing the laser Rabi frequency $\Omega_i(t)$ by looking at Eq. (5.44). Note that κ_i^{-1} must be smaller than τ. Otherwise, adiabatic following will imply coherent return to the initial state with $c_{D_i}(\tau) = 1$ with no external photon generated[Kuhn99] if $\kappa_i^{-1} \gg \tau$. We can define the pulse shape by the Fourier transform of the spectral evelope

$$f(t,\tau)_i = \frac{1}{\sqrt{2\pi}} \int_{-\infty}^{\infty} d\omega s(\omega,\tau)_i \mathrm{e}^{-\mathrm{i}\omega t}. \tag{5.45}$$

From Eq. (5.44), we see that the pulse shape is given by

$$f(t,\tau)_i = \sqrt{\kappa_i} \sin\vartheta_i(t) c_{D_i}(t) \tag{5.46}$$

For simplicity, we assume all parameters related to different i to be the same i.e. $(\Omega_i(t) = \Omega(t), g_i = g, \Gamma_i = \Gamma)$. We also assume that after a photon is generated, we recycle the state of the system from $|v_i\rangle$ to $|u_i\rangle$. In the ideal limit of strong cavity coupling $g^2 \gg \Gamma\kappa$ and adiabatic following, we are able to perform a deterministic mapping of the form

$$\sum_i \alpha_i |u_i\rangle|0\rangle_{\mathrm{cav}}|\mathrm{vac}\rangle \rightarrow \sum_i \alpha_i |u_i\rangle|0\rangle_{\mathrm{cav}} \int_{-\omega_b}^{\omega_b} d\omega s(\omega,t)_i b_i^\dagger(\bar{\omega})|\mathrm{vac}\rangle \tag{5.47}$$

This implies that we can encode the state of the atoms to the externally generated photons with a STIRAP process and was first demonstrated by Gheri *et. al.* [Gheri98] in the regime of Raman transfer with a large detuning.

Now, all these above calculations invoke the crucial assumption of adiabatic following. The adiabatic following condition is well defined in the limit where Γ_i and κ_i vanish. Specifically, the evolution time τ must be longer than the inverse of the frequency splitting gap between the dark state $|D_i(t)\rangle$ and the rest of the eigenstates [Kuhn99]. In our case, the gap δ is $\sqrt{g_i^2 + \Omega_i^2(t)}$ and the adiabatic condition is given by

$$(g_i^2 + \Omega_i^2(t))\tau^2 \gg 1. \tag{5.48}$$

Note that this condition does not imply adiabatic following when Γ_i and κ_i is non-

zero due to the atom-cavity system coupling to an infinite continum of modes. Therefore, a fuller description necessitates numerical simulation. Duan *et. al.* [Duan03] have already performed such simulations and showed that spontaneous emission loss is negligible in the limit of strong coupling where $g^2/\kappa\Gamma \gg 1$. Empirically, P_{spon} scales as $\kappa\Gamma/4g^2$. Furthermore, it was found that for strong coupling, the analytically calculated pulse shape $f(t,\tau)_i$ based on the adiabatic following ansatz agrees very well with numerical simulations. If we restrict ourselves to the less general case of a single Λ subsystem characterised for example by $\alpha_i = 0$, we recover exactly the usual single photon gun [Law97, Kuhn99].

Finally, we consider the case where the same laser driving pulse is offset by a time T_i and we operate in the single Λ subsystem, dropping all subscripts corresponding to subsystem for readability. For convenience, we can define the effective photon creation operator as $B^\dagger(t_i,\tau)$

$$B^\dagger(t,\tau) = \int_{-\omega_b}^{\omega_b} d\omega \mathrm{e}^{\mathrm{i}\omega t} s(\omega,\tau) b^\dagger(\bar{\omega}). \tag{5.49}$$

We find that when $|t_i - t_j| \gg \tau$ [Gheri98, Saavedra00],

$$\left[B^\dagger(t_i,\tau), B^\dagger(t_j,\tau)\right] \to 0. \tag{5.50}$$

This implies that photons created by laser driving pulse offset by a time separation much larger than the driving pulse duration τ can be considered to be in different modes and hence orthogonal. In fact,$\left[B^\dagger(t_i,\tau), B^\dagger(t_j,\tau)\right]$ which depends essentially on the temporal overlap of two identical pulses offset by $|t_i - t_j|$ approximately decay exponentially with the ratio $\frac{|t_i - t_j|}{\tau}$ and thus typically, a time-separation $|t_i - t_j|$ of the order of τ might already be sufficient to achieve the photon orthogonality condition [Saavedra00]. This leads us to the possibility of time-bin encoding in which photons are created by an early or late driving pulse with the appropriate time separation dependent on the initial ground state of the atom.

One way to implement such an encoding is to first swap the atomic states $|u_0\rangle$ and $|u_1\rangle$. Then a laser pulse with increasing Rabi frequency should excite the u_1-e_1 transition (see Fig. 5.2) at time t_0 for example. This transfers the atom into the state $|v_1\rangle$ and places one excitation into the field of the strongly coupled optical cavity, if the atom was initially prepared in $|u_0\rangle$. The photon then leaks out through the outcoupling mirror of the resonator. The encoding operation, which is feasible with present technology [Duan03], is completed by transfering $|v_1\rangle$ back into $|u_1\rangle$, swapping again the states $|u_0\rangle$ and $|u_1\rangle$ and repeating the above described photon

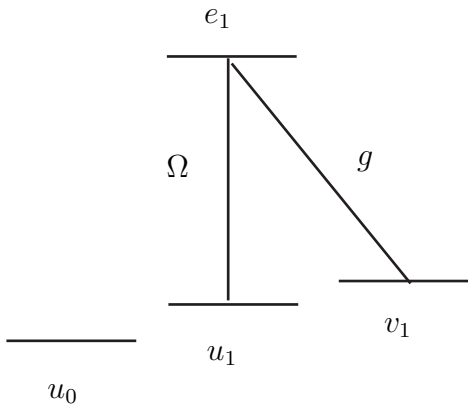

Figure 5.2: Schematic view of a single photon time-bin encoder and level configuration of the atomic structure containing the qubit.

generation process at a later time t_1. The above process therefore describes the mapping of a form

$$\sum_i \alpha_i |u_i\rangle|0\rangle_{\text{cav}}|\text{vac}\rangle \rightarrow \sum_i \alpha_i |u_i\rangle|0\rangle_{\text{cav}} B^\dagger(t_i,\tau)|\text{vac}\rangle \tag{5.51}$$

In general, time-bin encoding which requires a simpler energy level structure compared to polarisation encoding may find realisations in systems such as quantum dots and NV color centers where a double Λ-type configuration may not be easily found. We now proceed to the description of photon pair measurement.

5.4 Measurements on photon pairs

We give 2 examples of measurements on the photon pairs based on the concrete choice given in (5.15). The first method is suitable for polarisation encoded photon pairs. The second is suitable for dual-rail encoded photon pairs. In general, depending on the initial choice of encoding, conversion between encodings may be required. For example, one might need to convert time-bin encoding to either polarisation or dual-rail encoding and method 1 or 2 can be used respectively for photon pair measurements.

It is worth mentioning that our scheme has the same robustness from slow and unknown phase fluctutations along the photon paths due to the same reason outlined for example in Ref. [Simon03]. Due to the fact that we use coincidence measurement for our Bell-state detection, any slow phase error on the photons contributes

only to a global phase factor in the stationary qubits. This also implies that our scheme does not require interferometric stability as is the case of most schemes requiring coincidence detection. We first describe a canonical Bell-state measurement in polarisation encoding.

5.4.1 Canonical Bell-state measurement

Bell-state measurement on a photon pair is an important tool used widely in quantum information processing with photons. It is crucial for quantum teleportation [Bennett93], quantum dense coding [Bennett92] as well as entanglement swapping [Żukowski93]. Recently, Browne and Ruldoph [Browne05] have exploited Bell-state measurement for the efficient construction of a photonic cluster state. However, a complete Bell measurement cannot be realised with unit success probability in a purely linear optics based setup [Lütkenhaus99]. This can be thought as a main limitation to purely linear optics based quantum computation. We show here a canonical example of how a partial Bell measurement can be realised with the aid of a beam splitter [Braunstein95]. We recall the basis (1.2) states of a complete Bell basis as

$$
\begin{aligned}
|\Phi^{\pm}\rangle &= \frac{1}{\sqrt{2}}(a^{\dagger}_{1,h}a^{\dagger}_{2,v} \pm a^{\dagger}_{1,v}a^{\dagger}_{2,h})|0\rangle_{\text{vac}}\,, \\
|\Psi^{\pm}\rangle &= \frac{1}{\sqrt{2}}(a^{\dagger}_{1,h}a^{\dagger}_{2,h} \pm a^{\dagger}_{1,v}a^{\dagger}_{2,v})|0\rangle_{\text{vac}}\,.
\end{aligned} \tag{5.52}
$$

Here, $a^{\dagger}_{i,\lambda}$ refers to a photon creation operator for spatial mode i with polarisation λ. These 2-photon Bell states are sent, one in each input arm, into a 50:50 beam splitter which is described by the matrix $B(\frac{1}{2}, 1)$ in Chapter 2. We fix the convention that the spatial modes defined by the two input ports are defined as spatial modes 1 and 2 and that defined by the two output ports are defined as spatial mode 3 and 4. It can be shown that the basis Bell states at the input will transform to the output ports as

$$
\begin{aligned}
|\Phi^{+}\rangle &\rightarrow \frac{1}{\sqrt{2}}(a^{\dagger}_{4,v}a^{\dagger}_{4,h} - a^{\dagger}_{3,v}a^{\dagger}_{3,h})|0\rangle_{\text{vac}}\,, \\
|\Phi^{-}\rangle &\rightarrow \frac{1}{\sqrt{2}}(a^{\dagger}_{3,v}a^{\dagger}_{4,h} - a^{\dagger}_{4,v}a^{\dagger}_{3,h})|0\rangle_{\text{vac}}\,, \\
|\Psi^{+}\rangle &\rightarrow \frac{1}{2\sqrt{2}}((a^{\dagger}_{4,v})^2 + (a^{\dagger}_{4,h})^2 - (a^{\dagger}_{3,v})^2 - (a^{\dagger}_{3,h})^2)|0\rangle_{\text{vac}}\,, \\
|\Psi^{-}\rangle &\rightarrow \frac{1}{2\sqrt{2}}((a^{\dagger}_{4,v})^2 - (a^{\dagger}_{4,h})^2 - (a^{\dagger}_{3,v})^2 + (a^{\dagger}_{3,h})^2)|0\rangle_{\text{vac}}\,.
\end{aligned} \tag{5.53}
$$

We see that $|\Phi^{\pm}\rangle$ is indicated by detecting photons of different polarisations in the same and different output ports respectively. Unfortunately, $|\Psi^{\pm}\rangle$ cannot be distinguished by simple photon detection and hence, the simple beam splitter cannot implement a complete Bell measurement with unit efficiency. However, the following product states, $\frac{1}{\sqrt{2}}(|\Psi^{+}\rangle + |\Psi^{-}\rangle) = a^{\dagger}_{1,h}a^{\dagger}_{2,h}|0\rangle_{\rm vac}$ and $\frac{1}{\sqrt{2}}(|\Psi^{+}\rangle - |\Psi^{-}\rangle) = a^{\dagger}_{1,v}a^{\dagger}_{2,v}|0\rangle_{\rm vac}$ transform as $\frac{1}{2}((a^{\dagger}_{3,h})^2 - (a^{\dagger}_{4,h})^2)|0\rangle_{\rm vac}$ and $\frac{1}{2}((a^{\dagger}_{3,v})^2 - (a^{\dagger}_{4,v})^2)|0\rangle_{\rm vac}$ respectively. The output states in this case are distinguishable. Therefore, the measurement performed in this case is a partial Bell measurement with two Bell states and two product states constituting the measurement basis.

5.4.2 Measurement for polarisation encoded photon pair

We have shown that sending two polarisation encoded photons through the different input ports of a 50:50 beam splitter together with polarisation sensitive measurements in the $|\mathsf{h}\rangle/|\mathsf{v}\rangle$-basis in the output ports would result in a measurement of the states $\frac{1}{\sqrt{2}}(|\mathsf{hv}\rangle \pm |\mathsf{vh}\rangle)$, $|\mathsf{hh}\rangle$ and $|\mathsf{vv}\rangle$. To measure the states $|\Phi_i\rangle$ defined in Section 5.2.4 or 5.2.5, we therefore proceed as shown in Fig. 5.3(a) and perform the mapping $U_1 = |\mathsf{h}\rangle\langle\mathsf{a_1}| + |\mathsf{v}\rangle\langle\mathsf{a_2}|$ and $U_2 = |\mathsf{h}\rangle\langle\mathsf{b_1}| + |\mathsf{v}\rangle\langle\mathsf{b_2}|$ on the photon coming from source i. For the states defined Section 5.2.4, using Eq. (5.15), we see that this corresponds to the single qubit rotations

$$\begin{aligned} U_1 &= \tfrac{1}{\sqrt{2}}\left[\,|\mathsf{h}\rangle(\langle\mathsf{h}| + \langle\mathsf{v}|) + |\mathsf{v}\rangle(\langle\mathsf{h}| - \langle\mathsf{v}|)\,\right], \\ U_2 &= \tfrac{1}{\sqrt{2}}\left[\,|\mathsf{h}\rangle(\langle\mathsf{h}| + \langle\mathsf{v}|) - \mathrm{i}\,|\mathsf{v}\rangle(\langle\mathsf{h}| - \langle\mathsf{v}|)\,\right]. \end{aligned} \tag{5.54}$$

After leaving the beam splitter, the photons should be detected in the $|\mathsf{h}\rangle/|\mathsf{v}\rangle$-basis. A detection of two h (v) polarised photons indicates a measurement of $|\Phi_1\rangle$ ($|\Phi_2\rangle$). Finding two photons of different polarisation in the same (different) detectors corresponds to a detection of $|\Phi_3\rangle$ ($|\Phi_4\rangle$).

5.4.3 Measurement for dual-rail encoded photon pair

Alternatively, one can redirect the generated photons (for example, if the photons are time-bin encoded) to the different input ports of a 4×4 symmetric multiport beam splitter as shown in Fig. 5.3(b). A symmetric multiport redirects each incoming photon with equal probability to any of the possible output ports and can therefore be used to erase the which-way information of the incoming photons as we have mentioned in Chapter 2 and 3. If $a^{\dagger}_n$ ($b^{\dagger}_n$) denotes the creation operator for a

photon in input (output) port n, the effect of the multiport can be summarised as

$$a_n^\dagger \rightarrow \sum_m U_{mn} b_m^\dagger, \tag{5.55}$$

where U_{mn} is the probability amplitude to redirect a photon from the nth input port to the mth output port. For the implementation of either a two qubit universal phase gate or a parity filter, one should direct the input $|\mathsf{x_0}\rangle$ ($|\mathsf{x_1}\rangle$) photon from source 1 to input port 1 (3) and to direct a $|\mathsf{y_0}\rangle$ ($|\mathsf{y_1}\rangle$) photon from source 2 to input port 2 (4). If $|\text{vac}\rangle$ denotes the state with no photons in the setup, this results in the conversion $|\mathsf{x_0y_0}\rangle \rightarrow a_1^\dagger a_2^\dagger |\text{vac}\rangle$, $|\mathsf{x_0y_1}\rangle \rightarrow a_1^\dagger a_4^\dagger |\text{vac}\rangle$, $|\mathsf{x_1y_0}\rangle \rightarrow a_2^\dagger a_3^\dagger |\text{vac}\rangle$ and $|\mathsf{x_1y_1}\rangle \rightarrow a_3^\dagger a_4^\dagger |\text{vac}\rangle$. This conversion should be realised such that the photons enter the multiport at the same time. For two-qubit universal gate implementation, U_{mn} is given by

$$U_{mn} = \tfrac{1}{2}\, \mathrm{i}^{(m-1)(n-1)}. \tag{5.56}$$

In such a case, the multiport is also known as a Bell multiport which was introduced in Chapter 2. Using Eq. (5.55), one can show that the network transfers the basis states $|\Phi_i\rangle$, with the choice Eq. (5.15) as

$$\begin{aligned} |\Phi_1\rangle &\rightarrow \tfrac{1}{2}\left(b_1^{\dagger\,2} - b_3^{\dagger\,2}\right)|\text{vac}\rangle\,, \; |\Phi_2\rangle \rightarrow -\tfrac{1}{2}\left(\mathrm{b}_2^{\dagger\,2} - \mathrm{b}_4^{\dagger\,2}\right)|\text{vac}\rangle\,, \\ |\Phi_3\rangle &\rightarrow \tfrac{1}{\sqrt{2}}\left(b_1^\dagger b_4^\dagger - b_2^\dagger b_3^\dagger\right)|\text{vac}\rangle\,, \; |\Phi_4\rangle \rightarrow -\tfrac{1}{\sqrt{2}}\left(\mathrm{b}_1^\dagger \mathrm{b}_2^\dagger - \mathrm{b}_3^\dagger \mathrm{b}_4^\dagger\right)|\text{vac}\rangle\,. \end{aligned} \tag{5.57}$$

Finally, detectors measure the presence of photons in each of the possible output ports. The detection of two photons in the same output port, namely in 1 or 3 and in 2 or 4, corresponds to a measurement of the state $|\Phi_1\rangle$ and $|\Phi_2\rangle$, respectively. The detection of a photon in ports 1 and 4 or in 2 and 3 indicates a measurement of the state $|\Phi_3\rangle$, while a photon in the ports 1 and 2 or in 3 and 4 indicates the state $|\Phi_4\rangle$.

On the other hand, to implement a parity filter and hence teleportation with insurance, another symmetric multiport with U_{mn} given by

$$U = \tfrac{1}{2}\begin{pmatrix} 1 & 1 & 1 & 1 \\ 1 & 1 & -1 & -1 \\ 1 & -1 & 1 & -1 \\ 1 & -1 & -1 & 1 \end{pmatrix}$$

should be used. One can again show that the network transfers the appropriate

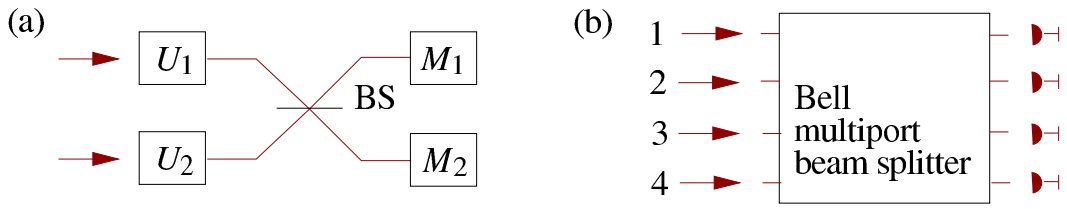

Figure 5.3: Linear optics networks for the realisation of a measurement of the basis states $|\Phi_i\rangle$ defined in Sections (5.2.4,5.2.5) after encoding the photonic qubits in the polarisation degrees of two photons (a) or into four different spatial photon modes (b) involving either a beam splitter (BS) or a 4×4 Bell multiport beam splitter.

basis states $|\Phi_i\rangle$ defined in Eq. (5.33) as

$$\begin{aligned} |\Phi_1\rangle &\rightarrow \tfrac{1}{2}\left(b_1^{\dagger 2} - b_3^{\dagger 2}\right)|\mathrm{vac}\rangle\,, \; |\Phi_2\rangle \rightarrow \tfrac{1}{2}\left(\mathrm{b}_2^{\dagger 2} - \mathrm{b}_4^{\dagger 2}\right)|\mathrm{vac}\rangle\,, \\ |\Phi_3\rangle &\rightarrow \tfrac{1}{\sqrt{2}}\left(b_1^{\dagger} b_2^{\dagger} - b_3^{\dagger} b_4^{\dagger}\right)|\mathrm{vac}\rangle\,, \; |\Phi_4\rangle \rightarrow \tfrac{1}{\sqrt{2}}\left(\mathrm{b}_1^{\dagger}\mathrm{b}_4^{\dagger} - \mathrm{b}_2^{\dagger}\mathrm{b}_3^{\dagger}\right)|\mathrm{vac}\rangle\,. \end{aligned} \tag{5.58}$$

The detection of two photons in the same output port, namely in 1 or 3 and in 2 or 4, corresponds to a measurement of the state $|\Phi_1\rangle$ and $|\Phi_2\rangle$, respectively as in the case for two-qubit phase gate implementation. However now, the detection of a photon in ports 1 and 4 or in 2 and 3 indicates a measurement of the state $|\Phi_4\rangle$, while a photon in the ports 1 and 2 or in 3 and 4 indicates the state $|\Phi_3\rangle$.

We now discuss an interesting feature of 2-photon coincidence measurement which we can exploit.

5.4.4 Time-resolved detection for non-identical photon sources

So far, we have assumed identical atom-cavity systems and therefore, photons generated from the photon sources only differ in their encoded degree of freedom (for example, polarisation, time-bin etc.). Non-identical atom-cavity systems in general yield different temporal photon pulse shapes as well as spatial modes and thus introduce an additional degree of freedom which allow for the origin of the photon pulse to be determined. Generally, this leads to errors in gate implementation as will be seen in this section. In principle, this can be fixed by pulse shape engineering if one has full knowledge of the cavity parameters. Otherwise, a time-resolved detection technique combined with spatial filters allows us to remove the which-way information due to non-identical pulse shapes. Recently, it has been shown how the Hong-Ou-Mandel dip, in which total photon indistinguishability is normally a neces-

sary requirement, can still be observed even with two distinguishable photons, provided one performs time-resolved postselection [Legero03, Legero04]. Time-resolved postselective detection is the essential mechanism that wipes away the which-way information as first suggested by Żukowski *et al.* [Żukowski93, Żukowski95].

It is convenient to start our discussion using the formalism of Legero *et al.* [Legero03, Legero04] with the simple situation where two distant atoms, labelled 1 and 2, are entangled with the aid of a beam splitter. Now, we consider a beam splitter where ports 1 and 2 are the input ports and ports 3 and 4 define the output ports, each containing an ideal photon detector. Correspondingly, the photon annihilation and creation operator for port j and polarisation i in frequency mode ω is denoted as $b_{ij}(\omega)$ and $b_{ij}^{\dagger}(\omega)$ respectively. By convention, the jth atom is placed at the jth input port. For each jth atom, we assume that its initial state is given by $c_{0j}|u_{0j}\rangle + c_{1j}|u_{1j}\rangle$. The jth atomic state is subsequently encoded (see Section 5.3.2) in the photon state as

$$|\psi\rangle_j = \sum_{i,k=0,1} c_{ij}|u_{ij}\rangle \int_{-\omega_b}^{\omega_b} d\omega s_j(\omega)\gamma_{ikj} b_{kj}^{\dagger}(\bar{\omega})|\mathrm{vac}\rangle. \tag{5.59}$$

such that the orthogonality condition $\sum_{k=0,1}\gamma_{ikj}\gamma_{lkj}^{*} = \delta_{il}$ is fulfilled. The coefficients γ_{ikj} are introduced to allow the generated photons to be transformed by arbitrary single qubit rotation. In addition, we have dropped the index for photon generation time τ since it is inconsequential to our discussion here. We have assumed perfect redundant encoding, where we have set without loss of generality, all cavity and laser driving parameters to be independent of polarisation. In principle, photon generation need not be perfect and there will generally be terms that do not contribute to any photon in the total atom-photon state vector. These terms can be neglected for our discussion as we use 2-photon detection to herald entanglement, thereby allowing us to disregard non-photon contributing terms. In contrast, this is not possible in 1-photon detection protocols. We then define the total input state as $|\Psi\rangle_{\mathrm{in}} = |\psi\rangle_1 \otimes |\psi\rangle_2$. We further define the unitary transformed total output state, before photon detection by $|\Psi\rangle_{\mathrm{out}} = S|\Psi\rangle_{\mathrm{in}}$ where S is a unitary operator that defines the beam splitter transformation. Specifically, we can set

$$\begin{aligned} S^{\dagger}b_{i3}(\omega)S &= U_{31,i}b_{i1}(\omega) + U_{32,i}b_{i2}(\omega)\,, \\ S^{\dagger}b_{i4}(\omega)S &= U_{41,i}b_{i1}(\omega) + U_{42,i}b_{i2}(\omega)\,, \end{aligned} \tag{5.60}$$

where $U_{mn,i}$ refers to the probability amplitude of redirecting a photon of polarisation i from input port n to output port m. Since we are dealing with time-resolved

detection, it is convenient to use the definition of the time-dependent electric field amplitude operator $E^+_{\lambda j}(t)$ for the jth port and polarisation $'\lambda'$ where $b_{\lambda j}(\omega) = \alpha_0 b_{0j}(\omega) + \alpha_1 b_{1j}(\omega)$ and $|\alpha_0|^2 + |\alpha_1|^2 = 1$ given by [Ou99b, Legero03]

$$E^+_{\lambda j}(t) = \frac{1}{\sqrt{2\pi}} \int_0^\infty d\omega K(\omega) \mathrm{e}^{-\mathrm{i}\omega t} b_{\lambda j}(\omega). \tag{5.61}$$

As in Legero *et al.* [Legero03] and Gardiner and Zoller [Gardiner04], we choose $K(\omega) \approx 1$ for reasons of normalisation and the fact that $s_j(\omega)$ is strongly peaked around ω_{cav}. Accordingly, using Eq. (5.60), the transformation of the electric field operator is thus given by

$$\begin{aligned} S^\dagger E^+_{\lambda 3}(t) S &= U_{31,\lambda} E^+_{\lambda 1}(t) + U_{32,\lambda} E^+_{\lambda 2}(t)\,, \\ S^\dagger E^+_{\lambda 4}(t) S &= U_{41,\lambda} E^+_{\lambda 1}(t) + U_{42,\lambda} E^+_{\lambda 2}(t)\,. \end{aligned} \tag{5.62}$$

It is convenient to note that for the input ports 1 and 2,

$$\begin{aligned} E^+_{\lambda j}(t)|\psi_j\rangle &= \sum_{i,k,l=0,1} \frac{c_{ij}}{\sqrt{2\pi}} |u_{ij}\rangle \int_{-\omega_b}^{\omega_b} d\omega \int_0^\infty d\tilde{\omega} \mathrm{e}^{-\mathrm{i}\tilde{\omega}t} \alpha_l b_{lj}(\tilde{\omega}) s_j(\omega) \gamma_{ikj} b^\dagger_{kj}(\bar{\omega}) |\mathrm{vac}\rangle \\ &= \sum_{i,k=0,1} \frac{c_{ij}\gamma_{ikj}\alpha_k}{\sqrt{2\pi}} |u_{ij}\rangle \mathrm{e}^{-\mathrm{i}\omega_{\mathrm{cav}}t} \int_{-\omega_b}^{\omega_b} d\omega \mathrm{e}^{-\mathrm{i}\omega t} s_j(\omega) |\mathrm{vac}\rangle \\ &= \sum_{i,k=0,1} c_{ij}\gamma_{ikj}\alpha_k \mathrm{e}^{-\mathrm{i}\omega_{\mathrm{cav}}t} f_j(t) |u_{ij}\rangle |\mathrm{vac}\rangle \end{aligned} \tag{5.63}$$

where

$$f_j(t) = \frac{1}{\sqrt{2\pi}} \int_{-\omega_b}^{\omega_b} d\omega \mathrm{e}^{-\mathrm{i}\omega t} s_j(\omega) \tag{5.64}$$

is the pulse shape of the photon [Duan03] in the jth input given by the Fourier transform of its frequency spectrum $s_j(\omega)$. We suppose that a photon is detected at port 3 at time t_3 with the polarisation $'a'$ and port 4 at time t_4 with the polarisation $'b'$. The unnormalised conditional state of the system, as in the formalism by Legero *et al.* [Legero03] and also Gardiner and Zoller [Gardiner04] is therefore given by $|\Psi\rangle_{\mathrm{cond}}$,

$$\begin{aligned} |\Psi\rangle_{\mathrm{cond}} &= E^+_{a3}(t_3) E^+_{b4}(t_4) |\Psi\rangle_{\mathrm{out}} \\ &= S S^\dagger E^+_{a3}(t_3) S S^\dagger E^+_{b4}(t_4) S |\Psi\rangle_{\mathrm{in}} \\ &= S(U_{31,a} U_{42,b} E^+_{a1}(t_3) E^+_{b2}(t_4) + U_{32,a} U_{41,b} E^+_{a2}(t_3) E^+_{b1}(t_4)) |\Psi\rangle_{\mathrm{in}}\,. \end{aligned} \tag{5.65}$$

For the sake of concreteness, we assume a 50:50 beam splitter so that $U_{mn,a} = U_{mn,b}$ is polarisation insensitive and $U_{31,k} = U_{41,k} = U_{32,k} = -U_{42,k} = \frac{1}{\sqrt{2}}$. We also set $\gamma_{ijk} = \delta_{ij}$ for simplicity. We further set $a =' 0'$ and $b =' 1'$ and require $c_{ij} = \frac{1}{\sqrt{2}}$. Using the relations given by Eq. (5.63), $|\Psi\rangle_{\text{cond}}$ can then be simplified to

$$|\Psi\rangle_{\text{cond}} = \frac{1}{4}(-f_1(t_3)f_2(t_4)|u_{01}\rangle|u_{12}\rangle + f_1(t_4)f_2(t_3)|u_{11}\rangle|u_{02}\rangle) \tag{5.66}$$

where we have conveniently dropped all the vacuum terms as well as the inconsequential global phase factor for readibility. For $|\Psi\rangle_{\text{cond}}$ to describe a maximally entangled singlet state (which we would like to prepare), it is necessary that the condition,

$$f_1(t_3)f_2(t_4) = f_1(t_4)f_2(t_3) \tag{5.67}$$

holds. This condition can be fulfilled unconditionally if the photon pulse shapes originating from both atoms are similar, i.e. $f_1(t) = \mathrm{k}f_2(t)$ for some complex constant k. This means the fidelity of the entangled state is guaranteed to be unity as long as a photon is detected in both output ports 3 and 4 irrespective of the time of detection. This is easily explained as the time of detection does not reveal the origin of the photon given that the photon pulse shapes are identical. In the case of distinguishable pulse shapes, one can still fulfil the condition given by Eq. (5.67) by setting $t_3 = t_4$, thus requiring perfect time-resolved coincidence detection. Note that this does not require any preknowledge of the pulse shape in either cavity to achieve arbitrary high fidelity. This is an illustration of the power of measurement-based approach to quantum computation in contrast to a fully coherent-based approach. Furthermore, since k is an unspecified constant that is complex, this implies that the introduction of any unknown slowly varying phase factor (with respect to the photon generation and detection time) in the path of the photons produces no observable effect on the fidelity of operation.

So far, we have assumed that the photon pulses from the 2 cavities have the same central frequency $\omega_1 = \omega_2 = \omega_{\text{cav}}$. Further, suppose that the 2 cavities are detuned relative to each other by $\Delta\omega = \omega_1 - \omega_2$, with everything else being identical. This is then equivalent to introducing a time-dependent phase factor to the pulse shape such that

$$f_1(t) = f_2(t)\exp(-\mathrm{i}\Delta\omega\mathrm{t}). \tag{5.68}$$

In this case, pulse similarity can still be obtained for $\Delta\omega(t_1 - t_2) = 2n\pi$. This condition was also previously predicted and used in the context of observing Hong-Ou-Mandel dip for photons of 2 different central frequencies but identical pulse shape

[Legero03, Legero04]. It is useful to determine analytically, within the approximation of adiabatic theorem, how the fidelity of entangled state preparation is degraded for 2 different cavity parameters. Firstly, it is convenient to recall formula for the pulse shape from Eq. (5.46)

$$f_j(t) = \sqrt{\kappa_j}\sin\theta_j(t)\exp(-\frac{\kappa_j}{2}\int_0^t d\tau \sin^2\theta_j(\tau)) \tag{5.69}$$

where

$$\sin\theta_j(t) = \frac{\Omega_j(t)}{\sqrt{\Omega_j^2(t)+g_j^2}} \tag{5.70}$$

and $\kappa_j, \Omega_j^2(t), g_j$ are the cavity decay, Rabi frequency of the driving laser and cavity coupling of the jth atom-cavity respectively. It is then obvious that the below condition with all other parameters being equal, guarantees pulse shape similarity, namely

$$\left|\frac{\Omega_1(t)}{g_1}\right| = \left|\frac{\Omega_2(t)}{g_2}\right|. \tag{5.71}$$

Assuming that this condition is fulfilled, we now consider $\kappa_1 \neq \kappa_2$. The time-dependent fidelity $F(t_3,t_4) = |\langle\Psi^-|\hat{\Psi}\rangle_{\rm cond}|^2$ given in terms of pulse shape functions is then given by[8]

$$F(t_3,t_4)) = \frac{(f_1(t_3)f_2(t_4)+f_1(t_4)f_2(t_3))^2}{2(f_1(t_3)^2f_2(t_4)^2+f_1(t_4)^2f_2(t_3)^2)}. \tag{5.72}$$

Following this, it is straightforward to show that the average fidelity $F_{\rm av}(b,a)$ with detectors integration time from $t=a$ to $t=b$ is given by

$$F_{\rm av}(b,a) = \frac{1}{2}\left(1+\frac{(\int_a^b dt f_1(t)f_2(t))^2}{\int_a^b dt f_1(t)^2\int_a^b dt f_2(t)^2}\right), \tag{5.73}$$

and is related to the overlap between the two pulse shape functions. It is interesting to also consider the case where the detected polarisation is the same. In this case, $|\Psi\rangle_{\rm cond}$ is given by

$$|\Psi\rangle_{\rm cond} = (-f_1(t_3)f_2(t_4)+f_1(t_4)f_2(t_3))\sum_{i=0,1}\alpha_i|u_{i1}\rangle\otimes\sum_{i=0,1}\alpha_i|u_{i1}\rangle. \tag{5.74}$$

For pulse similarity condition, this implies that $||\,|\Psi\rangle_{\rm cond}||^2$ vanishes, which is essentially the Hong-Ou-Mandel effect. As an example, we calculate the fidelity and

[8] $|\Psi^-\rangle = \frac{1}{\sqrt{2}}(|u_{01}\rangle|u_{12}\rangle - |u_{11}\rangle|u_{02}\rangle)$ and $|\hat{\Psi}\rangle_{\rm cond}\rangle = |\Psi\rangle_{\rm cond}\rangle/||\,|\cdot\rangle||$

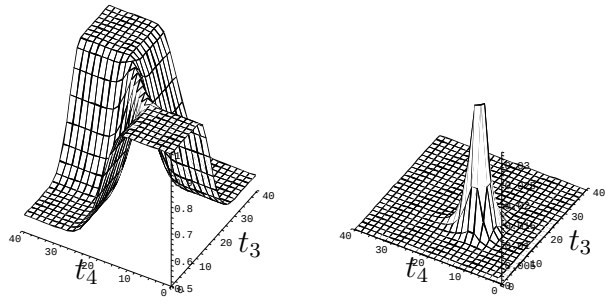

Figure 5.4: (a). Fidelity of entangled state and (b). Joint probability density of 2-photon coincidence detection for $\kappa_1 = 0.5\kappa_2$ for a guassian driving pulse with pulse width $\tau = 40/\kappa_2$,being centered in $20/\kappa_2$, with width $\sqrt{2}\tau/10$ and fixing $max(\Omega_j^2(t)/g_j^2) = 9$.

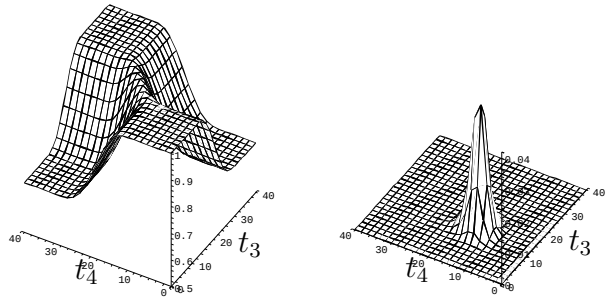

Figure 5.5: (a). Fidelity of entangled state and (b). Joint probability density of 2-photon coincidence detection for $\kappa_1 = 0.7\kappa_2$ for the same driving condition as above.

joint probability density of 2-photon coincidence detection for the case of a Gaussian driving pulse with pulse width $\tau = 40/\kappa_2$, being centered in $20/\kappa_2$, with width $\sqrt{2}\tau/10$, $\max(\Omega_j^2(t)/g_j^2) = 9$ and t_3 and t_4 normalised to κ_2^{-1}.

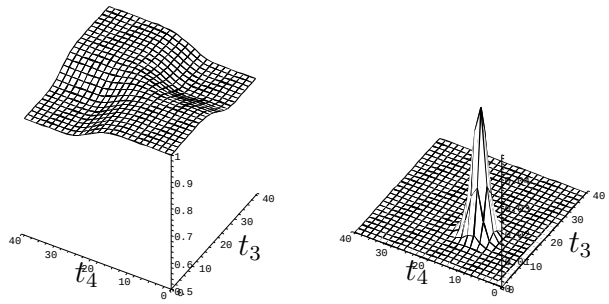

Figure 5.6: (a). Fidelity of entangled state and (b). Joint probability density of 2-photon coincidence detection for $\kappa_1 = 0.9\kappa_2$ for the same driving condition as above

From Fig. 5.4, Fig. 5.5 and 5.6 it can be seen that the fidelity is always unity for perfect coincidence. The more similar the cavities, the greater the tolerance of the fidelity. In the limit of identical cavities, coincidence photon pairs can be detected at any time interval with no effect on the fidelity. For comparision, the joint probability density for 2-photon detection is also calculated and the more different the cavities are, the lower the probability density of obtaining perfect coincidence generally. One observes the interesting trend of almost perfect fidelity at photon detection times at the leading and tail-end of the pulse even at non-perfect coincidence. This is attributed to the fact that the photon pulse shape at these times is relatively flat even for 2 non-identical cavities and in no way contributes to any which-way information. Mathematically, this corresponds to the condition where $f_1(t) \approx \mathrm{k} f_2(t)$ at the times t during the leading or tail-end of the photon pulses. Of course, the probability density for such coincidence is low as can be seen from the calculation. Without time-resolved detection, the average fidelity $F_{\mathrm{av}}(\infty, 0)$ corresponding to Fig. 5.4, Fig. 5.5 and 5.6 is 0.94, 0.98 and 0.99 respectively, consistent with the fact that dissimilarities of cavities generally yield lower fidelity.

We have given an example of how a time postselective 2-photon coincidence detection can yield high fidelity of entangled state preparation. It is straightforward to extend this to gate operation as described in this chapter. For example, one can assume the same setup as before except that now the following holds

$$\gamma_{001} = \gamma_{011} = \gamma_{101} = -\gamma_{111} = \gamma_{002} = \gamma_{102} = \mathrm{i}\gamma_{012} = -\mathrm{i}\gamma_{112}. \tag{5.75}$$

Repeating the same procedure as before and assuming the same detection syndrome with $a =' 0'$ and $b =' 1'$, one can show that the fidelity of gate operation is maximal when the pulse similarity condition is fulfilled.

5.5 Conclusions and discussions

We have shown that despite the fact that linear optics based Bell-state measurements on photons are incomplete, that does not prevent the deterministic implementation of a gate between distant qubits. Therefore, rather surprising, we show that it is not necessary to demonstrate deterministic entanglement generation in order to achieve a universal two-qubit gate with unit efficiency[9]. Furthermore, this scheme is intrin-

[9]The insurance aspect of this scheme allows processing of a single copy of unknown input state in principle. In contrast to cluster state implementation of two-qubit gates, the non-deterministic teleportation of an unknown unencoded input state into the cluster without insurance can destroy

sically interferometrically stable if one uses polarisation encoding and measurement due to the same reason as mentioned in Chapter 2. In the real world, nonideal situations of photon loss, inefficient photon detectors and photon generation would all lower the gate probability of success. Indeed, given photon number-resolving detectors (with no dark counts) of quantum efficiency p_d each, the probability of single-shot gate failure p_F, when two photons are not detected, is given by $1 - p_d^2$. One can also account for photon loss in the factor p_d. The solution towards fault-tolerant quantum computation in this scheme is to make a cluster state of high fidelity. High fidelity can be achieved because our scheme is a 2-photon heralded scheme. In the case where only one or no photon is detected, this is equivalent to tracing out the photon degrees of freedom. This effect can be removed by simply destroying the two qubits by measuring them in the computational basis in which an attempted cluster bond is required. This does not decrease the fidelity of the cluster state. Therefore, in the presence of imperfections such as photon loss and inefficient photon detectors, distributed quantum computation can still be performed with high fidelity by building a cluster state of distant qubits. Further discussions on cluster state buildup can be found in the work by Barrett and Kok [Barrett05] and Lim *et al.*[10] [Lim05a], and they lie out of the scope of this thesis. In addition, Benjamin *et al.* [Benjamin05] have also recently argued how the insurance scenario in our scheme can lead to a higher efficiency in building cluster states. We now proceed to the next chapter where we highlight an important application of the results of this chapter on generating photon entanglement on demand.

the input qubit if the teleportation fails.

[10]Details of efficient cluster state buildup based on the insurance scenario described in this chapter can be found here.

6

Distributed Photon Entanglement on Demand

In this short chapter, we highlight a useful result from Chapters 2 and 5 and show that distributed photon entanglement generation is possible on demand. In particular, we also demonstrate a duality relation that arises from our previous study of multiports which may give new perspectives in multiport design for quantum information processing.

6.1 Multiatom entanglement and multiphoton entanglement on demand

The key to multiphoton entanglement on demand lies in the initial creation of multiatom entanglement. We denote this step as the initialisation. Recalling Chapter 2 where we have mainly considered the Bell multiport, we place no restriction on the multiports considered in this chapter. We first allow each atom to be entangled with a photon and study what happens if the photons are passed through a multiport.

We assume that each ith atom is specified by two states $|\pm\rangle$ notated by $g^\dagger_{i\pm}|0\rangle$ using a second-quantised notation. Each of the atoms should first be maximally entangled with a photon feeding into each input of the $N \times N$ multiport such that we can write the total combined initial state as

$$|\Psi_{in}\rangle = \frac{1}{\sqrt{2^N}} \prod_{i=1}^{N} \Big(\sum_{\mu=+,-} g^\dagger_{i\mu}\, a^\dagger_{i\mu} \Big) |0\rangle. \tag{6.1}$$

Such a state preparation can be performed deterministically [Gheri98, Lim04] by an atom-cavity system as described in Chapter 5. The general atom-photon state $|\Psi_{in}\rangle$

after passing the photons through the multiport and upon collecting one photon per output port is then, up to normalisation and by analogy to Eq. (2.10), given by

$$|\Psi_{out}\rangle = \frac{1}{\sqrt{2^N}} \sum_{\sigma} \left[\prod_{i=1}^{N} U_{\sigma(i)i} \Big(\sum_{\mu=+,-} g_{i\mu}^{\dagger} b_{\sigma(i)\mu}^{\dagger} \Big) \right] |0\rangle \, . \tag{6.2}$$

Now, the next step is to choose a detection syndrome of the photons. Let the detection syndrome be defined by the postselected state

$$|\mathrm{S}\rangle = \prod_{j=1}^{N} \sum_{\mu} \alpha_{j\mu}^{*} b_{j\mu}^{\dagger} |0\rangle. \tag{6.3}$$

For example, $\alpha_{j\mu}^{*} b_{j\mu}^{\dagger}|0\rangle$ defines the state of a photon detected in output port j with polarisation μ. Note that we see a direct correspondance or analogy of $|\mathrm{S}\rangle$ to the input photon state (2.3). Applying the relevant projector, the multiatomic state $|\mathrm{A}\rangle$ can be shown to be projected onto

$$|\mathrm{A}\rangle = \frac{1}{\sqrt{2^N}} \sum_{\sigma} \left[\prod_{i=1}^{N} U_{\sigma(i)i} \Big(\sum_{\mu=+,-} \alpha_{\sigma(i)\mu} g_{i\mu}^{\dagger} \Big) \right] |0\rangle \tag{6.4}$$

Hence, a multiatomic state can be prepared by choosing an appropriate detection syndrome. Provided that the photons detectors have negligible dark counts, photon loss and inefficient detectors do not decrease the fidelity of state preparation. This is an advantage of choosing a coincidence (one photon per output port) detection syndrome. To get further insight, we can next substitute $i = \sigma^{-1}(j)$ and obtain

$$\begin{aligned} |\mathrm{A}\rangle &= \frac{1}{\sqrt{2^N}} \sum_{\sigma^{-1}} \left[\prod_{j=1}^{N} U_{j\sigma^{-1}(j)} \Big(\sum_{\mu=+,-} \alpha_{j\mu} g_{\sigma^{-1}(j)\mu}^{\dagger} \Big) \right] |0\rangle \\ &= \frac{1}{\sqrt{2^N}} \sum_{\sigma} \left[\prod_{i=1}^{N} U_{i\sigma(i)} \Big(\sum_{\mu=+,-} \alpha_{i\mu} g_{\sigma(i)\mu}^{\dagger} \Big) \right] |0\rangle \, . \end{aligned} \tag{6.5}$$

since σ^{-1} is just a dummy index for a permutation. A close comparision of (6.5) with (2.10) shows that this multiatomic state is of a similar[1] form to that of prepared multiphoton state given the input photon state (2.3), except that the input and output of the multiport are swapped. This suggests a duality relation of designing optical circuits aimed at preparing entangled atoms by examining how entangled photons(in analogy to the desired entangled atoms) can be prepared from product

[1]For simplicity, we have assumed bosonic statistics in the atoms for the discussion of the analogy with (2.10). In any case, (6.4) is the projected multiatomic state.

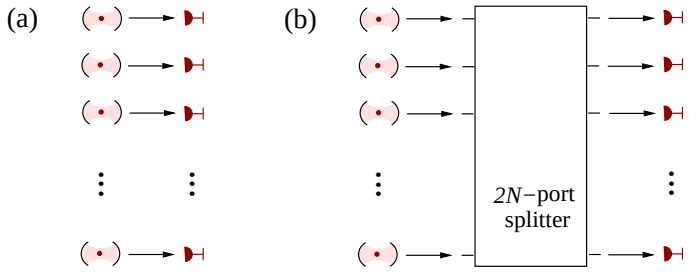

Figure 6.1: Experimental setup. (a) During the final "*push button*" step, the entanglement of N atom-cavity systems is mapped onto the state of N newly generated photons. (b) The initialisation of the system requires postselective measurements on the photon emission from the N cavities through a multiport beamsplitter.

states of photons(analogous to the detection syndrome).

An example of producing a three atom W-state was demonstrated using a 3×3 multiport [Zou04]. It was then conjectured, but not proven, that an $N \times N$ multiport may be used to prepare an N atom W-state. The work in this chapter qualifies this result rigourously for a Bell multiport.

In general, one can prepare or initialise a wide variety of atomic states with this method. One only needs to design the multiport that yields the desired mulitphoton state postselectively as described in Chapter 2. An alternative and more general way to create multiatom states by using universal two-qubit gates with insurance is described in Chapter 5.

Once the atomic qubits have been initialised, N photons in exactly the same state can be created by simply mapping the state of the sources onto the state of N newly generated photons whenever required [Lim04][2] (See Fig. 6.1). To accomplish this, the state of each photon source should first be encoded as in Chapter 5. Afterwards, the atomic qubits can be decoupled from the flying qubits by measuring again in a mutually unbiased basis with respect to the computation basis (i.e. the encoding basis) and performing a local operation on the photon whenever necessary. The generation of multiphoton entanglement on demand superficially resembles a remote state preparation of the state of N newly created photons by the multiatomic state. This mapping can also be accomplished more efficently without measurement by

[2] A very recent proposal by Kok *et al.* [Kok05a] built on the same point (i.e. initialise and map) to implement a multiphoton entanglement on demand source with a slightly different physical setup and procedure. The double-heralding step they used in the initialisation process can have the same advantages as coincidence detection. In addition, a cluster state is prepared offline and arbitrary multiatomic qubits can then be prepared by single qubit measurements to complete the initialisation process. Our scheme employs either the multiport approach for direct preparation of the atomic states or a series of universal two-qubit gates for atomic state initialisation.

choosing atomic levels similar to that in Lim *et al.* [Lim04]. For example, one can use a 5-level atom with ground states $|0\rangle$ and $|1\rangle$ constituting the logical qubit states as well as another ground state $|2\rangle$. The excited states are $|e_0\rangle$ and $|e_1\rangle$ where the cavity couples the transition $e_i - 2$ with a cavity photon of polarisation i. The exciting laser couples to the transition $e_i - i$ and drives an initialised atom similar to the description in Chapter 5, for example in the state $(\alpha|0\rangle + \beta|1\rangle) \otimes |\text{vac}\rangle$ to the state $|2\rangle \otimes (\alpha a_0^\dagger + \beta a_1^\dagger)|\text{vac}\rangle$ where $a_i^\dagger|\text{vac}\rangle$ denotes a photon with polarisation i in the external cavity field.

We can in principle create any arbitrary distributed N-photon state on demand in comparision with the schemes of Gheri *et al.* [Gheri98] and Schön *et al.*[3] [Schön05], where a restricted set of states on the same spatial mode can be created efficiently from a single atom-cavity system. Before we conclude our thesis, we observe that linear optics resources have been a crucial component in most parts of this thesis. We remove this resource next and consider entanglement generation with distant sources without cavities, i.e. in free space.

[3] I thank Christian Schön for stimulating discussions.

7

Photon Polarisation Entanglement from Distant Sources in Free Space

7.1 Introduction

In this chapter, we attempt to develop new perspectives to photon generation through distant sources in free space. There exist roughly two general approaches to create entangled photon pairs. Firstly, entangled photon pairs can be created within the *same* source as in atomic cascades [Aspect82], in parametric down conversion schemes [Kwiat95] and in the biexciton emission of a single quantum dot in a cavity [Stace03]. If the entanglement is not created within the same source, single photons can be brought together to overlap within their coherence time on a beamsplitter where a postselective entangling measurement can be performed on the output ports [Shih98]. A more detailed survey of single photon sources and entanglement generation is given in Chapter 2.

In contrast to this, we show that polarisation entanglement can also be obtained

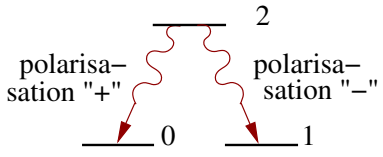

Figure 7.1: Λ-level configuration of the dipole source with the two degenerate ground states $|0\rangle$ and $|1\rangle$, the excited state $|2\rangle$ and optical transitions corresponding to the two orthogonal polarisations "+" and "−"

postselectively when the photons are created by *distant* sources in free space without having to control their photon collection times. As an example, we analyse the photon emission from two dipole sources that might be realised in the form of trapped atoms, diamond NV color centres, quantum dots or by using single atoms doped onto a surface. An interaction between the sources is not required. Each source should possess a Λ-type three-level configuration with the two degenerate ground states $|0\rangle$ and $|1\rangle$, the excited state $|2\rangle$ and optical transitions corresponding to the two orthogonal polarisations "+" and "−" along a well defined axis (see Fig. 7.1). Polarisation entanglement arises under the condition of the emission of two photons in different but carefully chosen directions independent from the initial state of the sources. Furthermore in our scheme, this leaves the dipoles in a maximally entangled state. Therefore, we can obtain both usable postselected 2-photon entanglement[1] and preselected dipole-dipole entanglement.

In order to understand how the scheme works, it is important to note that fluorescence from two distant dipole sources can produce an interference pattern on a far away screen, if the distance between the sources [Scully82, Eichmann93, Schön01] is comparable to the wavelength of the emitted photons. This can be understood as both sources contributing *coherently* to the creation of each photon. Consequently, the emission of one photon leaves a trace in the states of *all* its potential sources, depending on its polarisation and the direction of its wave vector [Schön01, Beige02], and can thus affect the state of the subsequently emitted photon. Such a picture is seen most directly using the quantum jump formalism [Hegerfeldt93, Dalibard92, Carmichael93].

The described interference pattern has already been observed [Eichmann93] in the intensity profile due to the flourescence of two four-level atoms scattered by laser light. Various attempts [Wong97, Itano98, Schön01, Agarwal02] to elucidate this have been made with the central theme that interference can only be observed when the which-way information is in principle absent. In addition, work aimed at investigating aspects of second-order photon or intensity-intensity correlations at perfect photon detection coincidences (i.e. at the same time) has also been made [Mandel83, Schön01, Agarwal02]. The modulation depth of such intensity-intensity correlations of the same polarisation is shown to be reachable to 100 % even when the intensity interference pattern may disappear. In other words, there exist a strong spatial antibunching of emitted photons of the same polarisation in free space where the detection of one photon does not permit the detection of another

[1] For example, postselected photon entanglement can be used for quantum cryptography

photon in certain directions at the same instant. Here, we exploit this feature for the generation of entangled photon pairs.

In this chapter, the detectors of Alice and Bob are placed such that all wave vector amplitudes contributing to the creation of a second photon with the same polarisation as the first one interfere destructively. In case of the collection of two photons (one by Alice and one by Bob) the shared pair has to be in a superposition of the state where Alice receives a photon with polarisation "+" and Bob a photon with polarisation "−" and the state where Alice receives a photon with polarisation "−" and Bob a photon with polarisation "+". Both share a maximally entangled pair, if the amplitudes for these two states are of the same size. In summary, polarisation entanglement is obtained with the help of postselection and interference effects. Related mechanisms have been proposed in the past to create atom-atom entanglement [Cabrillo99, Plenio99, Protsenko02, Simon03].

The pair creation scheme proposed in this paper is feasible with present technology and might offer several advantages to quantum cryptography. In contrast to parametric down conversion, the setup guarantees antibunching between subsequent photon pairs since the creation of a new pair is not possible without reexcitation of both sources. Furthermore, the scheme is robust with respect to the possible phase fluctuation in the exciting laser[2]. The final photon state does not depend on the initial state of the sources in case of a successful collection. Finally, the scheme may offer the possibility to generate *multiphoton* entanglement by incorporating more than two radiators in the setup.

7.2 Theory

Let us now discuss the creation of such an entangled photon pair in detail. We describe the interaction of the dipole sources with the surrounding free radiation field by the Schrödinger equation. The annihilation operator for a photon with wave vector $\mathbf{k}$, polarisation λ with polarisation vector[3] defined as $\epsilon_{\hat{\mathbf{k}}\lambda}$ is $a_{\mathbf{k}\lambda}$. The two dipole sources considered here are placed at the fixed positions $\mathbf{r}_1$ and $\mathbf{r}_2$ and should be identical in the sense that they have the same dipole moment $\mathbf{D}_{2j} = \langle 2|\mathbf{D}|j\rangle$ for the 2-j transition ($j = 0, 1$). The energy separation between the degenerate ground states and level 2 is $\hbar\omega_0$ while $\omega_k = kc$ and L^3 is the quantisation volume of the free radiation field. In addition, we define the ith atomic lowering and raising operator

[2] Axel Kuhn first brought this to my attention on discussion of this scheme.

[3] In this thesis, the notation is chosen such that $\hat{\mathbf{x}} \equiv \mathbf{x}/\|\mathbf{x}\|$.

as

$$S^-_{i,j} = |j\rangle_{ii}\langle 2|, \quad S^+_{i,j} = |2\rangle_{ii}\langle j|. \tag{7.1}$$

Using this notation, the system Hamiltonian becomes within the rotating wave approximation and with respect to the interaction-free Hamiltonian in the interaction picture,

$$\begin{aligned} H_{\mathrm{I}} &= \sum_{i=1,2}\sum_{j=0,1}\sum_{\mathbf{k},\lambda} \hbar g^{(j)}_{\mathbf{k}\lambda}\, \mathrm{e}^{-\mathrm{i}(\omega_0-\omega_k)t}\, \mathrm{e}^{-\mathrm{i}\mathbf{k}\cdot\mathbf{r}_i}\, a^\dagger_{\mathbf{k}\lambda}\, S^-_{i,j} + \mathrm{H.c.}\ , \\ &= \sum_{j=0,1} H^j_{\mathrm{I}1} + H^j_{\mathrm{I}2} \end{aligned} \tag{7.2}$$

which can be decomposed into terms $H^j_{\mathrm{I}i}$ relating only to each of the ith atom and

$$g^{(j)}_{\mathbf{k}\lambda} = \mathrm{i}e \left[\frac{\omega_k}{2\epsilon_0\hbar L^3}\right]^{1/2} (\mathbf{D}_{2j}, \epsilon_{\hat{\mathbf{k}}\lambda}) \tag{7.3}$$

is the coupling constant for the field mode $(\mathbf{k}, \lambda)$ to the 2-j transition of each source. With H_{I}, we can associate the unitary operator describing the evolution of the combined system from time t_1 to t_2 as $U_{\mathrm{I}}(t_2, t_1)$. The rotating wave approximation corresponds to neglecting the non-energy conserving terms that describe the excitation of atoms combined with the creation of a photon or the deexcitation of atoms combined with the annihilation of a photon. These effects are not unphysical [Knight73] but their contribution to the time evolution of the described system can be shown to be very small and almost impossible to observe.

7.2.1 Entangled photon and entanged dipole generation

To describe the effect of an emission on the state of the sources, we introduce the spontaneous decay rate of the 2-j transition $\Gamma_j \equiv (e^2\omega_0^3\,|\mathbf{D}_{2j}|^2)/(3\pi\epsilon_0\hbar c^3)$ and the reset or collapse operator $R_{\hat{\mathbf{k}},\lambda}$ which is associated with the quantum jump formalism [Hegerfeldt93, Dalibard92, Carmichael93]. A good review of the quantum jump approach can be found in Ref. [Plenio98]. For the sake of simplicity, we set $\Gamma_0 = \Gamma_1 = \Gamma$ in this chapter. The quantum jump formalism is an instance of a type of unravelling of the master equation describing the evolution of the dipole sources in an open environment such as the free radiation field. The source follows a so-called quantum state trajectory based on knowledge obtained from a real or ficticious continuous[4]

[4]More precisely, the measurement is not truly continuous but coarsed-grained at a timescale of Δt much larger than the transition optical period but also much smaller than the average timescale of atomic evolution. A truly continuous measurement will instead freeze the system due to the

time-resolved measurement that yields generally two types of observables. One of them is the no-photon observation and the other is a photon detection observation that can be direction and (or) polarisation specific. We first denote the free radiation field in the vacuum state $|0_{\rm ph}\rangle$ and define the reduced density operator of the dipole sources at time t as $\rho_a(t)$. We furthermore denote the 1-photon state of wave vector $\mathbf{k} = k\hat{\mathbf{k}}$ and polarisation λ by $|1_{k\hat{\mathbf{k}}\lambda}\rangle$. In the theory of quantum evolution of an open system, under the Born-Markovian approximation, the evolution of $\rho_a(t)$ given that at time t, the combined state is $\rho(t) = |0_{\rm ph}\rangle\rho_a(t)\langle 0_{\rm ph}|$, can be described by a superoperator $\mathcal{L}(\Delta t)$ that yields a Kraus operator sum representation given as

$$\rho_a(t) \to \mathcal{L}(\Delta t)\rho_a(t) = \rho_a(t+\Delta t) = \sum_\mu M_\mu \rho_a(t) M_\mu^\dagger \,. \tag{7.4}$$

Here $M_\mu = \langle \mu | U_{\rm I} | 0_{\rm ph}\rangle$ is associated with an observable μ and is also known as a Kraus operator. The above evolution is valid if we have no information of μ and puts $\rho_a(t+\Delta t)$ into a generally mixed state. This can be intepreted as an environment-induced measurement [Schön01] where the results of the measurement is not known. The situation changes if we perform a measurement and have full information on μ. The evolution is now described by

$$\rho_a(t) \to \mathcal{L}(\Delta t)\rho_a(t) = \rho_a(t+\Delta t) = \frac{M_\mu \rho_a(t) M_\mu^\dagger}{{\rm Tr}(M_\mu \rho_a(t) M_\mu^\dagger)} \,, \tag{7.5}$$

if the measurement in Δt yields an observable μ with probability ${\rm Tr}(M_\mu \rho_a(t) M_\mu^\dagger)$. The evolution of the source is thus generally stochastic leading to a quantum trajectory and the average of all stochastic evolutions yields the density operator obtained on solving the master equation, which gives an ensemble description. An instance of a stochastic evolution of the state is defined as a quantum trajectory of the quantum jump formalism. If a photon of polarisation λ and a wave vector pointing in the $\hat{\mathbf{k}}$ direction is detected within a coarse-grained time Δt small compared to the average timescale of the system evolution and large compared to the optical period, the evolution of the state of the source (see [Wong97, Schön01, Beige97] for more details) is given by

$$\rho_a(t+\Delta t) = \sum_k M_{\mu_k} \rho_a(t) M_{\mu_k}^\dagger / {\rm Tr}(\cdot) \approx R_{\hat{\mathbf{k}},\lambda} \rho_a(t_0) R_{\hat{\mathbf{k}},\lambda}^\dagger \Delta t / {\rm Tr}(\cdot) \,, \tag{7.6}$$

quantum Zeno effect.

with $M_{\mu_k} = \langle 1_{k\hat{\mathbf{k}}\lambda}|U_I(\Delta t + t, t)|0_{\rm ph}\rangle$ and[5]

$$R_{\hat{\mathbf{k}},\lambda} \equiv \sum_{i,j}\left[\frac{3\Gamma}{8\pi}\right]^{1/2}(\hat{\mathbf{D}}_{2j}, \epsilon_{\hat{\mathbf{k}}\lambda})\,\mathrm{e}^{-\mathrm{i}k_0\hat{\mathbf{k}}\cdot\mathbf{r}_i}\,S^-_{i,j}\ . \tag{7.7}$$

One can see that the detection of a photon within a short time Δt is always accompanied with a lowering or jump of the source within the same time Δt hence motivating the name "quantum jump" approach. Note that the probability density for the described emission is given by $\mathrm{Tr}(R_{\hat{\mathbf{k}},\lambda}\rho_a(t)R^\dagger_{\hat{\mathbf{k}},\lambda})$.

The no-photon time evolution of the system say between t_2 and t_1 is associated with a Kraus operator $M_0 = \langle 0_{\rm ph}|U_I(t_2,t_1)|0_{\rm ph}\rangle = U_{\rm cond}(t_2,t_1)$. More precisely, the state of the sources at t_2 after a no-photon event from t_1 is given by

$$\rho_a(t_2) = U_{\rm cond}(t_2,t_1)\rho_a(t_1)U^\dagger_{\rm cond}(t_2,t_1)/\mathrm{Tr}(\cdot) \tag{7.8}$$

where $U_{\rm cond}(t_2,t_1) = \mathrm{e}^{-\mathrm{i}H_{\rm cond}(t_2-t_1)/\hbar}$. This approach provides a non-Hermitian conditional Hamiltonian $H_{\rm cond}$ given by the following relation

$$I - \frac{\mathrm{i}}{\hbar}H_{\rm cond}\Delta t \approx U_{\rm cond}(\Delta t + t_0, t_0) = \langle 0_{\rm ph}|U_I(\Delta t + t_0, t_0)|0_{\rm ph}\rangle \tag{7.9}$$

where the r.h.s is evaluated by second-order perturbation theory for a coarse-grained time Δt similar to that of the timescale used in the derivation of the reset operator. In Eq. (7.9), $\langle 0_{\rm ph}|U_I(\Delta t + t_0, t_0)|0_{\rm ph}\rangle$ is given by

$$\begin{aligned}
&\langle 0_{\rm ph}|U_I(\Delta t + t_0, t_0)|0_{\rm ph}\rangle \qquad (7.10)\\
=\ &\langle 0_{\rm ph}|I - \frac{\mathrm{i}}{\hbar}\int_{t_0}^{\Delta t+t_0}dt' H_{\rm I}(t') - \frac{1}{\hbar^2}\int_{t_0}^{\Delta t+t_0}dt'\int_{t_0}^{t'}dt'' H_{\rm I}(t')H_{\rm I}(t'') + O(\Delta t^2)|0_{\rm ph}\rangle\\
=\ &I - \frac{1}{\hbar^2}\int_{t_0}^{\Delta t+t_0}dt'\int_{t_0}^{t'}dt''\langle 0_{\rm ph}|\Big[\sum_m H^m_{\rm I1}(t')H^m_{\rm I1}(t'') + H^m_{\rm I2}(t')H^m_{\rm I2}(t'')\\
&+\sum_{m\neq n} H^m_{\rm I1}(t')H^n_{\rm I1}(t'') + H^n_{\rm I2}(t')H^m_{\rm I2}(t'')\\
&+\sum_{m,n} H^m_{\rm I1}(t')H^n_{\rm I2}(t'') + H^n_{\rm I2}(t')H^m_{\rm I1}(t'')\Big]|0_{\rm ph}\rangle + O(\Delta t^2)
\end{aligned}$$

We further define the relative position vector $\mathbf{r} = \mathbf{r}_1 - \mathbf{r}_2$ where $r = \|\mathbf{r}\|$ is the distance between the atoms and denote $k_0 = \frac{\omega_0}{c}$. For the setup considered here, one

[5]Our analysis here apply only for degenerate levels $|0\rangle$ and $|1\rangle$ or in the case of non-degeneracies, when their frequency split $\Delta\omega$ is small enough such that $|\Delta\omega|\Delta t \approx 0$. For a more general discussion, see the formulation in Ref. [Hegerfeldt93].

finds in the absence of laser driving [Beige97, Wong97],

$$\begin{aligned} H_{\rm cond} &= \frac{\hbar}{2{\rm i}}\Big[\Gamma\sum_m (S^+_{1,m}S^-_{1,m}+S^+_{2,m}S^-_{2,m}) \\ &\quad +\sum_{m,n} C_{1m,2n}S^+_{1,m}S^-_{2,n}+C_{1n,2m}S^+_{1,n}S^-_{2,m}\Big], \end{aligned} \tag{7.11}$$

where $C_{in,jm}$ arises from dipole-dipole interaction and is given by

$$\begin{aligned} C_{in,jm} &= \frac{3\Gamma}{2}{\rm e}^{{\rm i}k_0 r}\Big[\frac{1}{{\rm i}k_0 r}((\hat{\mathbf{D}}_{2m},\hat{\mathbf{D}}_{2n})-(\hat{\mathbf{D}}_{2m},\hat{\mathbf{r}})(\hat{\mathbf{r}},\hat{\mathbf{D}}_{2m})) \\ &\quad +\Big(\frac{1}{(k_0r)^2}-\frac{1}{{\rm i}(k_0r)^3}\Big)((\hat{\mathbf{D}}_{2m},\hat{\mathbf{D}}_{2n})-3(\hat{\mathbf{D}}_{2m},\hat{\mathbf{r}})(\hat{\mathbf{r}},\hat{\mathbf{D}}_{2m}))\Big]. \end{aligned} \tag{7.12}$$

We consider only the cases where $C_{in,jm}$ is very small, or in other words, where the dipole-dipole interaction is insignificant. Without calculating the terms $C_{in,jm}$ explicitly, one can see that relative to the rate of spontaneous decay Γ, $C_{in,jm}$ scales as $(k_0r)^{-1}$ in the strongest possible dipole-dipole coupling scenario. This occurs when both dipoles are parallel with each other and orthogonal to the line joining both atoms. Therefore, in the limit of large k_0r, for example, $r > 25\lambda_0$ with $\lambda_0 = \frac{2\pi}{k_0}$, dipole-dipole coupling becomes insignificant.

The two-atom double slit experiment performed by Eichmann *et al.* [Eichmann93] also operates at this regime. We can thus simplify (7.11) and get

$$H_{\rm cond} = \frac{\hbar\Gamma}{2{\rm i}}\sum_m (S^+_{1,m}S^-_{1,m}+S^+_{2,m}S^-_{2,m}). \tag{7.13}$$

This Hamiltonian can also be derived by assuming that each atom couples to its own separate radiation field.

We now determine the state of the system under the condition of the collection of two photons, the first one at t_1 in the $\hat{\mathbf{k}}_{\rm X}$ direction with polarisation $\epsilon_{\hat{\mathbf{k}}_{\rm X}\lambda}$ and the second one at t_2 in the $\hat{\mathbf{k}}_{\rm Y}$ direction with polarisation $\epsilon_{\hat{\mathbf{k}}_{\rm Y}\lambda'}$. If the initial state of the dipole sources at $t=0$ is $|\varphi_0\rangle$, whilst the free radiation field is in its vacuum state, the unnormalised state of the dipole sources [Schön01] after the collection of the second photon is given by

$$\begin{aligned} |\psi(\epsilon_{\hat{\mathbf{k}}_{\rm Y}\lambda'}t_2|\epsilon_{\hat{\mathbf{k}}_{\rm X}\lambda}t_1)\rangle &= R_{\hat{\mathbf{k}}_{\rm Y},\lambda'}\,U_{\rm cond}(t_2,t_1)\,R_{\hat{\mathbf{k}}_{\rm X},\lambda}U_{\rm cond}(t_1,0)|\varphi_0\rangle \\ &= N(t_1,t_2)\langle 22|\varphi_0\rangle\sum_{i,j=0}^{1}((\hat{\mathbf{D}}_{2i},\epsilon_{\hat{\mathbf{k}}_{\rm Y}\lambda'})(\hat{\mathbf{D}}_{2j},\epsilon_{\hat{\mathbf{k}}_{\rm X}\lambda}){\rm e}^{-{\rm i}k_0\hat{\mathbf{k}}_{\rm Y}\cdot\mathbf{r}_1}{\rm e}^{-{\rm i}k_0\hat{\mathbf{k}}_{\rm X}\cdot\mathbf{r}_2} \\ &\quad +(\hat{\mathbf{D}}_{2j},\epsilon_{\hat{\mathbf{k}}_{\rm Y}\lambda'})(\hat{\mathbf{D}}_{2i},\epsilon_{\hat{\mathbf{k}}_{\rm X}\lambda}){\rm e}^{-{\rm i}k_0\hat{\mathbf{k}}_{\rm Y}\cdot\mathbf{r}_2}{\rm e}^{-{\rm i}k_0\hat{\mathbf{k}}_{\rm X}\cdot\mathbf{r}_1})|ij\rangle\,, \end{aligned} \tag{7.14}$$

with

$$N(t_1,t_2)=\frac{3}{8\pi}\,\Gamma \mathrm{e}^{-\Gamma(t_1+t_2)}\,. \tag{7.15}$$

Note that $\| \, |\psi(\hat{\mathbf{k}}_{\mathrm{Y}},t_2|\hat{\mathbf{k}}_{\mathrm{X}},t_1)\rangle \, \|^2$ yields the probability density for the corresponding event [Plenio98].

We now calculate the polarisation correlation $C_{\hat{\mathbf{k}}_{\mathrm{A}}\lambda,\hat{\mathbf{k}}_{\mathrm{B}}\lambda'}$ (i.e. the joint probability where Alice and Bob get a λ and λ' polarised photon respectively if Alice and Bob collect a photon each). It is simply given by

$$C_{\hat{\mathbf{k}}_{\mathrm{A}}\lambda,\hat{\mathbf{k}}_{\mathrm{B}}\lambda'}=||\psi(\epsilon_{\hat{\mathbf{k}}_{\mathrm{B}}\lambda'}t_2|\epsilon_{\hat{\mathbf{k}}_{\mathrm{A}}\lambda}t_1\rangle)|^2/\sum_{\lambda_1,\lambda_2}||\psi(\epsilon_{\hat{\mathbf{k}}_{\mathrm{B}}\lambda_1}t_2|\epsilon_{\hat{\mathbf{k}}_{\mathrm{A}}\lambda_2}t_1)\rangle|^2\,. \tag{7.16}$$

One can easily check that this is independent of t_1 and t_2 as all the time dependence cancels out in the normalising factor $N(t_1,t_2)$. We can use (7.16) to calculate the probability $C_{\pm}$ (C_{hv}) that both Alice and Bob get orthogonal polarisation if they each collect a photon in the circular (linear) basis. The importance of such a calculation lies in the fact that the circular and linear basis are mutually unbiased. This corresponds closely to the quantum cryptographic BB84 protocol where Alice and Bob perform measurements in a set of mutually unbiased bases. The existence of polarisation correlations in a set of mutually unbiased bases is a signature of entanglement (See Appendix A.).

To assure that Alice and Bob can receive a polarisation entangled pair, they should place their detectors in directions $\hat{\mathbf{k}}_{\mathrm{A}}$ and $\hat{\mathbf{k}}_{\mathrm{B}}$ with

$$\mathrm{e}^{-\mathrm{i}k_0(\hat{\mathbf{k}}_{\mathrm{A}}-\hat{\mathbf{k}}_{\mathrm{B}})\cdot(\mathbf{r}_1-\mathbf{r}_2)}=-1\,. \tag{7.17}$$

One can see that these positions are in general not unique. They have the physical interpretation of corresponding to a half-fringe interval in the far field of a double-slit experiment, in which the two atoms are replaced by pinholes which are symmetrically irradiated by a laser.

With condition (7.17), one obtains

$$\begin{aligned}
&|\psi(\epsilon_{\hat{\mathbf{k}}_{\mathrm{B}}\lambda'}t_2|\epsilon_{\hat{\mathbf{k}}_{\mathrm{A}}\lambda}t_1)\rangle=|\psi(\epsilon_{\hat{\mathbf{k}}_{\mathrm{A}}\lambda}t_2|\epsilon_{\hat{\mathbf{k}}_{\mathrm{B}}\lambda'}t_1)\rangle\\
&=N(t_1,t_2)2^{1/2}\,\mathrm{e}^{-\mathrm{i}k_0(\hat{\mathbf{k}}_{\mathrm{A}}\cdot\mathbf{r}_1+\hat{\mathbf{k}}_{\mathrm{B}}\cdot\mathbf{r}_2)}\,\langle 22|\varphi_0\rangle\\
&\Big[(\hat{\mathbf{D}}_{20},\epsilon_{\hat{\mathbf{k}}_{\mathrm{B}}\lambda'})(\hat{\mathbf{D}}_{21},\epsilon_{\hat{\mathbf{k}}_{\mathrm{A}}\lambda})-(\hat{\mathbf{D}}_{21},\epsilon_{\hat{\mathbf{k}}_{\mathrm{B}}\lambda'})(\hat{\mathbf{D}}_{20},\epsilon_{\hat{\mathbf{k}}_{\mathrm{A}}\lambda})\Big]\otimes|a_{01}\rangle
\end{aligned} \tag{7.18}$$

with $|a_{01}\rangle\equiv(|01\rangle-|10\rangle)/\sqrt{2}$. After two emissions, the dipole radiators are left in a maximally entangled state which is completely disentangled from the free radiation

field.

A coordinate system is introduced where the $\hat{\mathbf{z}}$-axis points in the direction of the line connecting the two sources and the $\hat{\mathbf{x}}$-axis coincides with the quantisation axis. In addition, we choose $\hat{\mathbf{k}}_{\mathrm{B}} = (1,0,0)^{\mathrm{T}}$, $\epsilon_{\hat{\mathbf{k}}_{\mathrm{B}}+} = \hat{\mathbf{D}}_{20} = (0,1,\mathrm{i})^{\mathrm{T}}/\sqrt{2}$ and $\epsilon_{\hat{\mathbf{k}}_{\mathrm{A}}-} = \hat{\mathbf{D}}_{21} = \hat{\mathbf{D}}^{*}_{20}$. Using the spherical coordinates (ϑ,φ) for Alice's detector position, one can write $\epsilon_{\hat{\mathbf{k}}_{\mathrm{A}}\pm} = \frac{1}{\sqrt{2}}(\epsilon_{\hat{\mathbf{k}}_{\mathrm{A}}h} \pm \mathrm{i}\epsilon_{\hat{\mathbf{k}}_{\mathrm{A}}v})$ with linear polarisations $\epsilon_{\hat{\mathbf{k}}_{\mathrm{A}}h} = (-\sin\varphi, \cos\varphi, 0)^{\mathrm{T}}$ and $\epsilon_{\hat{\mathbf{k}}_{\mathrm{A}}v} = (-\cos\vartheta\cos\varphi, -\cos\vartheta\sin\varphi, \sin\vartheta)^{\mathrm{T}}$ (see [Itano98]). Using (7.18), we have

$$C_{\pm} = C_{\hat{\mathbf{k}}_{\mathrm{A}}+,\hat{\mathbf{k}}_{\mathrm{B}}-} + C_{\hat{\mathbf{k}}_{\mathrm{A}}-,\hat{\mathbf{k}}_{\mathrm{B}}+} = \frac{(\cos\varphi + \sin\vartheta)^2 + (\cos\vartheta\sin\varphi)^2}{2(1+(\sin\vartheta\cos\varphi)^2)} \tag{7.19}$$

and

$$C_{hv} = C_{\hat{\mathbf{k}}_{\mathrm{A}}h,\hat{\mathbf{k}}_{\mathrm{B}}v} + C_{\hat{\mathbf{k}}_{\mathrm{A}}v,\hat{\mathbf{k}}_{\mathrm{B}}h} = \frac{(\cos\varphi)^2 + (\sin\vartheta)^2}{(1+(\sin\vartheta\cos\varphi)^2)}\,. \tag{7.20}$$

A straightforward evaluation of both equations for the range $\frac{\pi}{2} - 0.5 < \vartheta < \frac{\pi}{2} + 0.5$ and $-0.5 < \varphi < 0.5$ shows that[6]

$$C_{\pm} \approx C_{hv} \approx 1\,. \tag{7.21}$$

Therefore, having $\hat{\mathbf{k}}_{\mathrm{A}}$ pointing in a direction relatively close to the quantisation axis ($\vartheta = \pi/2, \varphi = 0$) which is the $\hat{\mathbf{x}}$-axis with a tolerance of ± 0.5 radians for both angles ϑ, φ together with condition (7.17) fulfilled will guarantee that Alice and Bob obtain an approximate postselected maximally entangled photon pair state which is maximally entangled in the ideal limit when $\hat{\mathbf{k}}_{\mathrm{A}} \to \hat{\mathbf{x}}$.

For illustration, we fix Alice's azimuthal angle $\varphi = 0$ and consider the case where $\theta \approx \frac{\pi}{2}$. Fig. 7.2 illustrates this case for both dipole separations at 25 and 26 wavelengths. As a comparision, Fig. 7.3 illustrates the case for both dipole separations at 25 and 27 wavelengths.

We observe that only when (7.17) is fufilled, Alice and Bob always collect photons of orthogonal polarisation each be it in the circular or linear basis, which therefore agrees with a postselected 2-photon entangled state in the singlet form. It can also be seen from both figures that even when an error of the dipole separation occurs within 2 wavelengths, the orthogonal polarisation correlation for collecting a photon pair can still above 90%. Therefore, strict Lamb-Dicke localisation of the dipole source is not essential. One may estimate the order of magnitude of the

[6]Note that $\vartheta = \pi/2$ should be excluded and intepreted as a limit point since we demand that condition (7.17) is fulfilled. At this limit where also $\varphi = 0$, then $C_{\pm} = C_{hv} = 1$ and we have a maximally entangled postselected state (See also Appendix A).

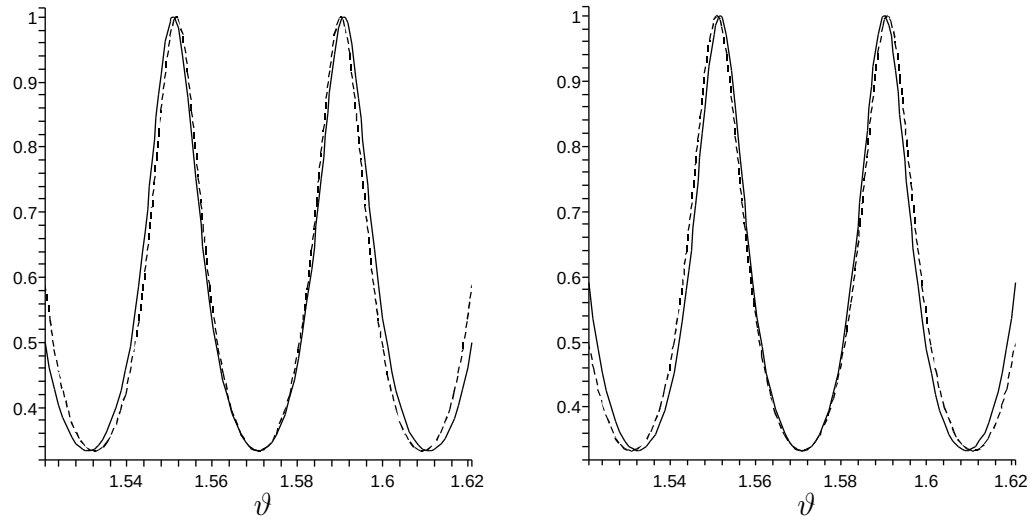

Figure 7.2: Photon-photon polarisation correlation for orthogonal polarisation as a function of the spherical coordinate ϑ of Alice's detector location while Bob collects photons in the $\hat{\mathbf{x}}$-direction in the circular(left) and vertical(right) basis for $r = 25\lambda_0$ (solid curve), and $r = 26\lambda_0$ (dotted curve).

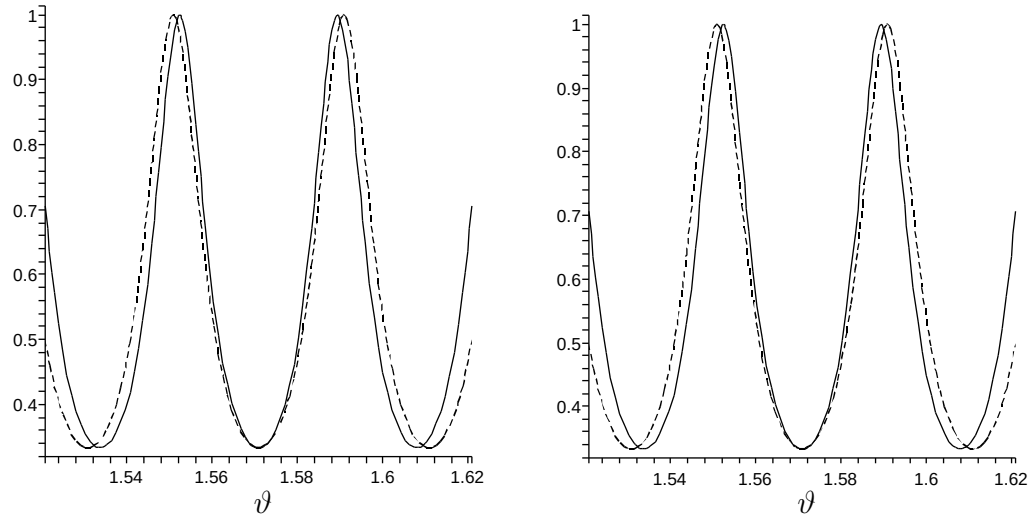

Figure 7.3: Photon-photon polarisation correlation for orthogonal polarisation as a function of the spherical coordinate ϑ of Alice's detector location while Bob collects photons in the $\hat{\mathbf{x}}$-direction in the circular(left) and vertical(right) basis for $r = 25\lambda_0$ (solid curve), and $r = 27\lambda_0$ (dotted curve).

probability of an entangled photon pair collection with the help of Fig. 7.2. One can then obtain the maximum count rate for detectors with solid angles Δ_A and Δ_B with the approximate formula $\frac{9}{64\pi^2}\Delta_A\Delta_B$ [Lim05b]. For example, for two detectors each of solid angular extent of 0.0225 steradians[7] yielding a minimum orthogonal polarisation correlation of 0.96, the order of magnitude for the collection probability P_c is approximately 10^{-6}. This is comparable to the scenario considered by Duan *et al.* [Duan04b] where he estimated the probability (also about $10^{-6} - 10^{-7}$) of entangling two distant ions in free space with the aid of a beamsplitter based on a similar scheme by Simon and Irvine [Simon03].

7.3 Experimental Implementation

As an example[8] we describe now a setup for entangled photon pair creation with two trapped ^{87}Rb atoms that is feasible with present technology [Schlosser01]. The ground states $|0\rangle$ and $|1\rangle$ are obtained from the $5^2S_{1/2}$ levels with $F = 1$ and have the quantum numbers $m_{\mathrm{F}} = -1$ and $m_{\mathrm{F}} = 1$. The excited state $|2\rangle$ is provided by the $5^2P_{3/2}$ level with $F = 0$. Suppose the atoms are initially in the $5^2S_{1/2}$ ground state with $F = 1$ and $m_{\mathrm{F}} = 0$ and a π polarised laser field is applied to excite to level 2 by a sharp π -pulse. After spontaneous emission into the ground states $|0\rangle$ and $|1\rangle$, another π polarised laser reinitialises the system by coupling these states to the $5^2P_{3/2}$ states with $F = 1$. From there the atoms return into the initial state via spontaneous decay. Due to their differences in polarisation and because of the detector locations, "+" (σ^+) and "−" (σ^-) polarised signal photons are distinguishable from the laser photons and spontaneously emitted π polarised photons. With a typical spontaneous decay time of order 10^{-8} s and assuming a rapid excitation with efficiency 90% and recycling time of order 10^{-7} with detection efficiency of 0.88 [Takeuchi99, Rosenberg05] and taking the estimate for collection efficiency P_c, the estimated count rate of entangled photons from this setup is expected to be $10^2 s^{-1}$. Compared to the yield possible in parametric downconversion being $10^6 s^{-1}$ [Kumar04], this scheme has relatively low yield. However, it does not require frequency filters for entangled photon detection and it also offers entanglement of the dipole sources as an attractive byproduct.

[7] Each detector consist of an array of slit detectors, with 15 slits each of 0.002×0.75 steradians at intervals fulfiling (7.17) for $r = 25\lambda_0$.

[8] I acknowledge Phillip Grangier for his kind discussion on experimental issues concerning this scheme during the 2003 summer school in Les Houches, Session 79, *Quantum Information and Entanglement*.

7.4 Conclusion

In conclusion, we proposed a scheme for the creation of polarisation entangled photon pairs by using two distant dipole radiators in free space. The entanglement is obtained by carefully choosing the detector positions with respect to the sources and arises under the condition of the collection of two photons independent of their emission times and the initial state of the sources. This also results in the source being maximally entangled. It is important to note that the photon entanglement detected can be used for quantum cryptography or Bell's inequality test. The scheme introduced in this chapter has the advantage of not requiring any linear optics and cavities compared to schemes in the previous chapters. Another application of the scheme would be to merely prepare two distant dipole sources in the maximally entangled ground state $|a_{01}\rangle$. In this case, no degeneracy of the atomic ground levels $|0\rangle$ and $|1\rangle$ is required. As in the case of Simon and Irvine [Simon03], this 2-photon detection protocol for preparing an entangled dipole state is robust against random laser phase fluctuations during the atomic excitation process as it contributes to just a trivial global phase factor. Furthermore, the 2-photon protocol can yield high fidelity of entangled state preparation more easily compared to the 1-photon protocol originally proposed by Cabrillo *et al.* [Cabrillo99]. This is due to the fact that in the 1-photon protocol, photons have to be gathered around the entire solid angle of emission to rule out the possibility of an undetected 2-photon emission which ruins the entanglement. This problem may be solved at the cost of a very weak excitation on the photon sources. The presented idea might find interesting applications in quantum computing with trapped atoms, diamond NV color centres, quantum dots or single atoms doped onto a surface and opens new possibilities for the creation of antibunched polarisation entangled photon pairs and even multiphoton entanglement by including more than two radiators in the setup.

Finally, we remark that the free-radiation field can be perceived roughly as a type of continuous beamsplitter, similar to a discrete multiport with infinite inputs and outputs. This leads generally to low entangled photon pair collection efficiency of 10^{-6} if we only gather photons in a well-defined directional spatial mode as explained earlier.

Photon entanglement schemes are therefore generally more realistic in the long-run with linear optics resources and single photon sources emitting on demand in well directed spatial modes as demonstrated in the rest of the thesis, owing to the higher success probability that can be obtained. Linear optics also offers flexibility in generating a wider variety of entangled states compared to the free space approach

described in this chapter. It is now time to conclude this thesis.

8

Summary and Outlook

The work of this thesis demonstrates various closely related aspects of quantum information processing with single photons as motivated in Chapter 1. Hopefully, it adds new perspectives to the relationship between single photons and their sources and the implication to quantum information processing in general. The summary of the main work is as follows.

In Chapter 2, we showed that a wide range of highly entangled multiphoton states, including W-states, can be prepared by interfering *single* photons inside a Bell multiport beam splitter and using postselection. The described setup, being photon encoding independent can be used to generate polarisation, time-bin and frequency encoded multiphoton entanglement, even when using only a single photon source. The success probability has a surprisingly non-monotonic decreasing trend as the number of photons increases.

In Chapter 3, we demonstrated how the HOM dip can be generalised to multiphoton coincidence detection in multiport beamsplitters. We considered the canonical symmetric Bell multiport and show that the HOM dip can be observed for all $N \times N$ Bell multiports where N is even but not necessarily when N is odd. Note that this observation applies generally to all bosons, of which photons are an example, thus having wide applicability. For the sake of completeness, we also discussed multifermionic scattering through a multiport and showed that identical fermions always leave the output ports of the multiport separately.

In Chapter 4, we proposed a scheme for implementing a multipartite quantum filter that uses entangled photons as a resource. It is shown that the success probability for the 2-photon parity filter can be as high as $\frac{1}{2}$, which is the highest that has so far been predicted without the help of universal two-qubit quantum gates.

Furthermore, the required number of ancilla photons is the least of all current parity filter proposals. Remarkably, the quantum filter operates with probability $\frac{1}{2}$ even in the N-photon case, regardless of the number of photons in the input state.

In Chapter 5 we described the efficient implementation of eventually deterministic two-qubit gate operations between single photon sources, despite the restriction of the no-go theorem on deterministic Bell measurement with linear optics. No entangled ancilla photons and photon-feed into cavities are needed. The key principle for our approach is based on source encoding to the photon that is generated as well as measurements in a mutually unbiased basis with respect to the computational basis. The described approach is highly general and lends wide implementation to various types of single photon sources. Furthermore, the scheme is still robust even in the case of dissimilarities of the photon sources, a testament to the unique character of a measurement-based approach to quantum computing. Our approach also gives fresh perspectives on the use of mutually unbiased basis in quantum computation, besides existing applications in quantum cryptography and for solving the Mean King's problem.

In Chapter 6, we used ideas from Chapters 2 and 5 to show how multiphoton entanglement on demand can be realised. Generally speaking, any multiphoton qubit state can be generated on demand in a distributed manner. At the same time, we also relate a duality relation between preparing photon entanglement and atom entanglement which may lead to new perspectives in multiport designs for entanglement generation.

In Chapter 7, we showed, using a setup closely resembling a Young double-slit experiment, that dipole-dipole as well as 2-photon entanglement can be generated with photons emitted from two distant dipole sources in free space (i.e. without the aid of linear optics setup). The scheme is highly robust to the dipole excitation imperfections. In the case of two sources, the entanglement arises under the condition of two emissions in certain spatial directions and leaves the dipoles in a maximally entangled state. This work adds new perspectives to current views on the entanglement generation using measurements.

The outlook and possible extensions to the work in this thesis are manifold. For example, the work in Chapter 2 and 3 is mainly restricted to Bell multiports due to a cyclic symmetry which we exploited. It is interesting to examine a greater variety of multiports defined by redirection or transfer matrices of various symmetries and their implications on multiphoton scattering and entanglement generation. Here, we have confined ourselves to analysing pure states and have not considered photon mixed-states for simplicity. This might lead to applications like the characterisation of

photons or multiports. We also did not consider EPR photon pairs as possible inputs to multiports which may yield exciting possibilities in multiphoton entanglement generation with higher probability of success. One could also extend this work to the investigation of POVMs with detectors and multiports. An extension of Chapter 3 may find application in experiments with particles with exotic statistics such as anyons[1]. Finally, multiports with weak nonlinearities may yield interesting prospects in enhanced multiphoton state preparation due to cooperative enhancement[2].

In Chapter 4, we have dealt with a simple setup for a multiphoton filter. It is interesting to see how this can be extended to arbitrary multiphoton gates and if the probability of success could be increased by combining approaches using an $N \times N$ multiport. With the aid of an arbitrary photon ancilla, generated perhaps by a multiphoton source on demand, one might be able to implement a programmable multiphoton gate. Further extensions to this work, hinted by the duality relation obtained in Chapter 6, might lead to a multiatom filter implementation.

Chapter 5 presents possible extensions to higher dimensional quNit operations or direct multiatom gate implementation. This might be implemented with the aid of a linear optics multiport. For example in this chapter, we have already used multiports for measurements leading to useful gate implementations. These techniques could be extended to new and interesting results. An intriguing observation of the choice of mutually unbiased basis used in this chapter yields, on suitable rearragement of the coefficents of the computational basis, a 4×4 Fourier transform matrix, which defines a Bell multiport[3]. The relationship between mutually unbiased basis and multiports may be worth investigating.

The work of Chapter 7 may in principle be extended to multiple dipoles or various energy level structures and by taking into account of dipole-dipole interaction or various means of dipole excitation. So far, we have restricted ourselves to the simplest case of two initially excited dipoles which is experimentally reasonable. Spatial polarisation correlations or intensity correlations may, for example be exploited for certain search tasks as demonstrated by Agarwal *et al.* [Agarwal04].

In this thesis, we have confined ourselves to discrete quantum information processing with photons and have said nothing about the equally rich field of continuous variable processing with photons or even a hybrid field of discrete-continuous variables. It may be that the work here can be extended to such domains and might lead to analogous applications.

[1] I thank Vlatko Vedral for stimulating discussions.
[2] I thank Jim Franson for stimulating discussions.
[3] I thank Thomas Durt for bringing this to my attention.

Finally, although we have focused our attention to single photons, many parts of this thesis may find analogous applications in other flying qubits such as electrons, which in contrast to photons, have fermionic statistics. It is noteworthy that many linear optical operations on photons can also be implemented on electrons. At the same time, there exist an intriguing prospect of setups, such as doped fibers, that modify the quantum statistics of the photons. One might envision new capabilities of quantum information processing with single photons using multiport setups consisting of such doped fibers in the future. It is hoped that the work in this thesis adds to the overall development as well as inspiring new research in quantum information processing.

A

Inferring the singlet state from polarisation statistics

We assume that Alice and Bob possess a shared reference frame of photon polarisation. They perform random measurements in two basis, one of which is the linear basis B_1 spanned by $|h\rangle$ and $|v\rangle$ and the other, the circular basis B_2 spanned by $|\pm\rangle = \frac{1}{\sqrt{2}}(|h\rangle \pm |v\rangle)$. We assume that the 2-photon state to be measured by Alice and Bob is in the general form ρ. We can write the POVM elements E_{1s} and E_{1d} for B_1 as

$$E_{1s} = |hh\rangle\langle hh| + |vv\rangle\langle vv| \ , E_{1d} = |hv\rangle\langle hv| + |vh\rangle\langle vh| \,, \tag{A.1}$$

and the POVM elements E_{2s} and E_{2d} for B_2 as

$$E_{2s} = |++\rangle\langle ++| + |--\rangle\langle --| \ , E_{2d} = |+-\rangle\langle +-| + |-+\rangle\langle -+| \,. \tag{A.2}$$

Note that $E_{1s} + E_{1d} = E_{2s} + E_{2d} = 1$. If Alice and Bob always detects orthogonal polarisations in B_1 and B_2, we wish to show that the only state consistent with this observation is the singlet state(which is maximally entangled) given by $\rho = |\Phi_-\rangle\langle\Phi_-|$[1] where $|\Phi-\rangle = \frac{1}{\sqrt{2}}(|hv\rangle - |vh\rangle)$. This approach does not require a full tomographic measurement and may shed new perspectives to the notion of optimal measurements in quantum tomography. We therefore have

$$\mathrm{Tr}(E_{1d}\rho) = 1 \tag{A.3}$$

[1] I thank Jens Eisert for his help in this problem.

and

$$\mathrm{Tr}(E_{2d}\rho) = 1\,. \tag{A.4}$$

We know that ρ must be positive semi-definite. This is to allow a valid probability interpretation should we choose to arbitrarily reduce the degree of freedom specifying ρ. This restriction together with Eq. (A.3) implies that ρ can only be of the form $\rho = a|hv\rangle\langle hv| + c|hv\rangle\langle vh| + c^*|vh\rangle\langle hv| + b|vh\rangle\langle vh|$ where $a+b = 1$ and a,b are positive real numbers. Adding condition (A.4) yields the further constraint $a = b = \frac{1}{2}$ as well as $c = -\frac{1}{2}$. This implies that $\rho = |\Phi_-\rangle\langle\Phi_-|$.

References

[Agarwal02] G. S. Agarwal, J. von Zantheir, C. Skornia and H. Walther, Phys. Rev. A., **65**, 053826 (2002).

[Agarwal04] G. S. Agarwal, G. O. Ariunbold, J. von Zanthier and H. Walther, *Non-classical imaging for a quantum search of trapped ions* (2004). Quant-ph/0401141.

[Aliferis04] P. Aliferis and D. W. Leung, Phys. Rev. A., **70**, 062314 (2004).

[Aspect82] A. Aspect, P. Grangier and G. Roger, Phys. Rev. Lett., **49**, 91 (1982).

[Barenco95] A. Barenco, C. H. Bennett, R. Cleve, D. P. DiVincenzo, N. Margolus, P. Shor, T. Sleator, J. A. Smolin and H. Weinfurter, Phys. Rev. A., **52**, 3457 (1995).

[Barnett98] S. M. Barnett, L. S. Phillips and D. T. Pegg, Opt. Comm., **158**, 45 (1998).

[Barrett04] M. D. Barrett, J. Chiaverini, T. Schaetz, J. Britton, W. M. Itano, J. D. Jost, E. Knill, C. Langer, D. Leibfried, R. Ozeri and D. J. Wineland, Nature, **429**, 737 (2004).

[Barrett05] S. D. Barrett and P. Kok, Phys. Rev. A., **71**, 060310 (2005).

[Bartlett05] S. D. Bartlett, T. Rudolph and R. W. Spekkens, *Dialogue concerning two views on quantum coherence: Factist and fictionist* (2005). Quant-ph/0507214.

[Beige97] A. Beige, *Kooperative Effekte in der Fluoreszenz zweier Atome*, Ph.D. thesis, Georg-August-Universität zu Göttingen, Göttingen, Germany (1997).

[Beige00] A. Beige, D. Braun, B. Tregenna and P. L. Knight, Phys. Rev. Lett., **85**, 1762 (2000).

[Beige02] A. Beige, C. Schön and J. Pachos, Fortschr. Phys., **50**, 594 (2002).

[Bell65] J. S. Bell, Physics, **1**, 195 (1965).

[Benjamin05] S. C. Benjamin, J. Eisert and T. M. Stace, *Optical generation of matter qubit graph states* (2005). Quant-ph/0506110.

[Bennett84] C. H. Bennett and G. Brassard, Proc. IEEE Int. Conf. Computers, Systems and Signal Processing, p. 175 (1984).

[Bennett92] C. H. Bennett and S. J. Wiesner, Phys. Rev. Lett., **69**, 2881 (1992).

[Bennett93] C. H. Bennett, G. Brassard, C. Crépeau, R. Jozsa, A. Peres and W. K. Wootters, Phys. Rev. Lett., **70**, 1895 (1993).

[Bennett96] C. H. Bennett, G. Brassard, S. Popescu, B. Schumacher, J. A. Smolin and W. K. Wooters, Phys. Rev. Lett., **76**, 722 (1996).

[Benson00] O. Benson, C. Santori, M. Pelton and Y. Yamamoto, Phys. Rev. Lett., **84**, 2513 (2000).

[Bergmann98] K. Bergmann, H. Theuer and B. W. Shore, Rev. Mod. Phys., **70**, 1003 (1998).

[Beveratos02] A. Beveratos, R. Brouri, T. Gacoin, A. Villing, J. P. Poizat and P. Grangier, Phys. Rev. Lett., **89**, 187901 (2002).

[Blinov04] B. B. Blinov, D. L. Moehring, L.-M. Duan and C. Monroe, Nature, **428**, 153 (2004).

[Bose99] S. Bose, P. L. Knight, M. B. Plenio and V. Vedral, Phys. Rev. Lett., **83**, 5158 (1999).

[Bose02] S. Bose and D. Home, Phys. Rev. Lett., **88**, 050401 (2002).

[Bourennane04a] M. Bourennane, M. Eibl, S. Gaertner, C. Kurtsiefer, A. Cabello and H. Weinfurter, Phys. Rev. Lett., **92**, 107901 (2004).

[Bourennane04b] M. Bourennane, M. Eibl, C. Kurtsiefer, S. Gaertner, H. Weinfurter, O. Gühne, P. Hyllus, D. Bruß, M. Lewenstein and A. Sanpera, Phys. Rev. Lett., **92**, 087902 (2004).

[Braunstein95] S. L. Braunstein and A. Mann, Phys. Rev. A., **51**, R1727 (1995).

[Brendel99] J. Brendel, N. Gisin, W. Tittel and H. Zbinden, Phys. Rev. Lett., **82**, 2594 (1999).

[Briegel98] H. J. Briegel, W. Dür, J. I. Cirac and P. Zoller, Phys. Rev. Lett., **81**, 5932 (1998).

[Briegel01] H. J. Briegel and R. Raussendorf, Phys. Rev. Lett., **86**, 910 (2001).

[Browne03] D. E. Browne, M. B. Plenio and S. F. Huelga, Phys. Rev. Lett., **91**, 067901 (2003).

[Browne05] D. E. Browne and T. Rudolph, Phys. Rev. Lett., **95**, 010501 (2005).

[Bužek96] V. Bužek and M. Hillery, Phys. Rev. A., **54**, 1844 (1996).

[Cabrillo99] C. Cabrillo, J. I. Cirac, P. Garcia-Fernandez and P. Zoller, Phys. Rev. A., **59**, 1025 (1999).

[Calarco04] T. Calarco, U. Dorner, P. Julienne, C. Williams and P. Zoller, Phys. Rev. A., **70**, 012306 (2004).

[Calderbank96] A. R. Calderbank and P. W. Shor, Phys. Rev. A., **54**, 1098 (1996).

[Calsamiglia01] J. Calsamiglia and N. Lütkenhaus, Appl. Phys. B., **72**, 67 (2001).

[Campos00] R. A. Campos, Phys. Rev. A., **62**, 013809 (2000).

[Carmichael93] H. Carmichael, *An Open Systems Approach to Quantum Optics, Lecture Notes in Physics* **18** ((Springer: Berlin), 1993).

[Cassettari00] D. Cassettari, B. Hessmo, R. Folman, T. Maier and J. Schmiedmayer, Phys. Rev. Lett., **85**, 5483 (2000).

[Cerf98] N. J. Cerf, C. Adami and P. G. Kwiat, Phys. Rev. A., **57**, R1477 (1998).

[Chen04] T. W. Chen, C. K. Law and P. T. Leung, Phys. Rev. A., **69**, 063810 (2004).

[Chen05] Y.-A. Chen, A.-N. Zhang, Z. Zhao, X.-Q. Zhou, C.-Y. Lu, C.-Z. Peng, T. Yang and J.-W. Pan, *Experimental quantum secret sharing and third-man quantum cryptography* (2005). Quant-ph/0502131.

[Chiaverini04] J. Chiaverini, D. Leibfried, T. Schaetz, M. D. Barrett, R. B. Balkestad, J. Britton, W. M. Itano, J. D. Jost, E. Knill, C. Langer, R. Ozeri and D. J. Wineland, Nature, **432**, 602 (2004).

[Chiaverini05] J. Chiaverini, J. Britton, D. Leibfried, E. Knill, M. D. Barrett, R. B. Blakestad, W. Itano, J. Jost, C. Langer, R. Ozeri, T. Schaetz and D. Wineland., Science, **308**, 997 (2005).

[Childs05] A. M. Childs, D. W. Leung and M. A. Nielsen, Phys. Rev. A., **71**, 032318 (2005).

[Cho04] J. Cho and H. W. Lee, *Controlled unitary operation between two distant atoms* (2004). Quant-ph/0409136.

[Ciaramicoli01] G. Ciaramicoli, P. Tombesi and D. Vitali, J. Opt. B: Quantum Semiclass. Opt., **3**, S72 (2001).

[Cirac95] J. I. Cirac and P. Zoller, Phys. Rev. Lett., **74**, 4091 (1995).

[Cirac97] J. I. Cirac, H. J. Kimble and H. Mabuchi, Phys. Rev. Lett., **78**, 3221 (1997).

[Cirac99] J. I. Cirac, A. Ekert, S. F. Huelga and C. Macchiavello, Phys. Rev. A., **59**, 4249 (1999).

[Clauser69] J. F. Clauser, M. A. Horne, A. Shimony and R. A. Holt, Phys. Rev. Lett., **23**, 880 (1969).

[Dalibard92] J. Dalibard, Y. Castin and K. Mølmer, Phys. Rev. Lett., **68**, 580 (1992).

[Deutsch85] D. Deutsch, Proc. Royal Soc. London A, **400**, 96 (1985).

[Deutsch92] D. Deutsch and R. Jozsa, Proc. Royal Soc. London A, **439**, 553 (1992).

[DiVincenzo95] D. P. DiVincenzo, Phys. Rev. A., **51**, 1015 (1995).

[DiVincenzo00] D. P. DiVincenzo, Fortschr. Phys., **48**, 771 (2000).

[Duan03] L. M. Duan, A. Kuzmich and H. J. Kimble, Phys. Rev. A., **67**, 032305 (2003).

[Duan04a] L. M. Duan, Phys. Rev. Lett., **93**, 100502 (2004).

[Duan04b] L. M. Duan, B. B. Blinov, D. L. Moehring and C. Monroe, Quant. Inf. Comp., **4**, 165 (2004).

[Duan05] L. M. Duan, B. Wang and H. J. Kimble, *Robust quantum gates on neutral atoms with cavity-assisted photon-scattering* (2005). Quant-ph/0505054.

[Dür00] W. Dür, G. Vidal and J. I. Cirac, Phys. Rev. A., **62**, 062314 (2000).

[Eibl03] M. Eibl, S. Gaertner, M. Bourennane, C. Kurtsiefer, M. Żukowski and H. Weinfurter, Phys. Rev. Lett., **90**, 200403 (2003).

[Eichmann93] U. Eichmann, J. C. Bergquist, J. J. Bollinger, J. M. Gilligan, W. M. Itano, D. J. Wineland and M. G. Raizen, Phys. Rev. Lett., **70**, 2359 (1993).

[Eisert00] J. Eisert, K. Jacobs, P. Papadopoulos and M. B. Plenio, Phys. Rev. A., **62**, 052317 (2000).

[Eisert05] J. Eisert, Phys. Rev. Lett., **95**, 040502 (2005).

[Ekert91] A. K. Ekert, Phys. Rev. Lett., **67**, 881 (1991).

[Englert01] B.-G. Englert, C. Kurtsiefer and H. Weinfurter, Phys. Rev. A., **63**, 032303 (2001).

[Enk97] S. J. van Enk, J. I. Cirac and P. Zoller, Phys. Rev. Lett., **79**, 5178 (1997).

[Enk98] S. J. van Enk, J. I. Cirac and P. Zoller, Science, **279**, 205 (1998).

[Enk02] S. J. van Enk and C. A. Fuchs, Phys. Rev. Lett., **88**, 027902 (2002).

[Fattal04] D. Fattal, K. Inoue, J. Vuckovic, C. Santori, G. S. Solomon and Y. Yamamoto, Phys. Rev. Lett., **92**, 037903 (2004).

[Feynman82] R. Feynman, *Simulating physics with computers*, International Journal of Theoretical Physics, **21**(6&7), 467 (1982).

[Fiurasek02] J. Fiurasek, Phys. Rev. A., **65**, 053818 (2002).

[Fiurasek03] J. Fiurasek, S. Massar and N. J. Cerf, Phys. Rev. A., **68**, 042325 (2003).

[Franson01] J. D. Franson and T. B. Pittman, Phys. Rev. A., **64**, 062311 (2001).

[Franson02] J. D. Franson, M. M. Donegan, M. J. Fitch, B. C. Jacobs and T. B. Pittman, Phys. Rev. Lett., **89**, 137901 (2002).

[Franson04] J. D. Franson, B. C. Jacobs and T. B. Pittman, Phys. Rev. A., **70**, 062302 (2004).

[Gardiner04] C. W. Gardiner and P. Zoller, *Quantum Noise* (Springer, 2004), third edition.

[Gasparoni04] S. Gasparoni, J.-W. Pan, P. Walther, T. Rudolph and A. Zeilinger, Phys. Rev. Lett., **93**, 020504 (2004).

[Gheri98] K. M. Gheri, C. Saavedra, P. Törmä, J. I. Cirac and P. Zoller, Phys. Rev. A., **58**, R2627 (1998).

[Gisin02] N. Gisin, C. G. Ribordy, W. Tittel and H. Zbinden, Rev. Mod. Phys., **74**, 145 (2002).

[Gottesman98] D. Gottesman, Phys. Rev. A., **57**, 127 (1998).

[Gottesman99] D. Gottesman and I. L. Chuang, Nature, **402**, 390 (1999).

[Grover96] L. K. Grover, *A fast quantum mechanical algorithm for estimating the median* (1996). Quant-ph/9607024.

[Grudka02] A. Grudka and A. Wojcik, Phys. Rev. A., **66**, 064303 (2002).

[Gulde03] S. Gulde, M. Riebe, G. P. T. Lancaster, C. Becher, J. Eschner, H. Häffner, F. Schmidt-Kaler, I. L. Chuang and R. Blatt, Nature, **421**, 48 (2003).

[Harrow03] A. W. Harrow and M. A. Nielsen, Phys. Rev. A., **68**, 012308 (2003).

[Hegerfeldt93] G. C. Hegerfeldt, Phys. Rev. A., **47**, 449 (1993).

[Hennrich00] M. Hennrich, T. Legero, A. Kuhn and G. Rempe, Phys. Rev. Lett., **85**, 4872 (2000).

[Hofmann02] H. F. Hofmann and S. Takeuchi, Phys. Rev. Lett., **88**, 147901 (2002).

[Hong87] C. K. Hong, Z. Y. Ou and L. Mandel, Phys. Rev. Lett., **59**, 2044 (1987).

[Horn85] R. A. Horn and C. R. Johnson, *Matrix Analysis* (Cambridge University Press, 1985).

[Horodecki96] M. Horodecki, P. Horodecki and R. Horodecki, Phys. Lett. A, **223**, 1 (1996).

[Hwang03] W.-Y. Hwang, Phys. Rev. Lett., **91**, 057901 (2003).

[Itano98] W. M. Itano, J. C. Bergquist, J. J. Bollinger, D. J. Wineland, U. Eichmann and M. G. Raizen, Phys. Rev. A., **57**, 4176 (1998).

[Jaksch99] D. Jaksch, H. J. Briegel, J. I. Cirac, C. W. Gardiner and P. Zoller, Phys. Rev. Lett., **82**, 1975 (1999).

[James01] D. F. V. James, P. G. Kwiat, W. J. Munro and A. G. White, Phys. Rev. A., **64**, 052312 (2001).

[Jeffrey04] E. Jeffrey, N. A. Peters and P. G. Kwiat, New J. Phys., **6**, 100 (2004).

[Joo03] J. Joo, Y.-J. Park, S. Oh and J. Kim, New J. Phys., **5**, 136 (2003).

[Kay04] A. Kay and J. K. Pachos, New J. Phys., **6**, 126 (2004).

[Keller04a] M. Keller, B. Lange, K. Hayasaka, W. Lange and H. Walther, Nature, **431**, 1075 (2004).

[Keller04b] M. Keller, B. Lange, K. Hayasaka, W. Lange and H. Walther, New J. Phys., **6**, 95 (2004).

[Kielpinsksi02] D. Kielpinsksi, C. Monroe and D. J. Wineland, Nature, **417**, 709 (2002).

[Kim99] J. Kim, O. Benson, H. Kan and Y. Yamamoto, Nature, **397**, 500 (1999).

[Kiraz04] A. Kiraz, M. Atature and A. Imamoglu, Phys. Rev. A., **69**, 032305 (2004).

[Kiraz05] A. Kiraz, M. Ehrl, T. Hellerer, O. E. Mustecaplioglu, C. Brauchle and A. Zumbusch, Phys. Rev. Lett. (2005).

[Knight73] P. L. Knight and L. Allen, Phys. Rev. A., **7**, 368 (1973).

[Knill01a] E. Knill, *Fermionic linear optics and matchgates* (2001). Quant-ph/0108033.

[Knill01b] E. Knill, R. Laflamme and G. J. Milburn, Nature, **409**, 46 (2001).

[Knill02] E. H. Knill and M. A. Nielsen, *Encyclopedia of Mathematics, Supplement III, ed. M. Hazewinkel* (Kluwer, 2002).

[Koashi04] M. Koashi, Phys. Rev. Lett., **53**, 120501 (2004).

[Kok01] P. Kok and S. Braunstein, Phys. Rev. A., **63**, 033812 (2001).

[Kok05a] P. Kok, S. D. Barrett and T. P. Spiller, J. Opt. B: Quantum Semiclass. Opt., **7**, S166 (2005).

[Kok05b] P. Kok and W. J. Munro, Phys. Rev. Lett., **95**, 048901 (2005).

[Kuhn99] A. Kuhn, M. Hennrich, T. Bondo and G. Rempe, Appl. Phys. B., **69**, 373 (1999).

[Kuhn02] A. Kuhn, M. Hennrich and G. Rempe, Phys. Rev. Lett., **89**, 067901 (2002).

[Kumar04] P. Kumar, P. Kwiat, A. Migdall, S. W. Nam, J. Vuckovic and F. N. C. Wong, Quant. Inf. Proc., **3**, 215 (2004).

[Kurtsiefer00] C. Kurtsiefer, S. Mayer, P. Zarda and H. Weinfurter, Phys. Rev. Lett., **85**, 290 (2000).

[Kurtsiefer01] C. Kurtsiefer, M. Oberparleiter and H. Weinfurter, Phys. Rev. A., **64**, 023802 (2001).

[Kurtsiefer02] C. Kurtsiefer, P. Zarda, M. Halder, H. Weinfurter, P. M. Gorman, P. R. Tapster and J. G. Rarity, Nature, **419**, 450 (2002).

[Kwiat95] P. G. Kwiat, K. Mattle, H. Weinfurter, A. Zeilinger, A. V. Sergienko and Y. H. Shih, Phys. Rev. Lett., **75**, 4337 (1995).

[Lange00] W. Lange and H. J. Kimble, Phys. Rev. A., **61**, 063817 (2000).

[Lapaire03] G. G. Lapaire, P. Kok, J. P. Dowling and J. E. Sipe, Phys. Rev. A., **68**, 042314 (2003).

[Law97] C. K. Law and H. J. Kimble, J. Mod. Opt., **44**, 2067 (1997).

[Lee02] H. Lee, P. Kok, N. J. Cerf and J. P. Dowling, Phys. Rev. A., **65**, R030101 (2002).

[Lee04] H. Lee, U. Yurtsever, P. Kok, G. M. Hockney, C. Adami, S. L. Braunstein and J. P. Dowling, J. Mod. Opt., **51**, 1517 (2004).

[Legero03] T. Legero, T. Wilk, A. Kuhn and G. Rempe, Appl. Phys. B., **77**, 797 (2003).

[Legero04] T. Legero, T. Wilk, M. Hennrich, G. Rempe and A. Kuhn, Phys. Rev. Lett., **93**, 070503 (2004).

[Leibfried03] D. Leibfried, B. DeMarco, V. Meyer, D. Lucas, M. Barrett, J. Britton, W. M. Itano, B. Jelenkovic, C. Langer, T. Rosenband and D. J. Wineland, Nature, **422**, 412 (2003).

[Lim04] Y. L. Lim and A. Beige, Proc. SPIE, **5436**, 118 (2004).

[Lim05a] Y. L. Lim, S. D. Barrett, A. Beige, P. Kok and L. C. Kwek, *Repeat-until-success distributed quantum computing with stationary and flying qubits* (2005). Quant-ph/0508218.

[Lim05b] Y. L. Lim and A. Beige, J. Phys. A., **38**, L7 (2005).

[Linden01] N. Linden and S. Popescu, Phys. Rev. Lett., **87**, 047901 (2001).

[Lütkenhaus99] N. Lütkenhaus, J. Calsamiglia and K. A. Suominen, Phys. Rev. A., **59**, 3295 (1999).

[Mancini04] S. Mancini and S. Bose, Phys. Rev. A., **70**, 022307 (2004).

[Mandel83] L. Mandel, Phys. Rev. A., **28**, 929 (1983).

[Matsukevich04] D. N. Matsukevich and A. Kuzmich, Science, **306**, 663 (2004).

[Mattle95] C. Mattle, M. Michler, H. Weinfurter, A. Zeilinger and M. Żukowski, Appl. Phys. B, **60**, S111 (1995).

[Mattle96] K. Mattle, H. Weinfurter, P. Kwiat and A. Zeilinger, Phys. Rev. Lett., **76**, 4656 (1996).

[Maurer04] C. Maurer, C. Becher, C. Russo, J. Eschner and R. Blatt, New J. Phys., **6**, 94 (2004).

[Mckeever04] J. Mckeever, A. Boca, A. D. Boozer, R. Miller, J. R. Buck, A. Kuzmich and H. J. Kimble, Science, **303**, 1992 (2004).

[Michler00] P. Michler, A. Imamoglu, M. D. Mason, P. J. Carson, G. F. Strouse and S. K. Buratto, Nature, **406**, 968 (2000).

[Mikami04] H. Mikami, Y. Li and T. Kobayashi, Phys. Rev. A., **70**, 052308 (2004).

[Milburn89] G. J. Milburn, Phys. Rev. Lett., **62**, 2124 (1989).

[Minc78] H. Minc, *Permanents, Encyclopedia of Mathematics and its applications, Volume 6, Section, Linear Algebra* (Addision-Wesley, 1978).

[Moehring04] D. L. Moehring, M. J. Madsen, B. B. Blinov and C. Monroe, Phys. Rev. Lett., **93**, 090410 (2004).

[Mølmer97] K. Mølmer, Phys. Rev. A., **55**, 3195 (1997).

[Munro05] W. J. Munro, K. Nemoto, R. G. Beausoleil and T. P. Spiller, Phys. Rev. A., **71**, 033819 (2005).

[Nemoto04] K. Nemoto and W. J. Munro, Phys. Rev. Lett., **93**, 250502 (2004).

[Nielsen00] M. A. Nielsen and I. L. Chuang, *Quantum Computation and Quantum Information* (Cambridge University Press, 2000).

[Nielsen04] M. A. Nielsen, Phys. Rev. Lett., **93**, 040503 (2004).

[O'Brien03] J. L. O'Brien, G. J. Pryde, A. G. White, T. C. Ralph and D. Branning, Nature, **426**, 264 (2003).

[Omar02] Y. Omar, N. Paunkóvic, S. Bose and V. Vedral, Phys. Rev. A., **65**, 062305 (2002).

[Oreg84] J. Oreg, F. T. Hioe and J. H. Eberly, Phys. Rev. A., **29**, 690 (1984).

[Ou88] Z. Y. Ou and L. Mandel, Phys. Rev. Lett., **61**, 50 (1988).

[Ou99a] Z. Y. Ou, J.-K. Rhee and L. J. Wang, Phys. Rev. Lett., **83**, 959 (1999).

[Ou99b] Z. Y. Ou, J.-K. Rhee and L. J. Wang, Phys. Rev. A., **60**, 593 (1999).

[Pan98a] J.-W. Pan, D. Bouwmeester, H. Weinfurter and A. Zeilinger, Phys. Rev. Lett., **80**, 3891 (1998).

[Pan98b] J.-W. Pan and A. Zeilinger, Phys. Rev. A., **57**, 2208 (1998).

[Pan03] J. W. Pan, S. Gasparoni, R. Ursin and G. Weihs, Nature, **423**, 417 (2003).

[Paunkóvic02] N. Paunkóvic, Y. Omar, S. Bose and V. Vedral, Phys. Rev. Lett., **88**, 187903 (2002).

[Pelton02] M. Pelton, C. Santori, J. Vuckovic, B. Zhang, G. S. Solomon, J. Plant and Y. Yamamoto, Phys. Rev. Lett., **89**, 233602 (2002).

[Peng05] C.-Z. Peng, T. Yang, X.-H. Bao, J. Zhang, X.-M. Jin, F.-Y. Feng, B. Yang, J. Yang, Q. Zhang, N. Li, B.-L. Tian and J.-W. Pan, Phys. Rev. Lett., **94**, 150501 (2005).

[Peres96] A. Peres, Phys. Rev. Lett., **77**, 1413 (1996).

[Pittman01] T. B. Pittman, B. C. Jacobs and J. D. Franson, Phys. Rev. A., **64**, 062311 (2001).

[Pittman02a] T. B. Pittman, B. C. Jacobs and J. D. Franson, Phys. Rev. A., **66**, 042303 (2002).

[Pittman02b] T. B. Pittman, B. C. Jacobs and J. D. Franson, Phys. Rev. Lett., **88**, 257902 (2002).

[Pittman03] T. B. Pittman, M. J. Fitch, B. C. Jacobs and J. D. Franson, Phys. Rev. A., **68**, 032316 (2003).

[Plenio98] M. B. Plenio and P. L. Knight, Rev. Mod. Phys., **70**, 101 (1998).

[Plenio99] M. B. Plenio, S. F. Huelga, A. Beige and P. L. Knight, Phys. Rev. A., **59**, 2468 (1999).

[Plenio05] M. B. Plenio and S. Virmani, *An introduction to entanglement measures* (2005). Quant-ph/0504163.

[Protsenko02] I. E. Protsenko, G. Reymond, N. Schlosser and P. Grangier, Phys. Rev. A., **66**, 062306 (2002).

[Pryde03] G. J. Pryde and A. G. White, Phys. Rev. A., **68**, 052315 (2003).

[Raussendorf01] R. Raussendorf and H. J. Briegel, Phys. Rev. Lett., **86**, 5188 (2001).

[Raussendorf03] R. Raussendorf, D. E. Browne and H. J. Briegel, Phys. Rev. A., **68**, 022312 (2003).

[Reck94] M. Reck, A. Zeilinger, H. J. Bernstein and P. Bertani, Phys. Rev. Lett., **73**, 58 (1994).

[Reck96] M. H. A. Reck, *Quantum Interferometry with Multiports: Entangled Photons in Optical Fibers*, Ph.D. thesis, Innsbruck University, Innsbruck, Austria (1996).

[Riebe04] M. Riebe, H. Häffner, C. F. Roos, W. Hansel, J. Benhelm, G. P. T. Lancaster, T. W. Korber, C. Becher, F. Schmidt-Kaler, D. F. V. James and R. Blatt, Nature, **429**, 734 (2004).

[Riedmatten04] H. de Riedmatten, I. Marcikic, W. Tittel, H. Zbinden, D. Collins and N. Gisin, Phys. Rev. Lett., **92**, 047904 (2004).

[Rosenberg05] D. Rosenberg, A. E. Lita, A. J. Miller and S. W. Nam, Phys. Rev. A., **71**, 061803 (2005).

[Saavedra00] C. Saavedra, K. M. Gheri, P. Törmä, J. I. Cirac and P. Zoller, Phys. Rev. A., **61**, 062311 (2000).

[Sagi03] Y. Sagi, Phys. Rev. A., **68**, 042320 (2003).

[Samuelsson04] P. Samuelsson, E. V. Sukhorukov and M. Büttiker, Phys. Rev. Lett., **92**, 026805 (2004).

[Santori00] C. Santori, M. Pelton, G. Solomon, Y. Dale and Y. Yamamoto, Phys. Rev. Lett., **86**, 1502 (2000).

[Santori02] C. Santori, D. Fattal, J. Vuckovic, G. S. Solomon and Y. Yamamoto, Nature, **419**, 594 (2002).

[Santori04] C. Santori, D. Fattal, J. Vuckovic, G. S. Solomon and Y. Yamamoto, New J. Phys., **6**, 89 (2004).

[Scheel03] S. Scheel, K. Nemoto, W. J. Munro and P. L. Knight, Phys. Rev. A., **68**, 032310 (2003).

[Scheel04a] S. Scheel, *Permanents in linear optics networks* (2004). Quant-ph/0406127.

[Scheel04b] S. Scheel, *Scaling of success probabilities for linear optics gates* (2004). Quant-ph/0410014.

[Schlosser01] N. Schlosser, G. Reymond, I. Protsenko and P. Grangier, Nature, **411**, 1024 (2001).

[Schlosser03] N. Schlosser, I. Protsenko and P. Grangier, Phil. Trans. Roy. Soc. Lond. A, **361**, 1527 (2003).

[Schmidt-Kaler03] F. Schmidt-Kaler, H. Häffner, M. Riebe, S. Gulde, G. P. T. Lancaster, T. Deuschle, C. Becher, C. F. Roos, J. Eschner and R. Blatt, Nature, **422**, 408 (2003).

[Schön01] C. Schön and A. Beige, Phys. Rev. A., **64**, 023806 (2001).

[Schön05] C. Schön, E. Solano, F. Verstraete, J. I. Cirac and M. M. Wolf, Phys. Rev. Lett., **95**, 110503 (2005).

[Scully82] M. O. Scully and K. Drühl, Phys. Rev. A., **25**, 2208 (1982).

[Sen(De)03] A. Sen(De), U. Sen, M. Wieśniak, D. Kaszlikowski and M. Żukowski, Phys. Rev. A., **68**, 062306 (2003).

[Shi05] B. S. Shi and A. Tomita, J. Mod. Opt., **52**, 755 (2005).

[Shih88] Y. Shih and C. Alley, Phys. Rev. Lett., **61**, 2921 (1988).

[Shih98] Y. H. Shih and C. O. Alley, Phys. Rev. Lett., **61**, 2921 (1998).

[Shor] P. Shor, Proc. 35th Annual Symp. Found. Computer Science, Santa Fe 1994, IEEE Computer Soc. Press 1994, p. 124.

[Shor95] P. W. Shor, Phys. Rev. A., **52**, 2493 (1995).

[Simon] D. Simon, Proc. 35th Annual Symp. Found. Computer Science, Santa Fe 1994, IEEE Computer Soc. Press 1994, p. 116.

[Simon03] C. Simon and W. T. M. Irvine, Phys. Rev. Lett., **91**, 110405 (2003).

[Sørensen98] A. Sørensen and K. Mølmer, Phys. Rev. A., **58**, 2745 (1998).

[Stace03] T. M. Stace, G. J. Milburn and C. H. W. Barnes, Phys. Rev. B., **67**, 085317 (2003).

[Steane96] A. Steane, Proc. R. Soc. Lond. A, **452**, 2551 (1996).

[Sun01] Y. Sun, M. Hillery and J. A. Bergou, Phys. Rev. A., **64**, 022311 (2001).

[Takeuchi99] S. Takeuchi, J. Kim, Y. Yamamoto and H. H. Hoguer, Appl. Phys. Lett., **74**, 1063 (1999).

[Terhal02] B. M. Terhal and D. P. DiVincenzo, Phys. Rev. A., **65**, 032325 (2002).

[Thew02] R. T. Thew, S. Tanzilli, W. Tittel, H. Zbinden and N. Gisin, Phys. Rev. A., **66**, 062304 (2002).

[Tittel98] W. Tittel, J. Brendel, H. Zbinden and N. Gisin, Phys. Rev. Lett., **81**, 3563 (1998).

[Törmä95] P. Törmä, S. Stenholm and I. Jex, Phys. Rev. A., **52**, 4853 (1995).

[Törmä98] P. Törmä, Phys. Rev. Lett., **81**, 2185 (1998).

[Toth05] G. Toth and O. Gühne, Phys. Rev. Lett., **94**, 060501 (2005).

[Tregenna02] B. Tregenna, A. Beige and P. L. Knight, Phys. Rev. A., **65**, 032305 (2002).

[Turhette95] Q. A. Turhette, C. J. Hood, W. Lange, H. Mabuchi and H. J. Kimble, Phys. Rev. Lett., **75**, 4710 (1995).

[Ursin04] R. Ursin, T. Jennewein, M. Aspelmeyer, R. Kaltenbaek, M. Lindenthal, P. Walther and A. Zeilinger, Nature, **430**, 849 (2004).

[Vaidman99] L. Vaidman and N. Yoran, Phys. Rev. A., **59**, 116 (1999).

[Vandersypen01] L. M. K. Vandersypen, M. Steffen, G. Breyta, C. Yannoni, R. Cleve and I. L. Chuang, Nature, **414**, 883 (2001).

[Verstraete04] F. Verstraete and J. I. Cirac, Phys. Rev. A., **70**, 060302 (2004).

[Walborn03] S. P. Walborn, A. N. Oliverira, S. Padua and C. . H. Monken, Phys. Rev. Lett., **90**, 143601 (2003).

[Walther05] P. Walther, K. Resch, T. Rudolph, E. Schenck, H. Weinfurter, V. Vedral, M. Aspelmeyer and A. Zeilinger, Nature, **434**, 169 (2005).

[Wang03] X.-B. Wang, Phys. Rev. A., **68**, 042304 (2003).

[Wong97] T. Wong, S. M. Tam, M. J. Collett and D. F. Walls, Phys. Rev. A., **55**, 1288 (1997).

[Wootters82] W. K. Wootters and W. H. Zurek, Nature, **299**, 802 (1982).

[Wootters89] W. K. Wootters and B. D. Fields, Annals of Physics, **191**, 363 (1989).

[Wu86] L.-A. Wu, H. J. Kimble, J. L. Hall and H. Wu, Phys. Rev. Lett., **57**, 2520 (1986).

[Xiao04] Y.-F. Xiao, X.-M. Lin, J. Gao, Y. Yang, Z.-F. Han and G.-C. Guo, Phys. Rev. A., **70**, 042314 (2004).

[Yoran03] N. Yoran and B. Reznik, Phys. Rev. Lett., **91**, 037903 (2003).

[You00] L. You and M. S. Chapman, Phys. Rev. A., **62**, 052302 (2000).

[Zhao03] Z. Zhao, T. Yang, Y.-A. Chen, A.-N. Zhang, M. Żukowski and J.-W. Pan, Phys. Rev. Lett., **91**, 180401 (2003).

[Zhao04] Z. Zhao, Y.-A. Chen, A.-N. Zhang, T. Yang, H. J. Briegel and J.-W. Pan, Nature, **430**, 54 (2004).

[Zhao05] Z. Zhao, A.-N. Zhang, Y.-A. Chen, H. Zhang, J.-F. Du, T. Yang and J.-W. Pan, Phys. Rev. Lett., **94**, 030501 (2005).

[Zhou05] X. F. Zhou, Y. S. Zhang and G. C. Guo, Phys. Rev. A., **71**, 064302 (2005).

[Zou02a] X. B. Zou, K. Pahlke and W. Mathis, Phys. Rev. A., **66**, 014102 (2002).

[Zou02b] X. B. Zou, K. Pahlke and W. Mathis, Phys. Rev. A., **66**, 064302 (2002).

[Zou04] X. Zou, K. Pahlke and W. Mathis, Phys. Rev. A., **69**, 013811 (2004).

[Zou05] X.-B. Zou and W. Mathis, Phys. Rev. A., **71**, 042334 (2005).

[Żukowski93] M. Żukowski, A. Zeilinger, M. A. Horne and A. K. Ekert, Phys. Rev. Lett., **71**, 4287 (1993).

[Żukowski95] M. Żukowski, A. Zeilinger and H. Weinfurter, Ann. N. Y. Acad. Science, **755**, 91 (1995).

[Żukowski97] M. Żukowski, A. Zeilinger and M. A. Horne, Phys. Rev. A., **55**, 2564 (1997).